SILICA- AND ORGANIC POLYMER-BASED MONOLITHIC STATIONARY PHASES FOR MODERN LIQUID PHASE SEPARATIONS

By

HENGWEN ZHONG

Master of Science in Chemistry

Oklahoma State University

Stillwater, Oklahoma

2005

Submitted to the Faculty of the
Graduate College of the
Oklahoma State University
in partial fulfillment of
the requirements for
the Degree of
DOCTOR OF PHILOSOPHY
December, 2008

SILICA- AND ORGANIC POLYMER-BASED

MONOLITHIC STATIONARY PHASES FOR

MODERN LIQUID PHASE SEPARATIONS

Dissertation Approved:

Dr. Ziad El Rassi

Dissertation Adviser

Dr. Ricard A. Bunce

Dr. Haobo Jiang

Dr. Barry Lavine

Dr. LeGrande M. Slaughter

Dr. A. Gordon Emslie

Dean of the Graduate College

ACKNOWLEDGMENTS

I would like to thank all the people who have made this dissertation possible and an enjoyable experience for me. First of all I would like to express my sincere gratitude to Dr. Ziad El Rassi, my research advisor, who has kindly given me his guidance throughout my graduate studies. He shares with me his knowledge and shows his expertise in the separation sciences which not only enriches my theoretical knowledge but also strengthens my research ability in science exploration. My research experience under his supervision will surely have a great impact in my future career.

I would also like to thank my committee members, Dr. Richard Bunce, Dr. Barry K. Lavine, Dr. LeGrande Slaughter and Dr. Haobo Jiang for their support and suggestions. Their dedication to research and teaching has helped progress my learning experience to become a better researcher.

I want to express my best regards to all of the members in Dr. El Rassi's research group, who showed their kindness and offered help whenever I encountered a problem in the laboratory.

Finally, I would like to express my gratitude to my parents Youye Zhong and Songfang Huang, my sisters Hengbing and Hengzhen and my brother Hengchang, for their endless love and support in every aspect of my life. Without their unconditional love, understanding and encouragement, I could not have achieved any goal or made any success.

TABLE OF CONTENTS

Chapter Page

Chapter Page

LIST OF TABLES

Table Page

Chaper III

Chapter V

Table Page

Chapter VI

LIST OF FIGURES

Figure Page

Chapter I

Chapter III

Figure Page

Chapter IV

Figure Page

Chapter V

Figure Page

Chapter VI

Figure Page

Figure Page

LIST OF SYMBOLS

a	hydrodynamic radius
α	selectivity factor
κ	Debye-Huckel constant
Δp	pressure drop
$\Delta\mu_{ep}$	difference of electrophoretic mobility
D	diffusion coefficient
δ	thickness of the electrical double layer
d_p	particle diameter
e	electronic charge
E	electrical field strength
ε	dielectric constant
ε'	porosity of the stationary phase
ε_o	permittivity of the vacuum
η	viscosity of the electrolyte solution
I	ionic strength
k'	chromatographic retention factor
k^*	retention factor in CEC
k^*_{cc}	peak locator in CEC
k^*_{ep}	velocity factor

L	total length of the column
l	effective length of column to detection point
ρ	charge density of the surface
N	number of theoretical plates
q	ionic charge
θ	conductivity
μ_{app}	apparent electrophoretic mobility
μ_{eo}	electroosmotic mobility in CZE
μ_{ep}	electrophoretic mobility
R_s	resolution
σ_t	peak standard deviation
σ_L	statistical equivalence of the variance of the migrating zone width
t	elution time
t_m	migration time of charged species
t_o	migration time of inert and neutral tracer
t_R	migration time of neutral species
u_{eo}	electroosmotic velocity in CEC
V	applied voltage
ν,	average flow velocity in pressure driven flow
ν_{eo}	electroosmotic velocity in CZE
ν_{ep}	electrophoretic velocity
w	width of peak at base
w_h	width of peak at half height

w_i	width of peak at inflection point
φ_d	potential at the interface between compact and diffuse regions
φ_o	potential at the interface between the surface and the solution
ζ	zeta potential
ζ_p	zeta potential on a stationary particle

LIST OF ABBREVIATIONS

2-AB	2-Aminobenzamide
ACN	Acetonitrile
AIBN	2,2'-Azobis(isobutyronitrile)
CD	Cyclodextrin
CE	Capillary electrophoresis
CEC	Capillary electrochromatography
Con A	Concancavalin A
CZE	Capillary zone electrophoresis
DAD	Diode array detector
DMF	*N,N*-Dimethylformamide
EDMA	Ethylene dimethacrylate
EOF	Electroosmotic flow
GalNAc	*N*-Acetyl galactosaminide
GlcNAc	*N*-Acetyl glucosaminide
GMA	Glycidyl methacrylate
HILIC	Hydrophilic interaction liquid chromatography
HPLC	High performance liquid chromatography
I.D.	Inner diameter
IDCN	1*H*-Imidazole-4,5-dicarbonitrile

LAC	Lectin affinity chromatography
LC	Liquid chromatography
Nano-LC	Nano-liquid chromatography
NP	Normal phase
NPC	Normal phase chromatography
oNP	*o*-nitrophenyl
PEG	Poly(ethylene glycol)
pNP	*p*-nitrophenyl
RCA	*Ricinus communis* agglutinin
RP	Reversed phase
SNA	*Sambucus Nigra* agglutinin
TMOS	Tetramethylorthosilicate
TRIM	Trimethylolpropane trimethacrylate
WGA	Wheat germ agglutinin

CHAPTER I

SCOPE OF THE STUDY AND GENERAL BACKGROUND

Introduction and Scope of the Study

This dissertation involved three liquid phase separation techniques including capillary electrochromatography (CEC), nano-liquid chromatography (nano-LC) and to a lesser extent capillary electrophoresis (CE). Since nano-LC is simply a miniaturization of the traditional high performance liquid chromatography (HPLC) in terms of columns used and instrumentation, which involves the delivery of nano flow (i.e, a few nL/min), no explicit background on nano-LC is provided in this chapter. On the other hand, some basic backgrounds on CEC will be provided since CEC is a more recent separation technique, and only limited analytical textbooks describe this newly emerging technique. CEC is hybrid of CE and HPLC, and therefore most of the backgrounds given in this chapter about CEC relate very closely to CE and LC.

The hybrid nature of CEC provides the technique with features that combine CE and HPLC, i.e., high separation efficiency resulting from the CE component and unique selectivity originating from the chromatographic capillary column. It was for this reason that CEC has been developed rapidly over the last decade. CEC involves an electrical field which is applied to a fused silica capillary of 25-100 μm ID filed up with a given

stationary phase. Separation in CE is based on differences in charge-to-mass ratio among the separated solutes, while separation in HPLC is based on differences of solutes partitioning between mobile and stationary phases. Thus, CEC separation of neutral solutes parallels that obtained in HPLC. In this case, CEC is simply an LC approach with no moving parts, i.e., absence of mechanical pumps, because the mobile phase flow is insured from within the column by the electroosmosis phenomenon under the influence of a direct electric field. For charged species, CEC separation is based on both differences in charge-to-mass ratio and interaction with the stationary and mobile phase among the charged solutes. Similar to CE, CEC is characterized by a plug-like flow profile thus yielding higher separation efficiency than HPLC, which possesses a laminar flow profile. Also, as in CE the electroosmotic flow (EOF) transports the mobile along with the solutes through the capillary column filled up with the stationary phase. In addition to its unique selectivity and high separation efficiency, CEC also has other advantages such as low consumption of sample and mobile phase, ease of transforming it to a miniaturized format (e.g., chip CEC), and mechanical simplicity of the system.

The scope of this dissertation encompasses the development, characterization and application of novel silica-based and organic polymer-based polar and affinity monolithic stationary phases for normal phase and affinity chromatography of polar species including glycoconjugates, e.g., glycoproteins and their glycan fragments.

This chapter is to introduce some fundamental aspects and some basic operational principles of CEC. It gives an overview of the history of CEC development and brief descriptions of some basic concepts and equations pertinent to CEC separation technique. Chapter II gives an overview of the progress made in silica-based and organic polymer-

based monoliths including the fabrication methods and their applications in separation. Chapter III illustrates the factors that affect the column performance of silica-based polar monoliths and their investigation in the separation and profiling of glycans derived from standard glycoproteins by CEC and nano-LC. In Chapter IV, the generation of silica-based lectin affinity monoliths and their affinity characterization with glycoproteins and monosaccharides are described. Chapter V is concerned with the development of a novel acrylate-based polar stationary phase. Various fabrication methods are investigated. Column performances are evaluated and comparisons with the traditionally used acylate-based monoliths are presented. Further investigation of the acrylate-based monolith in the development of lectin affinity stationary phases and the study of the affinity interactions between the immobilized lectins and glycoconjugates are covered in Chapter VI.

Furthermore, the rationale and significance of the various studies pursued in this dissertation are portrayed in Chapter II along with a literature overview of the progress made in the various interrelated topics pertinent to our investigation. This is also supplemented by more pertinent rationale in the introduction of each chapter that follows Chapter II and describes the investigations undertaken in this dissertation.

Brief History of CEC Development

The first use of electrophoresis was by a Swedish scientist Arne Tiselius in 1937 [1, 2]. Mould and Synge were in the first place to apply EOF to the separation of polysaccharides on a collodion membrane [3]. The development of capillary

electrophoresis had not been reported until Stellan Hjerten demonstrated initially the use of a 3 mm ID glass tube in 1967 [4]. In 1974, Pretorius *et al*. initiated the use of EOF as the driven force for the solvent in a 1 mm glass tube packed with particles of 75-125 μm I.D. [5]. Fourteen years later, Jorgenson and Lukacs started the use of fused-silica capillaries of 75 μm I.D., which was successful in the separation of amino acids with a column efficiency as high as 400,000 plates/meter [6]. Jorgenson and Lukacs also reported the feasibility of CEC employing octadecyl-silica (ODS) particles as the stationary phase media packed in a glass capillary of 170 μm I.D. In the late 1980's and early 1990's, Knox *et al*. [7-10] demonstrated the development of CEC in the separation of a polyaromatic hydrocarbon mixture. Ever since their success with capillaries packed with C_{18}-coated silica particles for CEC separations, CEC has received much attention and has been developed extensively over the last decade.

Basic Principles of Capillary Electrochromatography

Theory of Electrophoresis and Electroosmotic Flow

Electrophoresis is the migration of charged molecules or ions under the influence of an electric field [11]. In an electric field, ions or charged species move at a steady electrophoretic migration velocity. The electrophoretic mobility (μ_{ep}, $cm^2/V{\cdot}s$) is given by the electrophoretic velocity (ν_{ep} , cm/s) per unit of the electric field strength (E, V/cm) as follows:

$$\mu_{ep} = \frac{\nu_{ep}}{E}$$

The electrophoretic mobility is affected by the viscosity of the medium and the size and charge of the species. Small and highly charged species have higher mobilities while large and less charged species have lower mobilities. The factors that affect the electrophoretic mobility can be expressed by the following equation:

$$\mu_{ep} = \frac{q}{6\pi\eta a}$$

where q is the ionic charge, η is the viscosity and a is the hydrodynamic radius of the species or radius of the solvated ion.

In a fused silica capillary, the silanol groups on the wall of the capillary start to ionize and form a negatively charged surface when the pH of the electrolyte solution is above 3.5. Cations from the running electrolyte accumulate on the silica surface thus forming the so called the compact region of the electric double layer. Due to thermal motion, some of these ions in the compact region diffuse into the bulk solution to produce the diffusion region of the electric double layer at liquid solid interface (see Figure 1). An electric double layer that includes the compact region and the diffuse region is thus formed. This distribution of ions creates a gradient potential from the charged surface to the bulk solution (see Figure 2). As shown in Figure 2, the electric potential decreases linearly in the compact region and exponentially in the diffusion region. The ψ_o and ψ_d represent the potentials on the solid surface and the potential at the interface, respectively. The distance from the interface to where the potential value is 0.37 ψ_d is the thickness of the electric double layer (δ). δ can be calculated from the Debye-Hückel constant κ:

$$\delta = \frac{1}{\kappa}$$

The Debye-Hückel constant is given by:

$$\kappa = \sqrt{\frac{8\pi e^2 I}{\varepsilon kT}}$$

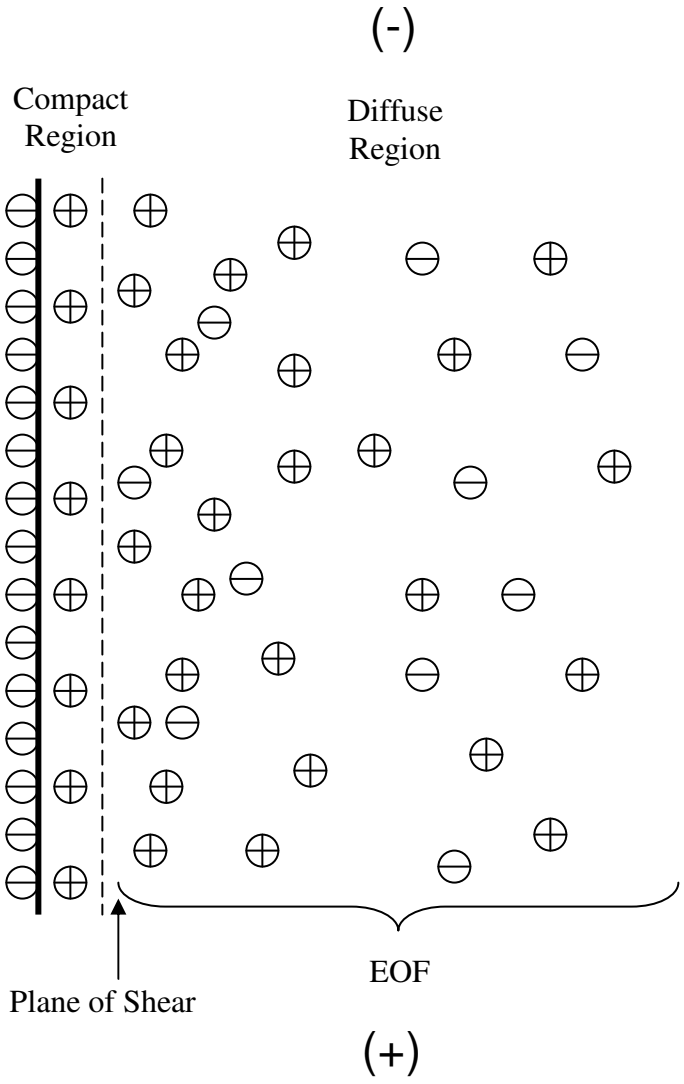

Figure 1. *Schematic of an electrical double layer at a charged surface (adapted from reference [12]).*

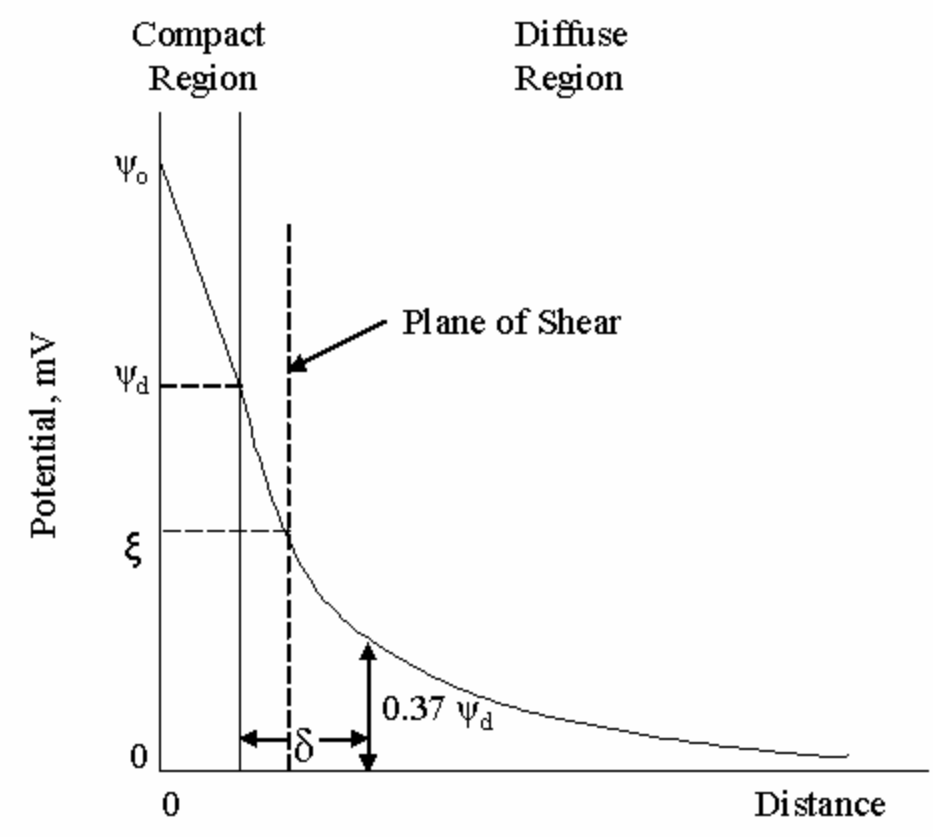

Figure 2. *Potential gradient in the Stern-Gouy-Chapman layer model.*

where e is the electronic charge, k is the Boltzman constant and I is the ionic strength. I is expressed as follows:

$$I = \frac{1}{2}\sum C_i Z_i^2$$

where C is the ion concentration and Z is the ion valence. The plane of shear (see Figure 2) is where the bulk solution flows tangentially to the surface. The potential value at the plane of shear is known as the zeta potential (ζ), which is defined as:

$$\zeta = \frac{4\pi\delta\rho}{\varepsilon}$$

where ε is dielectric constant, ρ is the charge density of the surface.

When an electrical potential is applied to the electrolyte solution inside the capillary, the ions in the diffuse region move toward the oppositely charged electrode. The movement of the solvated ions drags the bulk solution and as a result a liquid flow is generated. This flow of the bulk solution is called electroosmotic flow, which is generally abbreviated as EOF. EOF mobility is expressed as follows:

$$\mu_{eo} = \frac{\zeta \varepsilon}{\eta}$$

or

$$\mu_{eo} = \frac{\nu_{eo}}{E} = \frac{4\pi\rho}{\eta\kappa} \propto \frac{1}{\sqrt{I}}$$

The above equation indicates that EOF is proportional to the applied potential and inversely proportional to the ionic strength and viscosity of the electrolyte solution.

The equation for the EOF in a column packed with porous or nonporous non-conductive particles (e.g., CEC column) is suggested by Overbeek [13] as follows:

$$u_{eo} = -\frac{\varepsilon \varepsilon_o \zeta_p E}{\eta}\left(\frac{\theta_{packed}}{\theta_{open}}\right)$$

where ε is the dielectric constant of the medium, ε_o is the permittivity of the vacuum, ζ_p is the zeta potential at the surface of the packing material, E is the electric field strength, η is the viscosity of the bulk solution and θ_{packed} and θ_{open} are the conductivities in a packed column and an open tube, both filled with electrolyte solution, respectively. The conductivity ratio of $\theta_{packed}/\theta_{open}$ is introduced to account for the effect of the particles on the EOF. Since a packed capillary has a lower conductance than an open capillary, the EOF in a packed capillary is usually lower than that in an open capillary under equivalent

conditions. The difference in conductivity between packed and open capillaries can be estimated from the difference of the currents generated in the two capillaries.

Although the Overbeek's equation does not include the particle size parameter, it is suggested to use particles with sizes above 0.5 μm for CEC columns to avoid the problem of electric double layer overlap which might lead to the elimination of EOF [9, 14].

Different from EOF is the average flow velocity in the pressure driven flow (ν'), which is given by the Kozeny-Carman equation[15] as follows:

$$\nu' = \frac{\varepsilon'^2 d_p^{\,2} \Delta p}{180(1-\varepsilon')^2 \eta L}$$

where ε' is the porosity, d_p is the diameter of the particle of the stationary phase and Δp is the pressure drop over the length of the column (L). As shown in the equation ν' decreasing particle size would have a two-fold effect on the flow velocity because porosity decreases with decreasing the particle size. The equation also indicates that an increase of the applied pressure would increase the average flow velocity.

When the surface of the capillary or the packing material is negatively charged, the direction of the EOF is from the cathode to the anode. Under this condition, the apparent mobility of positively charged species is faster than their electrophoretic mobility μ_{ep},. Since negatively charged species move in the opposite direction to the EOF, they either move in a speed which is slower than the EOF in the same direction, or do not move at all when their electrophoretic mobilities equal the EOF, or even move in the opposite direction when their electrophoretic mobilities are higher than the EOF. Neutral species move at the same speed of the EOF. The mobility of charged species

under the influence of an electric field and EOF is called apparent mobility (μ_{app}). The apparent mobility is the sum of electrophoretic mobility (μ_{ep}) and EOF (μ_{eo}) as follows:

$$\mu_{app} = \mu_{ep} + \mu_{eo}$$

The schematic in Figure 3 shows the mobility differences between cations, anions and neutral species and their elution order reflected on the electropherogram. The mechanism illustrated above also applies when the surface of the capillary is positively charged.

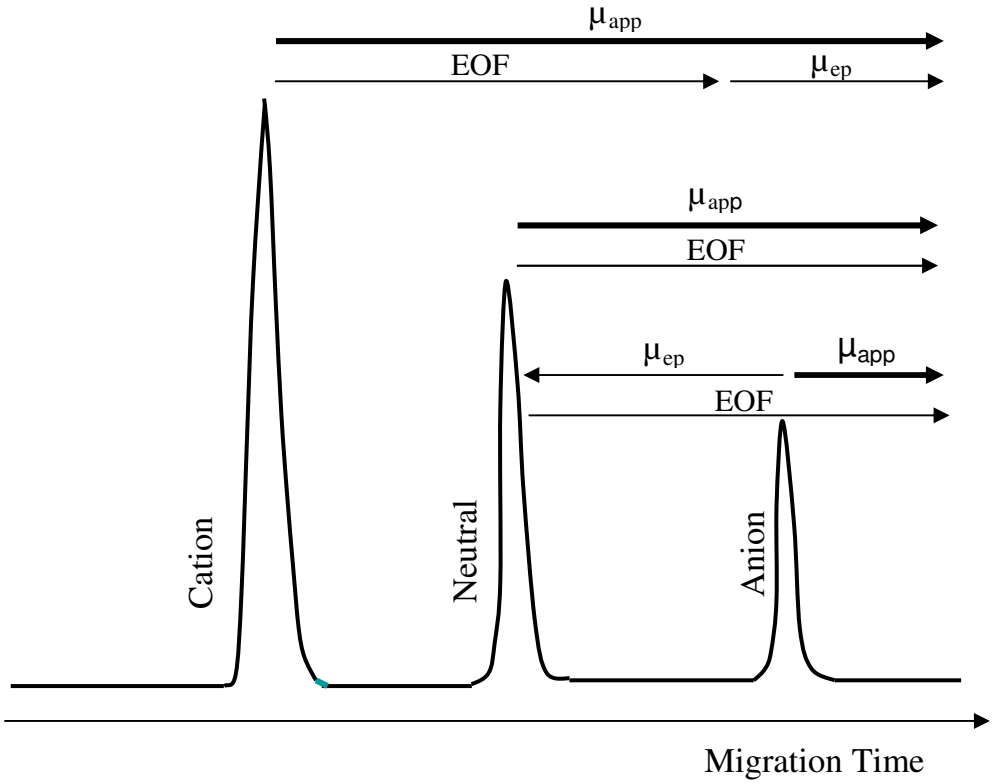

Figure 3. *Schematic showing the direction of EOF, effective mobility and apparent mobility.*

The thickness of an electric double layer in microchannels is in the range of 10-1000 nm [16] and a typical value of 1-10 nm was suggested for the electric double layer in CE/CEC[17]. The thickness of the electric double layer can be ignored compared to

the internal diameter of the capillary (50-100 μm). Therefore the flow profile of EOF can be considered as plug-like flow profile. Figure 4 shows the flow profiles of EOF in CE and CEC. As a comparison, the flow profile in pressure-induced flow (i.e. flow in HPLC) is also presented. The laminar flow profile in pressure-induced flow results from the fact that liquid flows faster in larger channels and therefore solutes move at different speeds which lead to band broadening.

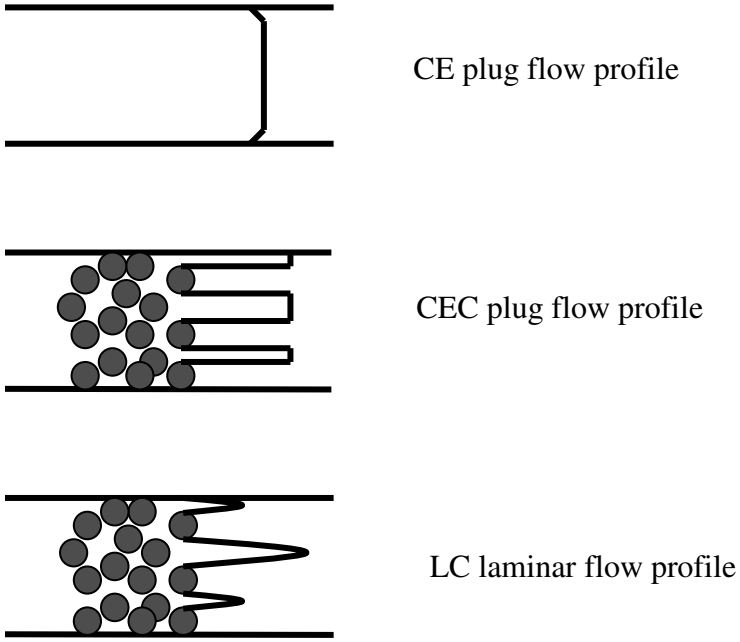

Figure 4. *Flow profiles of EOF and pressure-induced flow.*

Analytical Parameters in CE/CEC

Mobility EOF is the electroosmotic flow velocity (v_{eo}) per unit of applied field strength (E) as follows:

$$\mu_{eo} = \frac{v_{eo}}{E} = \frac{lL}{t_o V}$$

where l is the capillary effective length from the inlet to the detection window, L is the capillary total length, t_o is the migration time of a neutral species and V is the applied voltage. The apparent mobility of a charged species in CE can be calculated by

$$\mu_{app} = \frac{v_{app}}{E} = \frac{lL}{t_m V}$$

where v_{app} is the apparent velocity and t_m is the migration time of a charged species. Since,

$$\mu_{app} = \mu_{ep} + \mu_{eo}$$

μ_{ep} can be calculated in CE by:

$$\mu_{ep} = \mu_{app} - \mu_{eo} = \frac{lL}{V}\left(\frac{1}{t_m} - \frac{1}{t_o}\right)$$

Efficiency, resolution and selectivity in CE Column separation efficiency is defined as the plate number N given by[18]:

$$N = \frac{l^2}{\sigma_L^{\,2}}$$

Where σ_L is the statistical equivalence of the variance of the migrating zone width:

$$\sigma_L^{\,2} = 2Dt_m = \frac{2DlL}{\left(\mu_{ep} + \mu_{eo}\right)V}$$

where D is the diffusion coefficient of the species. When L = l, which means the detection is at the tip of the capillary, N is given by

$$N = \frac{l^2}{\sigma_L^{\,2}} = \frac{\left(\mu_{ep} + \mu_{eo}\right)Vl}{2DL} = \frac{\left(\mu_{ep} + \mu_{eo}\right)V}{2D}$$

This equation shows that, in CE, N increases with increasing μ_{app} and decreasing D. N can also be calculated from the electropherogram by the following equation, which is the same equation as that used for CEC (from the electrochromatogram) or LC (from the chromatogram):

$$N = \frac{t_R^{\,2}}{\sigma_t^{\,2}} = 16\left(\frac{t_m}{w}\right)^2 = 5.54\left(\frac{t_m}{w_h}\right)^2 = 4\left(\frac{t_m}{w_i}\right)^2$$

where w, w_h and w_i are the widths of the peak at base, half height and inflection point, respectively.

Resolution of two adjacent peaks in CE is defined by:

$$R_s = \frac{1}{4}\sqrt{N}\,\frac{\Delta\mu_{ep}}{\overline{\mu}_{app}} = \frac{1}{4\sqrt{2}}\,\Delta\mu_{ep}\sqrt{\frac{Vl}{DL\left(\overline{\mu}_{ep} + \mu_{eo}\right)}}$$

Also, R_s can be calculated from the electropherogram in CE, electrochromatogram in CEC or chromatogram in LC by

$$R_s = \frac{2\left(t_{m2} - t_{m1}\right)}{w_1 + w_2}$$

where t_{m1} and t_{m2} are the migration times of species 1 and 2, w_1 and w_2 are the peak widths of species 1 and 2. In CEC and LC, the term retention time is used instead of migration time.

Selectivity factor α of two neighboring peaks in CE is given by

$$\alpha = \frac{\Delta\mu_{ep}}{\overline{\mu}_{app}} = \frac{\Delta\mu_{ep}}{\overline{\mu}_{ep} + \mu_{eo}}$$

where $\Delta\mu_{ep}$ is the difference of electrophoretic mobility between species 1 and 2, $\overline{\mu_{ep}}$ is the average of electrophoretic mobility of species 1 and 2.

For neutral species in CEC, α can be calculated using the equation

$$\alpha = \frac{t_{R2}^{'}}{t_{R1}^{'}} = \frac{k_2^{'}}{k_1^{'}}$$

where, t_{R1}' and t_{R2}' are the adjusted retention time of species 1 and 2, respectively (t_{R1}'= t_{R1}- t_o, t_{R2}'= t_{R2}- t_o), and k_1' and $k_2^{'}$ are the retention factors of species 1 and 2, respectively.

For a neutral species, the retention factor k' in CEC is defined as

$$k^{'} = \frac{t_R - t_o}{t_o}$$

where t_R is the retention time of the solute and t_o is the migration time of a neutral EOF tracer (i.e., unretained solute).

For a charged solute in CEC, the retention factor is represented by k^*:

$$k^* = \frac{t_m\left(1 + k_{ep}^*\right) - t_o}{t_o}$$

where t_m is the migration time of the charged solutes, t_o is the migration time of EOF marker and k^*_{ep} is the velocity factor defined as follows:

$$k_{ep}^* = \frac{\nu_{ep}}{\nu_{eo}}$$

Both k^* and k^*_{ep} are measured in CEC, ν_{ep} is measured in CE with the same conditions used in CEC. If the solute is neutral, $\nu_{ep} = 0$, $k^*_{ep} = 0$, and thus $k^* = k$'.

In CEC, peak locator k^*_{cc} is used to describe the elution order of charged species. k^*_{cc} is given by

$$k_{cc}^* = \frac{t_m - t_o}{t_o}$$

For neutral solutes, the definitions of the analytical parameters for efficiency, and resolution in CEC are similar to those used in HPLC, which are not included in this chapter. More details and principles about HPLC can be found in textbooks [19, 20].

Column Technology

Most of the stationary phases for packed columns in CEC were inherited or transferred from HPLC. In CEC, three types of columns have been developed, i.e., open tubular columns, particles packed columns and monolithic columns. One basic requirement for the stationary phases in CEC is that there must be charged or ionizable groups on the surface for generation of EOF [17]. A brief overview of the column technology is presented in the following sections. More about the development and application of the stationary phases will be introduced in Chapter II.

Open tubular columns Open tubular columns are prepared by attaching the stationary phases onto the inner wall of the capillaries (10-25 μm I.D.) *via* either physical or dynamical adsorptions or chemical reactions [21]. The adsorption is based on the electrostatic interactions between the capillary silica surface and the desired coating material. Dynamically adsorbed stationary phases usually need a mobile phase containing the adsorbed agent to maintain the interaction between the stationary phase and the capillary wall [22]. Chemically bonded stationary phases used in open tubular columns are similar to monolithic stationary phases, which will be illustrated in the following

sections. Compared to packed columns, open tubular columns have higher EOF because higher voltage can be used due to fast heat dissipation in the open tube. In addition, open tubular columns are easier to fabricate. The major disadvantage of the open tubular columns is their small sample capacity due to the limited surface area [17].

Particles packed columns Particles packed columns used in CEC resemble the conventional HPLC particles packed columns. As in HPLC, column packing and frits preparation are needed for the column fabrication. The pore size of the particle used that assures the generation of a significant EOF should be higher than 200 Å. The packing methods include solvent slurry packing, supercritical CO_2 slurry packing, centripetal packing and electrokinetic packing [17]. The solvent slurry packing is the most widely used method. The materials that are used for the on-column frit fabrication include silicate or silica gels, sintered packing material, sol gel glued packing materials and porous polymers [17]. Packed columns have higher surface area and in turn higher sample capacity than the open tubular columns. However, in addition to the difficulty to make end-frits, the particles packed columns have other problems associated with the use of frits, e.g., lower porosity and, thus, are easily contaminated or even clogged when 'dirty' samples are used [17]. To avoid the use of frits and packing, new monolithic materials, which are continuous porous rods, have been developed for stationary phases used in both LC and CEC since mid 1990's.

Monolithic columns Monolith is a continuous porous rigid material which can be made through particle fixing [23, 24] or *in situ* polymerizations (see Chapter II). The

in situ polymerization is now used widely for monolith fabrications. Monoliths can be sorted into two primary types, namely, inorganic silica-based monolith and organic polymer-based monolith.

The silica-based monolith is generally produced *via* the so-called sol-gel process that involves three steps, i.e., hydrolysis, condensation and successive polycondensation as illustrated in the following reactions:

$$Si(OR)_4 + H_2O \rightarrow Si(OH)(OR)_3 + ROH \qquad (1)$$

$$Si\text{-}OH + Si\text{-}OH \rightarrow Si\text{-}O\text{-}Si + H_2O \qquad (2)$$

$$Si\text{-}OH + Si\text{-}OR \rightarrow Si\text{-}O\text{-}Si + R\text{-}OH \qquad (3)$$

where R stands for an alkyl group (C_nH_{2n+1}).

The successive condensation yields oligomers which finally grow into a gel network [25]. The most often used sol-gel precursors are tetramethylorthosilicate (TMOS) and tetraethylorthosilicate (TEOS). Poly (ethylene glycol) (PEG) is often employed as porogen to help generate porous structure for silica monolith. The preparation of the silica monolith involves *in situ* polymerization, mesopore tailoring, aging and surface modification [26].

Organic polymer-based monoliths can be produced by *in situ* thermally initiated polymerization [27], photopolymerization [28] or γ-radiation-initiated polymerization [29]. The organic polymer-based monoliths can be identified as acrylate-based monolith, styrene-based monolith and acrylamide-based monolith based on the monomer used. Among these polymers, the acrylate-based monolith is the most popular and successful porous material [30]. Glycidyl methacrylate (GMA) is widely employed as monomer for the acrylate-based monolith. Ethylene dimethacrylate (EDMA) and trimethylolpropane

trimethacrylate (TRIM) are the popular crosslinkers for the polymers. The porogen for organic polymer-based monolith is an organic solvent (or a binary solvent mixture) such as toluene, hexanol, dodecanol, etc. The preparation of organic polymer-based monoliths involves only one-step polymerization, and in some instances an additional step(s) of surface modification for specific ligand introduction.

Compared to the particles packed column, the monolith columns have many advantages including simplicity of the *in situ* preparation, no column packing and frit required, no bubble formation problem, ease to control the pore structure and ease to modify the surface. More about the monolithic columns will be presented in the later chapters.

Instrumentation

The major components of a CE/CEC instrument are a high-voltage power supply, a capillary, two electrodes, an autosampler, a detector and a data processor (Figure 5). The CEC column format may be any one of the columns described above in the preceding section. The capillary is held in a cartridge with its window located on the aperture of the cartridge for UV detection. The inlet and outlet of the capillary and two electrodes are immersed into two vials (usually 1 mL) serving as mobile phase reservoirs. The power supply provides voltage in the range of 1.0 kV-30 kV under which analytes move from the anode to the cathode or in the reverse direction. Sample injections can be achieved by voltage (1-10 kV) or pressure (0-20 psi). Detectors that are used in the CE/CEC system are mainly UV-vis, fluorescence, mass spectrometric, nuclear magnetic

resonance, refractive index, conductivity, amperometric and radiometric [31]. UV-vis and mass spectrometric detectors are the most widely used detectors for quantitation and structural identification, respectively. The UV source of the UV-vis detector is a deuterium lamp with a spectrum in the range of 190-330 nm. Electropherograms or electrochromtograms, which are plots of detection signal versus time are displayed in real time by the data handling system.

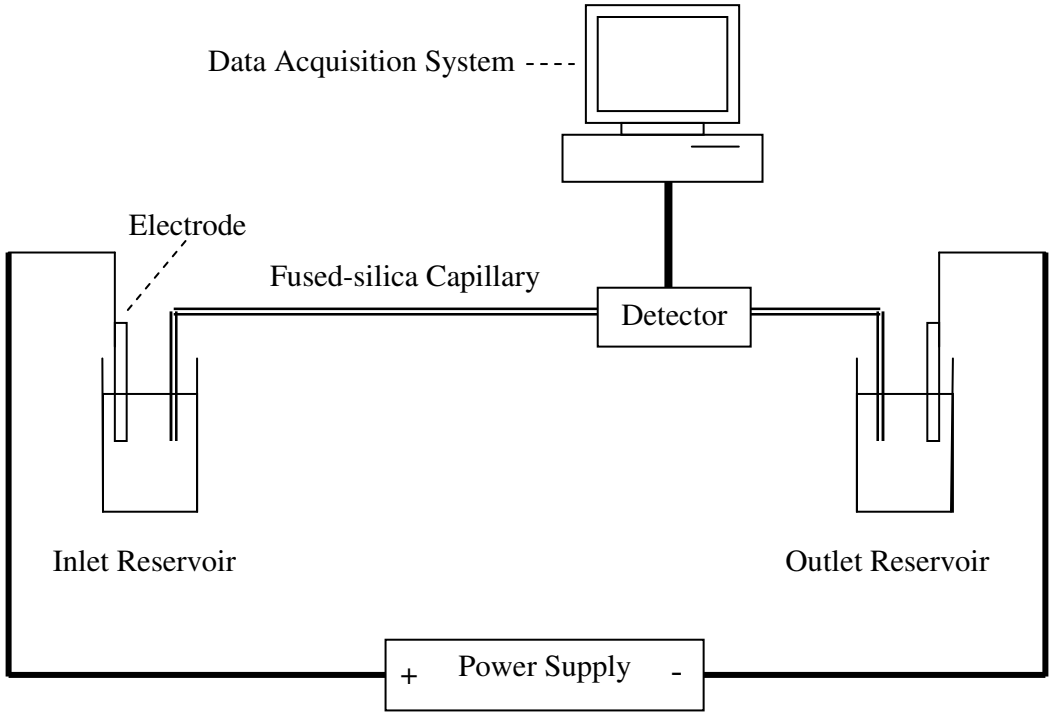

Figure 5. *Schematic illustration of a CE/CEC instrument.*

Conclusions

This chapter has (i) outlined the scope of this dissertation; (ii) provided the historical background of the development of CEC; (iii) explained the basic principle and

performance parameters used in CE and CEC; (iv) overviewed the column technology and (v) illustrated the CE/CEC instrumentation.

REFERENCES

[1] Tiselius, A., *J. Exp. Med.* **1937**, *65*, 641.

[2] Tiselius, A., *Biochem. J.* **1937**, *31*, 313.

[3] Mould, D. L., Synge, R. L., *Analyst* **1952**, *77*, 964.

[4] Hjerten, S., *Chromatogr. Rev.* **1967**, *9*, 122.

[5] Pretorius, V., Hopkins, B. J., Shieke, J. D., *J. Chromatogr.* **1974**, *99*, 23.

[6] Jorgenson, J. W., Luckas, K. D., *Anal. Chem.* **1981**, *53*, 1298.

[7] Knox, J. H., *Chromatographia* **1988**, *26*, 329.

[8] Knox, J. H., Grant, I. H., *Chromatographia* **1987**, *24*, 135.

[9] Knox, J. H., Grant, I. H., *Chromatographia* **1991**, *32*, 317.

[10] Knox, J. H., McCormack, K. A., *J. Liq. Chromatogr.* **1989**, *12*, 2435.

[11] Krull, I. S., Stevenson, R. L., Mistry, K., Swartz, M. E., *Capillary Electrochromatography and Pressurized Flow Capillary Electrochromatography*, HNB Pubishing, New York **2000**.

[12] Heiger, D. N., *High Performance Capillary Electrophoresis*, Hewlett-Packard Company, France **1992**.

[13] Overbeek, J. T. G., *Colloid Science*, Elsevier, New York **1952**.

[14] Smith, N. W., Evans, M. B., *Chromatographia* **1995**, *4*, 197.

[15] Giddings, J. C., *Unified Separation Science*, Wiley, New York **1991**.

[16] Gong, L., Wu, J., *Appl. Mathematics and Mechanics* **2006**, *27*, 1391.

[17] Tang, Q., Lee, M. L., *Trends Anal. Chem.* **2000**, *19*, 648.

[18] Frossman, P. D., Colburn, J. C., *Capillary Electrophoresis Theory & Practice*, Academic Press, Inc, San Diego **1992**.

[19] Meyer, V. R., *Practical High-Performanc Liquid Chromatography*, Wiley, Bodmin, Cornwall **2004**.

[20] Miller, J. M., *Chromatography*, John Wiley & Sons, Inc., Hoboken, New Jersey **2005**.

[21] Pesek, J. J., Matyska, M. T., *Open tubular approches to capillary electrochromatography*, in: Deyl, Z., Svec, F. (Eds.), *Capillary Electrochromatography*, Elsevier, Amsterdam **2001**, pp. 241.

[22] Liu, Z., Wu, R., Zou, H., *Electrophoresis* **2002**, *23*, 3954.

[23] Asiaie, R., Huang, X., Farnan, D., Horvath, C., *J. Chromatogr. A* **1998**, *806*, 251.

[24] Chirica, G., Remcho, V. T., *Electrophoresis* **1999**, *20*, 50.

[25] Nakanishi, K., *J. Porous Mater.* **1997**, *4*, 67.

[26] Minakuchi, H., Nakanishi, K., Soga, N., Ishizuka, N., Tanaka, N., *Anal. Chem.* **1996**, *68*, 3498.

[27] Mihelic, I., Koloni, T., Podgornik, A., *J. Appl. Polym. Sci.* **2003**, *87*, 2326.

[28] Lee, D., Svec, F., Frechet, J. M. J., *J. Chromatogr. A* **2004**, *1051*, 53.

[29] Safrany, A., Beiler, B., Laszlo, K., Svec, F., *Polymer* **2005**, *46*, 2862.

[30] Vlakh, E. G., Tennikova, T. B., *J. Sep. Sci.* **2007**, *30*, 2801.

[31] Weston, A., Broun, P. R., *HPLC and CE: Principles and Practice*, Academic Press, San Diego **1997**.

CHAPTER II

OVERVIEW OF SILICA-BASED AND ORGANIC-BASED POLAR AND AFFINITY MONOLITHIC COLUMNS

Introduction

Monoliths used in CEC or LC falls into two primary types, i.e., inorganic silica-based monoliths and organic polymer-based monoliths. Both of the two monolithic types of columns have the same merits over the conventional particles packed columns including (i) packing and frit fabrication are not required, (ii) simple *in situ* polymerization, (iii) good controllability of porous structures, and (iv) easy modification of surfaces. While silica-based monoliths have the advantages of mechanical stability and high specific surface area, which allows high separation efficiency, organic polymer monolithic columns have the merits of simplicity of preparation and stability in aqueous and alkaline mobile phase environment.

In the past decade, the development of the monoliths for CEC and LC has received much attention and gained increasing interest [1-3]. Monolithic stationary phases have been widely used in the separation of small molecules and large biomolecules as stationary phases for reversed phase chromatography (RPC) [4-7], normal phase chromatography (NPC) [8-11], affinity chromatography [10-12] and ion

chromatography [13, 14], etc. Among these chromatographic methods, the development and applications of polar monolithic stationary phases are still very limited and need more explorations. On the other hand, affinity monolithic columns seem to be the promising support materials for affinity chromatography due to their fast mass transfer and low backpressure [10, 11, 15, 16]. In this regard, this chapter will give a review focusing on the recent developments and applications of the polar and affinity monolithic stationary phases in CEC and LC separations.

Silica-Based Monolithic Columns

Fabrication of Silica-Based Monoliths

Most of silica-based monoliths were synthesized *via* the so-called sol-gel technology which was firstly reported by Minakuchi *et al.* [17]. The sol-gel process involves the following reactions, i.e., (i) hydrolysis of the silica alkoxide to form silanol groups (Si-OH); (ii) alcohol condensation between the alkoxide and the silanols to produce the siloxane bonds (Si-O-Si); (iii) water condensation between the silanol groups to generate Si-O-Si bonds. The subsequent condensation reactions will finally lead to the formation of a Si-O-Si crosslinked network (see Chapter I). The sol-gel method usually employed tetramethoxysilane as the functional monomer, poly(ethylene glycol) (PEG) or other alternatives with similar structure as the porogen and acetic acid as the catalyst [18]. The morphology of silica monolith was affected by a variety of factors such as

ratios of monomer, porogen and solvent, and mesopore treatment time and temperature, etc [19].

The following describes the general procedures that were involved in the preparation of silica monolithic capillary columns [3, 20]. The fused-silica capillary was firstly treated hydrothermally or with a sodium hydroxide solution followed by hydrochloric acid treatment to generate silanol groups for further bonding reactions. The sol-gel precursor solution was then introduced into the capillary and an *in-situ* polymerization was conducted at a warm temperature for a certain time (usually 12 h). The resulted monolith skeleton was stabilized by a heating treatment at a high temperature. The monolith was then ready for surface modification, e.g., polar or nonpolar ligands attachment or protein immobilization.

Polar Silica-Based Monoliths for Normal Phase Chromatography (NPC) and Capillary Electrochromatography (NP-CEC)

Normal-phase chromatography (NPC) is a complementary separation technique to reversed-phase chromatography (RPC). Compared to reversed-phase separation, NPC with polar sorbents is more powerful in the separation of polar solutes. In NPC, the stationary phase, which usually bears polar functionalities such as cyano, diol or amino, is more polar than the mobile phase. The mobile phase in NPC is usually a mixture of organic solvents such as chloroform and methanol. Sample retention increases with decreasing the polarity of the mobile phase [21], that is by increasing the content of the least polar organic solvent component of the mobile phase. Since a wide range of polar

stationary phases (e.g., bare silica gels, silica bonded polar phases, ion exchange resins, etc.) can be utilized to achieve NPC of polar species [22], a more generic term "hydrophilic interaction liquid chromatography (HILIC)" was coined by Alpert [23]. In this chapter and throughout this dissertation, the more traditional acronym NPC will be utilized.

Due to its high separation efficiency and its suitability for the separation of a wide variety of solutes especially those with low polarity, RPC is the most widely used method in liquid chromatography. Similar to the traditional silica particles packed in columns used in RPC, silica-based reversed-phase monoliths have been investigated by many researchers [7, 24-27]. In contrast, there are only a few reports regarding polar silica-based monolithic columns for normal phase CEC and LC of polar species. An overview regarding the development and applications of columns packed with polar silica-based particles as well as silica monolithic columns before 2005 was presented in the MS thesis by the author of this dissertation [28]. The following section gives an overview of the most recent development and applications of polar silica monolithic stationary phases with an emphasis on their applications in NPC. The last section gives a summary of the development of polar silica monoliths in our research group. Other types of modified silica monoliths such as stationary phases for chiral separations and ion-exchange chromatography (IC) can be found in recent review articles by Qin et al. (chiral separations in CEC) [29], Schaller *et al.* (IC) [13], Chambers *et al.* (IC) [14] and Nunez *et al.* (IC) [3].

Tanaka's research group is regarded as the pioneer in the development of the silica-based monoliths. They first successfully fabricated silica-based monoliths bonded

with C_{18} and used them in HPLC in 1996. Recently, they started the work on monolithic silica capillary columns modified with other functionalities to introduce polar columns that can be used in NPC [30]. Silica-based monoliths prepared by the sol-gel process were modified with *N*-(3-trimethoxysilyl-propyl) methacrylamide as the anchor groups by passing a 1:1 mixture of the silane [i.e., *N*-(3-trimethoxysilyl-propyl) methacrylamide] and pyridine through the monolith at 80 ˚C for 24 h. The monolith thus formed with the methacrylamide functionality was charged with a solution containing acrylamide and 3-aminopropyltriethoxysilane and allowed to react at 60 ˚C for 1 h. The polyacrylamide-modified monolithic silica columns thus obtained were denoted PAMS(100)-x by the authors [30]. The PAMS columns obtained had permeability of 2.3×10^{-14} -7.9×10^{-14} m^2 and plate height of 16-21 μm. These polar columns were applied to the separations of nucleic acid bases and nucleoside mixtures containing 9 solutes and sugar mixtures including 14 carbohydrates using 70-90 % v/v acetonitrile. The comparison of the synthesized column with the commercial amide-type particle packing column (TSK gel Amide-80) showed that the synthesized column had slightly higher column separation efficiency and 3 folds higher permeability [30]. In order to increase the retention factors of sugars on monolithic silica capillary columns modified with *N*-(3-trimethoxysilyl-propyl)methacrylamide anchor groups, Tanaka's research group prepared poly(acrylic acid) coated monolithic silica capillary column by allowing the column with the methacrylamide functionality to react with a mixture of 30 μL acrylic acid and 5 mg ammonium persulfate in 1.0 mL water at 60 ˚C for 2 h [31]. The poly(acrylic acid) modified monolithic silica capillary column thus obtained was referred to by the authors as MAS-AA columns. The MAS-AA columns were successful in the separations of

pyridylamino derivatized sugars and peptides of the tryptic digest of bovine serum albumin in the NPC mode by LC. In addition, the MAS-AA columns were able to separate proteins and nucleosides in the mode of weak cation-exchange at high linear flow velocity [31]. The high polarity of the carboxylic acid functionality improved the intermolecular interaction and thus increased solute retention in NPC. It was suggested that the poly(acrylamide) coated columns are suitable for the separation of longer polymers of sugar derivatives, while poly(acrylic acid) coated columns are useful for oligosaccharide separations. Also, the columns were shown to be suitable for highly polar solutes separation in LC-MS [31]. In addition, the study on the column performance of the poly (acrylic acid) coated columns indicated that the column used in the NPC mode can be an alternative to RPC mode for polar compounds in both isocratic and gradient elution [32].

Other approaches to make hybrid silica-based monoliths possessing both organic and inorganic moieties as well as mixed-mode stationary phase that can be used in different separation modes such as RPC, NPC, and CEC, etc., were also reported recently. Ye *et al.* produced monolithic silica columns with surface-bound amino functionalities by modifying silica-based monolith with 3-aminopropyltrimethoxysilane for NPC applications. The amino groups served as a weak anion-exchanger and made contribution to the generation of EOF in CEC. Nucleotides were separated by a mixed mode including hydrophilic interaction, weak anion-exchange and electrophoresis. Polar compounds such as phenols, nucleic acid bases and nucleosides were separated by normal phase CEC mode [33]. Another silica-based monolith with reversed-phase mode and weak anion-exchange mode for high performance liquid chromatography was

reported by Nogueira *et al* [34]. In this work, *N*-(10-undecanyl)-3-aminoquinuclidine was immobilized onto thiol-modified monolithic silica columns. The mixed mode column gave complementary selectivity to the reversed phase mode and were found to be particularly useful for separations of hydrophilic acidic peptides [34]. Ding *et al.* mixed three monolith precursors of tetraethoxysilane, aminopropyltriethoxysilane and octyltriethoxysilane to make a monolithic stationary phase, which combined reversed-phase mode and weak anion-exchange mode [35]. The amino groups acted as weak anion exchange functionalities and also dominated the charge on the surface of the stationary phase to generate EOF in CEC at acidic pH. Some aromatic acids and basic compounds were well separated with proper mobile phases, and neutral compounds were separated based on reversed-phase mechanism [35].

In investigations conducted by our research group, polar ligands such as 3-hydroxypropionitrile [20] and 1H-imidazole-4,5-dicarbonitrile [36] were employed to modify the surface of silica-based monoliths in order to yield polar stationary phases which could be used in NPC. The monoliths were produced by a modified sol-gel process [37] and the polar ligands were introduced to the surface of the silica monolith *via* an epoxy ring opening reaction [28]. The monolith modified with the ligand 3-hydroxypropionitrile (denoted CN-OH monolith) yielded a strong EOF and gave rapid separation of the polar compounds including phenols and chloro-substituted phenols, nucleosides, nucleic acid bases and mono and oligosaccharides. The monolith modified with the 1H-imidazole-4,5-dicarbonitrile (denoted 2CN-OH monolith) showed higher retention toward polar solutes while still possessing high column separation efficiency compared to the CN-OH column [36]. The retention factors of the solutes tested on the

2CN-OH column were about twice higher than those obtained on the CN-OH column under otherwise identical conditions. The increased retention resulted from the highly polar nature of the 2CN-OH monolith, which possessed two polar cyano functions and two basic groups for each immobilized ligand. The 2CN-OH monolith showed its high separation efficiency in the CEC separations of maltooligosaccharides, peptides and basic compounds [38]. It is expected that the 2CN-OH monolith with its significant polar property will be useful for the separation of a wide range of polar molecules in NPC.

Silica-Based Affinity Monoliths

Silica-based monoliths have higher surface area than organic polymer-based monoliths. A recent study showed that the surface coverage of immobilized α_1-acid glycoprotein ligands on the surface of a silica-based monolith was higher than that on silica particles packed in columns by 18% and than that on the surface of polymer-based monoliths prepared from GMA and EDMA by 61% [39]. In addition, the silica monolith contained 1.5-3.6 times more α_1-acid glycoprotein per unit volume compared to the silica particles packed in columns or the polymer-based monoliths. This kind of affinity monolith was evaluated in terms of retention, efficiency and resolving power by testing the separation of two chiral analytes, i.e., R/S-warfarin and R/S-propranolol. Compared to silica particles packed in columns and GMA/EDMA monoliths, the silica-based monolith exhibited higher retention, better resolution and higher separation efficiency in the separation of those chiral molecules. Moreover, silica-based monoliths had lower backpressures and separation impedances. Human serum albumin immobilized silica-

based monolith gave the same results as α_1-acid glycoprotein immobilized silica-based monolith [40].

Other than the investigations mentioned above, most publications on the development and application of silica-based monoliths were about enzyme-immobilized stationary phases. The most recent research in this area is done by Brennan and his coworkers who tried to develop protein-doped silica monolithic columns for screening small molecule-protein interactions *via* frontal chromatography. The enzyme dihydrofolate reductase was mixed with the sol-gel precursor liquids to make the monolith [41-43]. A summary of the research work in this area can be found in the review articles by Sevc [44] and by Josic and Buchacher [45].

Thus far, most reports on silica-based lectin affinity columns involved silica particles packed in columns, and the following is a brief description of the research work involving lectins immobilized on silica particles. Honda *et al.* prepared wheat germ agglutinin (WGA) and concanavalin A (Con A) columns to differentiate glycopeptides *via* immobilization of lectin to the surface of silica particles that possess hydroxyl groups. The identification of glycopeptides was based on the binding constants obtained from their retention times [46]. Madera *et al.* immobilized four lectins including Con A, *Sambuccus nigra* agglutinin (SNA-I), *Ulex europaeus*-I (UEA-I) and phytohaemagglutinin-L (PHA-L) onto silica particles packed in microcolumns and used the lectin microcolumns for glycoprotein enrichment from μL volumes of human blood serum. Individual injections of sample onto the lectin affinity microcolumns was followed by offline reversed-phase prefractionation and nano-LC/MS/MS, permitted identification of 108 proteins in the lectin-bound fractions. In contrast, multi-lectin

microcolumn affinity chromatography could identify 67 proteins [47]. The same group also combined Con A and SNA microcolumns to fractionate complex glycopeptides mixtures and to identify protein glycosylation sites [48]. *Lotus tetragonolobus* agglutinin (LTA) was employed by Xiong *et al.* to modify the surface of silica particles packed in columns for selective capturing of glycopeptides that carry disease-associated modification in their carbohydrates from the tryptic digests of serum samples. Glycopeptides possessing an α-L-fucose residue that were retained by the lectin column were deglycosylated by peptide-*N*-glycosidase (PNGase F) and then transferred to a reversed-phase (RP) column. The fractions obtained from the RP column were finally analyzed by MALDI-MS and ESI-MS [49]. Cartellieri *et al.* established a one-step procedure for separation of fetuin from fetal bovine serum by a WGA modified tresylated silica particles packed in columns. It was reported that 21.6 mg of fetuin was collected from 1 mL of serum by the affinity method [50]. In addition to the lectin columns, one paper reported the immobilization of DNA on silica particles packed in column. This column was used in one-dimensional chromatography as well as two-dimensional chromatography, which employed silica monolithic ODS column and the DNA column. The study showed that 7 and 14 compounds from the two traditional Chinese medicines *Coptis chinensis Franch* and *Rheum palmatum L.*, respectively, were found to have affinity to the immobilized DNA [51].

Although enzyme immobilized silica monolithic columns have been explored by some researchers, other types of silica-based affinity monoliths were rarely reported, and silica monoliths for lectin affinity chromatography have not been reported so far. Because silica-based affinity monolithic columns have many attractions in their

applications [39, 40], more efforts need to be invested to further their development. Such efforts are represented by the development and application of silica monolithic lectin affinity columns, as described in more details in the following chapters.

Organic Based Monolithic Columns

Fabrication of Acrylate-Based Monoliths

The most widely used polymers for organic polymer-based monoliths are polymethacrylate, polystyrene, ploy acrylamide and some natural polymers such as cellulose and agarose. These polymeric monoliths were usually produced by an *in situ* polymerization reaction in the presence of a crosslinker, a porogen and an initiator. Typically, the production of a given methacrylate-based monolithic capillary column can be described as follows. A fused-silica capillary column is initially treated with sodium hydroxide followed by hydrochloric acid and dried with acetone. Thereafter, the wall of the capillary column is vinylized by reacting the wall with methoxysilylmethacrylate. A polymerization solution prepared by mixing a functional monomer (e.g., glycidyl methacrylate, GMA) with a crosslinker (e.g., EDMA) and porogenic solvent mixture (e.g., dodecanol and toluene) is then introduced into the capillary for an *in situ* polymerization in the presence of a radical initiator such as 2,2'-azobisisobutyronitrile (AIBN) *via* UV light or thermal initiation. The polymerization is usually allowed to proceed until a white rod is formed inside the capillary. The monolith thus formed is then subjected to further surface modifications [52].

Polymer-Based Polar Monoliths for NPC and NP-CEC of Polar Compounds

Similar to silica-based monoliths, while reversed-phase organic polymer-based monoliths have been investigated by many researchers [53-56], polar polymer-based monoliths have not yet undergone enough development to separate polar solutes which are difficult to resolve by reversed-phase columns. The following is an overview of the recent development and application of polar polymer-based monoliths.

Since some functional monomers possess polar moieties, polar polymer-based monoliths can be obtained in principle by *in situ* polymerization in a single step. For example, Holdsvendova *et al.* fabricated a polar acrylate-based monoliths by using *N*-(hydroxymethyl) methacrylamide (HMMAA) as the functional monomer, EDMA as the crosslinker, the mixture of propane-1-ol and butane-1,4-diol as the porogens and AIBN as the initiator [57]. The column, which had hydroxyl groups as its functionalities, was used to separate oligonucleotides in the NPC mode. Gradient elution with mobile phase possessing acetonitrile and 100 mM triethylamine acetate was investigated to optimize the conditions for oligoneuleotide separation [57].

Que and Novotny separated a complex fractions of *O*-linked glycans derived from the bile-salt-stimulated-lipase on an amino monolithic column with a mobile phase of acetonitrile/water/ammonium formate (240 mM, 55/44/1, v/v/v), pH 3.0 using EOF as the driving force. They also prepared a cyano monolithic column to separate a mixture of linkage-positional isomers, e.g., maltoheptose $(Glc)_7$ (1→4) and dextran dp7 $(Glc)_7$ (1→6), using the mobile phase of acetonitrile/water/ammonium formate (240 mM,

65/34/1, v/v/v), pH 3.0. The polymerization solution for the cyano monolith fabrication contained acrylamide, bisacrylamide, 2-cyanoethyl acrylate, vinylsulfonic acid and polyethylene glycol (PEG). The polymerization mixture for preparing the amino column consisted of acrylamide, bisacrylamide, 3-amino-1-propanol vinyl ether, [2-(acryloyloxy)ethyl]trimethylammonium methyl sulfate and PEG [58, 59].

Lysine was immobilized on GMA/EDMA monoliths for NP-CEC separation of phenols, anilines, aromatic acids, and basic pharmaceuticals. Due to the amphoteric property of lysine, the column generated anodic or cathodic EOF depending on the pH of the mobile phase. Ionic and ionizable solutes were separated based on hydrophobic and electrostatic interactions with the stationary phase as well as differences in electrophoretic mobility, while neutral compounds were separated based solely on hydrophobic interaction [60].

A copolymerization of butyl methacrylate, ethylene dimethacrylate, methacrylic acid and 2-(dimethylamino) ethyl methacrylate as the functional monomers and 1-propanol and 1,4-butanediol as the porogens to generate a zwitterionic monolith was described by Fu *et al.* [61]. The tertiary amine and acrylic acid groups of the monoliths made it possible for the monolith to generate anodic and cathodic EOF under different pH conditions. Neutral and ionic compounds were separated at different pH of the mobile phase. While less polar solutes such as alkylbenzenes and polyaromatic hydrocarbons were separated based on a reversed-phase mechanism, electrostatic interactions affected the separation of peptides.

The above overview has discussed recent investigations involving polar organic polymer-based monolithic columns. Other studies associated with chiral separations and

ion chromatography employing polymers as the supporting materials can be found in recent review articles [3, 13, 14, 29]. Compared to polar silica-based monoliths, polar polymer-based monoliths can be prepared readily by one step polymerization due to the availability of different kinds of monomers bearing polar functionalities.

Polymer-Based Affinity Monoliths

Organic polymer-based monoliths have been employed recently as the supporting materials for affinity stationary phases due to their relatively low mass-transfer resistance than the conventional stationary phase materials and their ease of fabrication [62]. Many reports on the development and application of the affinity polymer-based monoliths have been published during the past decade. This includes enzyme affinity [44, 45], immunoaffinity [63, 64], lectin affinity [11, 16], protein A affinity [65, 66], protein G affinity [67, 68], immobilized metal affinity [69, 70], sugar-based affinity [10, 71], and aptamer affinity [72]. Among these affinity stationary phases, the enzyme affinity monoliths have been investigated the most. The relevant findings have been summarized in the review articles by Svec [44] and Josic and Buchacher [45]. The followings are some examples of the affinity monolithic columns based on the GMA-EDMA/TRIM polymerization.

In protein G monolithic affinity column fabrication, protein G was immobilized on a monolith fabricated by *in situ* co-polymerization of the functional monomer GMA and the cosslinker TRIM in the presence of the radical initiator 2,2-dimethoxy-2-phenylacetophenone (DMPA) using the porogenic solvent mixture consisting of

cyclohexanol, methanol and hexane. The monolith with immobilized protein G thus obtained was used as an on-line preconcentrator for protein enrichment [67]. The affinity monolith was also coupled to a nonpolar monolithic column made from butyl methacrylate and ethylene dimethacrylate for on-line removal of γ-immunoglobulin (IgG) as well as for preconcentration of low abundance proteins [68]. Similarly, Pan *et al.* prepared protein A affinity column by immobilizing the protein A onto a monolith made by *in situ* polymerization of GMA as the monomer, EDMA and TRIM as the crosslinkers. The resulting monolith was employed for the determination of IgG concentration in human serum [65].

Though organic polymer-based affinity monoliths have been investigated to some extent, the development and application of the organic polymer-based monoliths with immobilized lectins have not been explored yet to their full potentials. Major contributions to the development and application of the acrylate-based affinity monolithic columns originated from El Rassi's research group. This research group immobilized different biomolecules such as mannan [10], protein A, protein G' and antibodies [63, 64], and lectins (e.g., Con A, WGA and *lens culinaris* agglutinin (LCA)) [11, 16] on the acrylate-based monoliths and successfully fractionated or enriched the particular biomolecules. In the immobilization of mannan, two kinds of acrylate-based monoliths were developed, namely a neutral poly (glycidyl methacrylate-*co*-ethylene dimethacrylate) and a cationic poly (glycidyl methacrylate-*co*-ethylene dimethacrylate-*co*-[2-(-(methacryloxy) ethyl] trimethyl ammonium chloride). The neutral polymeric monolith immobilized with mannan was useful in affinity nano-LC while the cationic polymer could be used in both nano-LC and CEC. The affinity monoliths were able to

isolate and concentrate mannose/mannan binding proteins such as LCA and Con A [10]. Lectins such as Con A and WGA were also immobilized on the same monoliths for the separation of glycoconjugates. Evaluation of the affinity of the lectin monoliths using a wide range of glycoprotiens including peroxidase, ovalbumin, ribonuclease B, transferrin, glucose oxidase, glycophorin A, conalbumin and α_1-acid glycoprotein showed that the lectin monoliths exhibited strong affinity with the particular glycoproteins [11]. To enhance separation of glycoproteins, Okanda and El Rassi coupled different lectin columns immobilized with LCA and WGA in series. By using different eluting mobile phases containing 0.2 M *N*-acetylglucosamine (GlcNAc) and 0.2 M methyl-α-D-mannopyranoside, respectively, lipoxidase could be separated from avidin, fetuin and α_1-acid glycoprotein in the nano-LC mode. α_1-Acid glycoprotein, fetuin, κ-casein, avidin, human transferrin and collagen were separated from each other in the CEC mode [16]. Protein A, protein G' and antibodies were also employed to modify the surface of the monoliths made from GMA and EDMA in the microscale depletion of high abundance proteins from human serum. The monoliths that possessed high permeability in pressure-driven flow were good supporting materials for long tandem affinity columns and insured simultaneous protein depletion successfully. The loading capacities of the various affinity columns immobilized with six proteins including anti-HSA, protein G', protein A, anti-human α_1-antitrypsin, anti-human transferrin, anti-human haptoglobin and anti-human α_2-macroglobulin were evaluated. It was found that protein A and protein G' had much higher loading capacities than the antibody-based affinity columns. The tandem affinity columns were used to deplete the top eight most abundant proteins in human serum [63].

In addition to the mannan column described above, lectin separations based on lectin-carbohydrate interaction using carbohydrate immobilized monoliths were also reported by Tetala *et al.* [71]. The polymeric monolith was made by using 2-hydroxyethyl methacrylate (HEMA) as the monomer, (+)-*N, N'*-diallyltartardiamide and piperazine diacrylamide as the crosslinkers, and the monosaccharides β-galactose, β-gluctose and α-mannose as the ligands. The carbohydrates were connected to an alkene terminated tetraethylene glycol spacer through the reducing ends, and the immobilized carbohydrates acted as functional monomers along with the HEMA to form affinity monoliths. LCA and Con A were eluted from the carbohydrate-immobilized column with a mobile phase containing 0.1 M methyl-α-mannopyranoside, and peanut agglutinin (PNA) was eluted with the mobile phase containing 0.1 M β-galactose. In addition to the enrichment of lectins and sugar-binding toxins, the columns could also be used to determine the carbohydrate-protein dissociation constants when operated in frontal affinity chromatography.

A GMA/EDMA acrylate-based monolith with immobilized *pisum sativum* agglutinin (PSA) was employed to fabricate an integrated lectin affinity microfluidic chip by Mao et al. [73]. The polymerization was based on an UV-initiated synthesis where GMA, EDMA and 2,2-dimethoxy-2-phenylacetophenone acted as the functional monomer, crosslinker and initiator, respectively. Different porogen solvents including cyclohexanol/decylalcohol and dodecanol were used. The former porogen resulted in a monolith that had smaller pores, which made desorption of glycoproteins from the column more difficult than from the monolith that used dodecanol as the porogen. The later monolith had larger pore structure and was selected for the elution of the particular

glycoproteins. The chip with the monolith was able to separate three glycoproteins, i.e., turkey ovalbumin, chicken ovalbumin and ovamucoid using electroosmosis as the liquid driving force across the separation channel of the chip. These glycoproteins were labeled with 5-(6)-carboxytetramethylrhodamine succinimidyl ester and purified by a Sephadex G-50 column before they were detected by an UV/Vis spectrophotometer with the detection wavelength set at 280 nm.

Bedair and Oleschuk immobilized Con A on a GMA/EDMA monolith and applied the Con A monolith as a nanoelectrospray (ESI) emitter for an MS/MS system. Porogenic solvents such as methanol, ethanol, propanol, hexanol, octanol and dodecanol were employed to study their effects on the amount of immobilized Con A and the stability of the ESI spray. It was found that the alcohol with the higher alkyl chain helped to increase the surface area and thus increase the amount of the immobilized Con A. The glycopeptides with the high mannose type glycans derived from the glycoprotein ribonuclease B were captured and preconcentrated by the emitter before they were detected by the tandem mass spectrometer. This system was expected to be useful for screening glycosylation of proteins and peptides especially by microfluidic devices [15].

Conclusions

This chapter provided an overview on the recent development and application of silica-based and organic polymer-based polar and affinity monoliths. For polar monoliths, silica-based monoliths are still in their early stages of development and need more investigation and exploration of their full potentials. Although polar polymer-based

monoliths are easier to obtain compared to the silica monoliths, they do not offer sufficient specific surface area for ensuring the required retention and selectivity for small polar molecules. To address the lack of sufficient specific surface area, hybrid type polar monoliths, which have the features of both silica and polymer functionalities have been introduced recently. They overcame the lack of polar ligands for silica-based monolith and at the same time still possessed high surface area due to the silica backbone. Although hybrid type polar monoliths seem to provide an alternative solution to the inherent relatively low specific surface area of organic polymer-based monoliths, polar organic polymer monoliths are still awaiting further development and investigations.

Both silica-based affinity monoliths and organic polymer-based affinity monoliths exhibit good permeability compared to the conventional particles packed in columns. Silica affinity monoliths distinguish themselves from the other types of monoliths for their high mechanical strength, high specific surface area and higher amount of affinity ligands immobilized. It is believed that silica-based monoliths are suitable stationary phases especially for small molecule separations, while polymer-based monoliths are appealing stationary phases due to their ease of fabrication. Finally, although affinity monoliths in general and lectin monoliths in particular have made some progress in recent years, their development is still underway and the exploitation of their full potentials is yet to come.

REFERENCES

[1] Wu, R., Hu, L. G., Wang, F. J., Ye, M. L., Zou, H., *J. Chromatogr. A* **2008**, *1184*, 369.

[2] Svec, F., *J. Sep. Sci.* **2005**, *28*, 729.

[3] Nunez, O., Nakanishi, K., Tanaka, N., *J. Chromatogr. A* **2008**, *1191*, 231.

[4] Yang, C., Ikegami, T., Hara, T., Tanaka, N., *J. Chromatogr. A* **2006**, *1130*, 175.

[5] Rieux, L., Lubda, D., Niederlander, H. A. G., Verpoorte, E., Bischoff, R., *J. Chromatogr. A* **2006**, *1120*, 165.

[6] Hara, T., Kobayashi, H., Ikegami, T., Nakanishi, K., Tanaka, N., *Anal. Chem.* **2006**, *78*, 7632.

[7] Allen, D., El Rassi, Z., *Electrophoresis* **2003**, *24*, 408.

[8] Wu, R., HU, L., Wang, F., Ye, M., Zou, H., *J. Chromatogr. A* **2008**, *1184*, 369.

[9] Xie, C., Fu, H., Hu, J., Zou, H., *Electrophoresis* **2004**, *25*, 4095.

[10] Bedair, M., El Rassi, Z., *J. Chromatogr. A* **2004**, *1044*, 177.

[11] Bedair, M., El Rassi, Z., *J. Chromatogr. A* **2005**, *1079*, 236.

[12] Okanda, F. M., El Rassi, Z., *Electrophoresis* **2007**, *28*, 89.

[13] Schaller, D., Hilder, E. F., Haddad, P. R., *J. Sep. Sci.* **2006**, *29*, 1705.

[14] Chambers, S. D., Glenn, K. M., Lucy, C. A., *J. Sep. Sci.* **2007**, *30*, 1628.

[15] Bedair, M., Oleschuk, R. D., *Analyst* **2006**, *131*, 1316.

[16] Okanda, F. M., El Rassi, Z., *Electrophoresis* **2006**, *27*, 1020.

[17] Minakuchi, H., Nakanishi, K., Soga, N., Ishizuka, N., Tanaka, N., *Anal. Chem.* **1996**, *68*, 3498.

[18] Tanaka, N., Kobayashi, H., Nakanishi, K., Nakanishi, K., Ishizuka, N., *Anal. Chem.* **2001**, 421A.

[19] Nakanishi, K., *J. Porous Material* **1997**, *4*, 67.

[20] Allen, D., El Rassi, Z., *J. Chromatogr. A* **2004**, *1029*, 239.

[21] Snyder, L. R., Kirkland, J. J., Glajch, J. L., *Practical HPLC Method Development*, John Wiley & Sons, Inc., New York **1997**.

[22] Ye, M., Zou, H., Kong, L., Lei, Z., Wu, R., Ni, J., *The Appl. Notebook* **2002**, 41.

[23] Alpert, A. J., *J. Chromatogr. A* **1990**, *499*, 177.

[24] Kobayashi, H., Smith, C., Hosoya, K., Ikegami, T., Tanaka, N., *Anal. Chem.* **2002**, *18*, 89.

[25] Fujimoto, C., *J. High Resolut. Chromatogr.* **2000**, *23*, 89.

[26] Rieux, L., Niederlander, H., Verpoorte, E., Bischoff, R., *J. Sep. Sci.* **2005**, *28*, 1628.

[27] Luo, Q., Shen, Y., Hixson, K. K., Zhao, R., Yang, F., Moore, R. J., Mottaz, H. M., Smith, R. D., *Anal. Chem.* **2005**, *77*, 5028.

[28] Zhong, H., *Polar Bonded Stationary Phases Consisting of Silica-Based Monoliths for Normal Phase Capillary Electrochromatography,* Oklahoma State University, Stillwater, **2005**, 71 pp

[29] Qin, F., Xie, C., Yu, Z., Kong, L., Ye, M., Zou, H., *J. Sep. Sci.* **2006**, *29*, 1332.

[30] Ikegami, T., Fujita, H., Horie, K., Hosoya, K., Tanaka, N., *Anal. Bioanal. Chem.* **2006**, *386*, 578.

[31] Ikegami, T., Horie, K., Jaafar, J., Hosoya, K., Tanaka, N., *J. Biochem. Biophys. Methods* **2007**, *70*, 31.

[32] Horie, K., Ikegami, T., Hosoya, K., Saad, N., Fiehn, O., Tanaka, N., *J. Chromatogr. A* **2007**, *1164*, 198.

[33] Ye, F., Xie, Z., Wong, K., *Electrophoresis* **2006**, *27*, 3373.

[34] Nogueira, R., Lubda, D., Leitner, A., Bicker, W., Maier, N. M., Lammerhofer, M., Lindner, W., *J. Sep. Sci.* **2006**, *29*, 966.

[35] Ding, G., Da, Z., Yuan, Z., J.J., B., *Electrophoresis* **2006**, *27*, 3363.

[36] Zhong, H., El Rassi, Z., *J. Sep. Sci.* **2006**, *29*, 2031.

[37] Ishizuka, N., Miakuchi, H., NIakanishi, K., Soga, N., Nagayama, H., Hosoya, K., *Anal. Chem.* **2000**, *72*, 1275.

[38] Zhong, H., El Rassi, Z., *J. Sep. Sci.* **2006**, *29*, 2023.

[39] Mallik, R., Xuan, H., Hage, D. S., *J. Chromatogr. A* **2007**, *1149*, 294.

[40] Mallik, R., Hage, D. S., *J. Pharm. Biomed. Anal.* **2008**, *46*, 820.

[41] Hodgson, R. J., Chen, Y., Zhang, Z., Tleugabulova, D., Long, H., Zhao, X., Organ, M., Brook, M. A., Brennan, J. D., *Anal. Chem.* **2004**, *76*, 2780.

[42] Besanger, T. R., Hodgson, R. J., Guillon, D., Brennan, J. D., *Anal. Chimi. Acta* **2006**, *561*, 107.

[43] Lebert, J. M., Forsberg, E. M., Brennan, J. D., *Biochem. Cell Biol.* **2008**, *86*, 100.

[44] Svec, F., *Electrophoresis* **2006**, *27*, 947.

[45] Josic, D., Buchacher, A., *J. Biochem. Biophys. Methods* **2001**, *49*, 153.

[46] Honda, S., Suzuki, S., Nitta, T., Kakehi, K., *J. Chromatogr.* **1988**, *438*, 73.

[47] Madera, M., Mechref, Y., Klouckova, I., Novotny, M. V., *J. Chromatogr. B* **2007**, *845*, 121.

[48] Madera, M., Mechref, Y., Novotny, M. V., *Anal. Chem.* **2005**, *77*, 4081.

[49] Xiong, L., Andrews, D., Regnier, F., *J. Proteome Res.* **2003**, *2*, 618.

[50] Cartellieri, S., Hamer, O., Helmholz, H., Niemeyer, B., *Biotechnol. Appl. Biochem.* **2002**, *35*, 83.

[51] Su, X., HU, L., Kong, L., Lei, X., Zou, H., *J. Chromatogr. A* **2007**, *1154*, 132.

[52] Okanda, F. M., El Rassi, Z., *Electrophoresis* **2005**, *26*, 1988.

[53] Yan, W., Zhang, Z., Gao, R., Yan, C., Wang, J., *J. Liq. Chromatogr. Rel. Tech.* **2002**, *25*, 2965.

[54] Huang, X., Wang, Q., Yan, H., *J. Chromatogr. A* **2005**, *1062*, 183.

[55] Umemura, T., Ueki, Y., Tsunoda, K., Katakai, M., Tamada, M., Harguchi, H., *Anal. Bioanal. Chem.* **2006**, *386*, 566.

[56] Trojer, L., Lubbad, S. H., Bisjac, C. P., Wieder, W., Bonn, G. K., *J. Chromatogr. A* **2007**, *1146*, 216.

[57] Holdsvendova, P., Suchankova, J., Buncek, M., Backovska, V., Coufal, P., *J. Biochem. Biophys. Methods* **2007**, *70*, 23.

[58] Que, A. H., Novotny, M. V., *Anal. Bioanal. Chem.* **2003**, *375*, 599.

[59] Que, A. H., Konse, T., Baker, A. G., Novotny, M. V., *Anal. Chem.* **2000**, *72*, 2703.

[60] Dong, C., DOng, J., Qu, J., Zhu, Y., Zou, H., *Electrophoresis* **2006**, *27*, 2518.

[61] Fu, H., Xie, C., Dong, J., Huang, X., Zou, H., *Anal. Chem.* **2004**, *76*, 4866.

[62] Hahn, R., Jungbauer, A., *Anal. Chem.* **2000**, *72*, 4853.

[63] Jmeian, Y., El Rassi, Z., *J. Proteome Res.* **2007**, *6*, 947.

[64] Jiang, T., Mallik, R., Hage, D. S., *Anal. Chem.* **2005**, *77*, 2362.

[65] Pan, Z., Zou, H., Mo, W., Huang, X., Wu, R., *Anal. Chim. Acta* **2002**, *466*, 141.

[66] Berruex, L. G., Freitag, R., Tennikova, T. B., *J. Pharm. Biomed. Anal.* **2000**, *24*, 95.

[67] Armenta, J. M., Gu, B., Humble, P. H., Thulin, C. D., Lee, M. L., *J. Chromatogr. A* **2005**, *1097*, 171.

[68] Armenta, J. M., Gu, B., Thulin, C. D., Lee, M. L., *J. Chromatogr. A* **2007**, *1148*, 115.

[69] Luo, Q., Zou, H., Xiao, H., Guo, Z., *J. Chromatogr. A* **2001**, *926*, 255.

[70] Vizioli, N. M., Rusell, M. L., Carbajal, M. L., Carducci, C. N., Grasselli, M., *Electrophoresis* **2005**, *26*, 2942.

[71] Tetala, K. K. R., Chen, B., Visser, G. M., van Beek, T. A., *J. Sep. Sci.* **2007**, *30*, 2828.

[72] Zhao, Q., Li, X., X.C., L., *Anal. Chem.* **2008**, *80*, 3915.

[73] Mao, X., Luo, Y., Dai, Z., Wang, K., Du, Y., Lin, B., *Anal. Chem.* **2004**, *76*, 6941.

CHAPTER III

DEVELOPMENT OF NOVEL POLAR SILICA-BASED MONOLITHIC COLUMNS FOR NORMAL PHASE NANO LIQUID CHROMATOGRAPHY AND ELECTROCHROMATOGRAPHY OF POLAR SPECIES INCLUDING GLYCANS

Introduction

Monolithic columns are characterized by a bimodal pore morphology consisting of macropores (or wide channels for mobile phase flow) and mesopores (or domains of relatively narrow pores providing most of solute adsorption capacity onto the column). This bimodal porous structure within the monolith has direct effects on the specific surface area and permeability of the monolithic column. A previous study has shown that the column separation efficiency is affected firstly by the ratio of the silica monomer to the porogen and the solvent and secondly by the subsequent mesopore treatment by ammonium hydroxide [1]. This study has further investigated these factors that affect the column separation efficiency in order to gain more insight into the underlying phenomena.

Silica-based monoliths can be subjected to surface modification in the aim of attaching a given chromatographic ligand for providing the proper retention mechanism for separating particular compounds. One surface modification process that is reported in this chapter involves the conversion of silica-based monoliths into polar stationary phases for normal phase chromatography (NPC) of polar compounds including glycans (i.e., the sugar chains attached to proteins). It consistes of the covalent attachment of polar ligands to the surface of the silica monolith. As discussed in Chapter II, RPLC has a shortcoming as far as the separation of polar analytes such as glycans is concerned due to the weak interaction of the solute with the nonpolar stationary phase [2]. In addition, only a limited amount of work has been reported so far on silica-based monolithic columns for NPC [2-5]. Thus, further investigation in this area is in order.

Glycosylation is an important posttranslational modification of proteins. Glycans play important biological roles in the functions of glycoproteins. Many diseases are associated with aberrant glycosylation or systems failing to recognize carbohydrates. For example, diabetes results in chemical glycation of proteins, glycosyltransferase abnormal expression leads to blood clotting defect, IgG glycosylation alteration causes rheumatoid arthritis and glycosylation changes are correlated with cancer, etc [6]. In this regards, glycans are recognized as the biomarkers of some diseases [6]. Therefore, there exists the urgency and necessity for improved separation technology for glycans.

With a few exceptions, there are two types of glycosidic link in proteins: (i) an *N*-glycosidic link, which contains *N*-acetylglucosamine (GlcNAc) linked *via* the amide nitrogen of an asparagine (Asn) residue yielding the so called *N*-glycans and (ii) an *O*-glycosidic link *via* the reducing end of an *N*-acetylgalactosamine (GalNAc) residue in a

linkage to the hydroxyl group of serine (Ser) or threonine (Thr) and to a lesser extent tyrosine, hydroxy-lysine or hydroxyproline yielding the so called *O*-glycans. This type of glycans is also called "mucin-type".

Most *O*-glycans are short chains and can remain as a monosaccharide, but often a complex structure is built by stepwise addition of monosaccharides such as fucose (Fuc), galactose (Gal), *N*-acetylneuraminic, *N*-glycolylneuraminic acid, 2-keto-3-deoxynonulosonic acid and glucuronic acid. *O*-Glycans can also contain sulfate and phosphate residues. Mannose (Man) and glucose have been found as components of the mucin-type *O*-glycans, but they are not common [7]. In the larger mucin-type *O*-glycan chains three domains can be distinguished. These are a core, a backbone and a peripheral region (see Figure 1A). At least nine core classes have been described for mucin-type *O*-glycans [7].

Structures of *N*-glycans fall into three types: high mannose-type, complex-type and hybrid-type (Figure 1B). They share the common core structure Manα1–3(Manα1–6) Manβ1–4GlcNAcβ1–4GlcNAc, but differ in their outer branches or antennae. High mannose glycans have 2 to 6 additional α-Man linked to the core structure. Typical complex glycans contain 2 to 4 outer branches with sialyllactosamine sequence. Hybrid structures have the features of both high mannose-type and complex-type glycans and most of them contain bisecting GlcNAc that is linked β1–4 to the β-linked Man residue of the core structure. In addition, a type of carbohydrate chain, called poly-*N*-acetyllactosamine-type, has been described [8, 9] whose outer branches have a characteristic structure composed of *N*-acetyllactosamine repeating units.

(A) *O*-Glycans

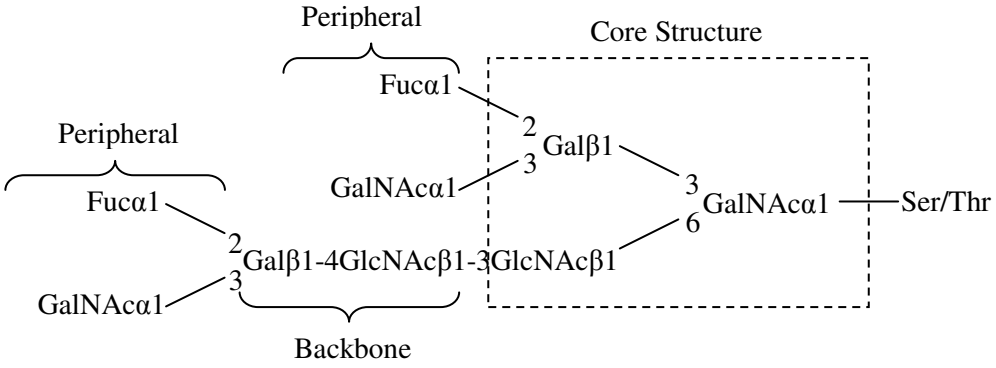

(B) *N*-Glycans

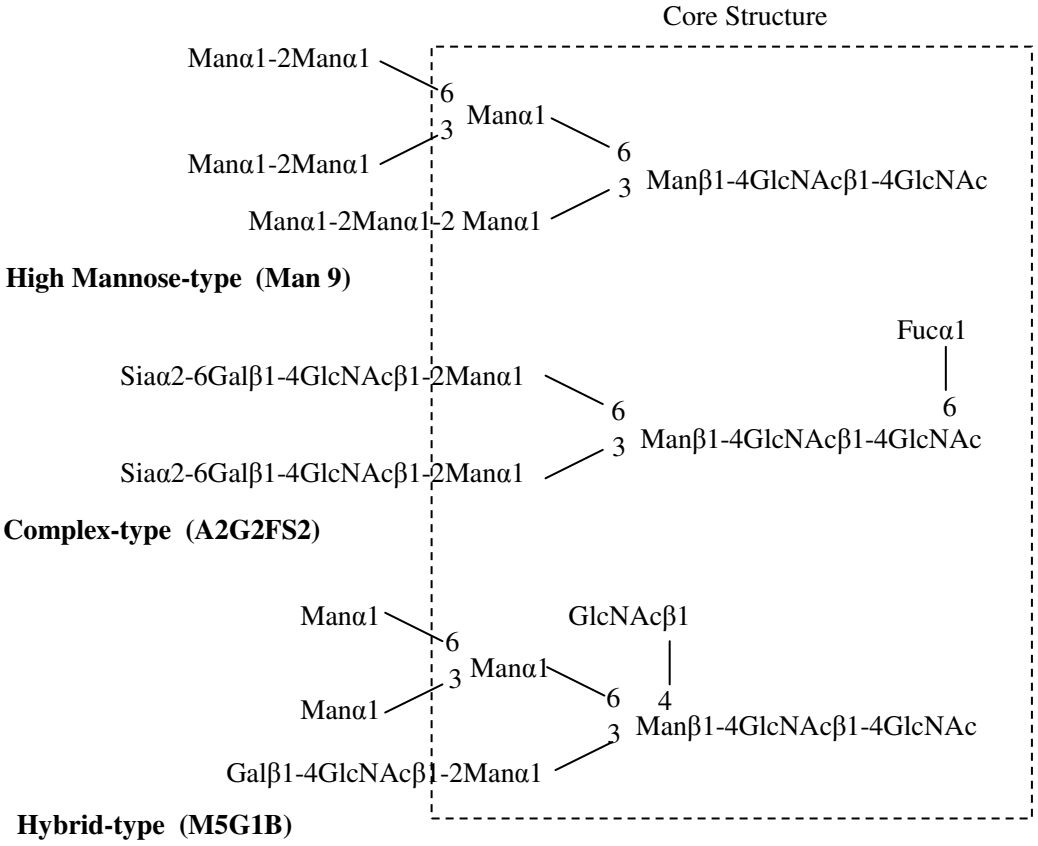

Figure 1. *(A) Example of an O-glycan structure. (B) Typical structures and designations of N-glycans. Nomenclature for describing N-glycan structures: A(1,2,3,4) indicates the number of antennae linked to the trimannosyl core; G(0-4) indicates the number of terminal galactose (Gal) residues; F, core fucose (Fuc); B, bisecting N-acetylglucosamine (GlcNAc); S, sialic acid (Sia), M, mannose (Man).*

Protein glycosylation can occur at more than one position in the amino acid sequence, and the glycans at even a single position may be heterogeneous or may be missing from some molecules. This leads to populations of glycosylated variants of a single protein, called glycoforms [10]. The relative proportions of glycoforms are found to be reproducible, not random, and depend mainly on the environment in which the protein is glycosylated [11].

Carbohydrate separations have been studied extensively using CE [12-15] and to a lesser extent CEC [16]. Also, different modes of HPLC have been used in carbohydrate analysis [14, 15] including RP-HPLC [17-19], NP-HPLC [20, 21], graphitized carbon column technology [22, 23], ion-exchange HPLC [21, 24], size exclusion chromatography [25, 26] and affinity chromatography [27]. However, the separation of glycans by NP-HPLC and NP-CEC using monolithic column technology has not been fully developed yet and there still exists ample room for further improvement (for detailed discussion and background, see Chapter II). This study investigated the separation and retention behaviors of glycans on novel polar monolithic columns. In this regard, the previously developed cyano silica-based monolith (referred to as 2CN-OH monolith) [28] is further exploited in this investigation for the separation of glycans.

Experimental

Instrumentation

The instruments used were a P/ACE 5010 capillary electrophoresis system from Beckman Instruments (Fullerton, CA, USA) equipped with a UV detector and a data handling system comprised of an IBM personal computer and P/ACE Station software, and an HP^{3D}CE system from Hewlett-Packard (Waldbornn, Germany) equipped with a photodiode array detector. A Sigma 3 Gas Chromatograph from Perkin-Elmer (Norwalk, CT, USA) was employed for temperature programming. An Isotemp refrigerated circulator (Model 910) for heat treatment and an Isotemp oven (Model 615G) for incubations were from Fisher Scientific (Fair Lawn, NJ, USA). The dry-bath for derivatization of saccharides was the Thermolyne Type 17600 (Dubuque, IA, USA). The SpeedVac SC 110 was from Savant Instruments, Inc. (Holbrook, NY, USA).

Reagents and Materials

Fused silica capillaries (100 μm I.D. and 375 μm O.D.) were from Polymicro Technologies (Phoenix, AZ, USA). Poly(ethylene glycol) (PEG) and tetramethylorthosilicate (TMOS) were from Aldrich Chemical Co., Inc (Milwaukee, WI, USA). Hydrochloric acid, sulfuric acid, toluene and acetonitrile (ACN) were from Fisher Scientific (Fair Lawn, NJ, USA). PNGase F (or N-glycosidase F) and avidin were from EMD Biosciences, Inc. (La Jolla, CA, USA). γ-Glycidoxypropyltrimethoxysilane was

from Hüls America Inc. (Bristol, PA, USA). Acetic acid (HAc) was from EM science (Gibbstown, NJ, USA). 1*H*-Imidazole-4,5-dicarbonitrile was from Nippon Soda Co. LTD (Chiyoda-ku, Tokyo, Japan). Glycoclean^{TM} R Cartridge and Glycoclean^{TM} S Cartridge were from Prozyme (San Leandro, CA, USA). Ovalbumin, human α_1-acid glycoprotein and human transferrin were from Sigma-Aldrich Fine Chemicals (St. Louis, MO, USA).

Silica Monolith Fabrication

The method to fabricate the silica-based monolith is similar to the previously published one [28-30]. The inner wall of the fused-silica capillary (37 cm × 100 μm ID) was treated with a 1.0 M sodium hydroxide solution for 30 min followed by a 0.2 M hydrochloric acid solution for 30 min. The capillary was then rinsed with water and dried with helium. A 198.8 mg of PEG was dissolved in 1250 μL of 0.01 M acetic acid and the solution obtained was incubated with stirring at 0 °C for 10 min. A 1250 μL of TMOS was added and mixed with the solution. The mixture was stirred at 0 °C for 45 min, then injected into the pretreated capillary leaving 13 cm at one end empty. The inlet and the outlet ends were connected with a piece of Teflon tubing. The capillary was kept in an Isotemp refrigerated circulator previously set at 40 °C for 14 h. The resulting siliceous monolith was rinsed with water followed by a 0.01 M ammonium hydroxide solution and was incubated in an oven at a temperature of 120 °C for 1 h. The capillary was washed with water followed by ethanol and dried with helium. Finally, it was subjected to a gradient heating treatment in a GC oven with an initial temperature of 30 °C for 2 min followed by 180 °C for 1 h and finally 330 °C for 20 h.

Introduction of Polar Functionalities to the Surface of the Silica Monolith

The method for ligand attachment to the surface of the silica monolith is similar to the previously published method [28-30]. A solution containing γ-glycidoxypropyltrimethoxysilane in toluene (1:10 v/v) was introduced into the monolith prepared as described in the previous section, which was later put in an oven set at 110 °C for 2 h. This procedure was repeated three times. The column was rinsed with toluene, DMF, H_2O before a solution containing 0.1 M 1*H*-imidazole-4,5-dicarbonitrile (pH 7.0) was pushed into the monolithic capillary column. The column thus filled with 1*H*-imidazole-4,5-dicarbonitrile was incubated at 70 °C for 14 h. This step was repeated three times. The column was rinsed with water and the detection window was made 13 cm from the outlet end by dissolving the polyimide coating with a fuming sulfuric acid. The ends of the column were then cut to have an 8-cm length from detection window to the outlet and 25-cm length from detection window to the inlet.

Specific Surface Area Measurement by BET

The surface area of the monolith was measured by a Quantachrome Nova 1200 instrument using a conventional BET (Brunauer-Emmet-Teller) multilayer nitrogen adsorption method. Briefly, a 0.100-g sample was weighed and put in a tube that was later heated and degassed overnight to remove water, other solvent or impurities. The mass of the sample was measured before the tube was placed back into the instrument for

surface area measurement with nitrogen as the adsorbent at 77 K. The specific surface area was calculated by the B.E.T. equation.

Preparation of Glycans

The PNGase F was employed to catalyze the hydrolysis of asparagine-linked high-mannose, hybrid and complex oligosaccharides from glycoproteins [31, 32]. Glycoprotein of 2 mg was added to an Eppendorf tube, to which a 350 µl of deionized water was added to dissolve all of the protein. Then 100 µL of 0.05 M dibasic sodium phosphate aqueous solution, pH 7.5, and 25 µL of a denaturation buffer containing 1 M β-mercaptoethanol and 2% (w/w) sodium dodecyl sulfate (SDS) were added to the Eppendorf tube. The solution obtained was mixed by a Vortex before it was subjected to heat treatment at 100 °C for 5 min. After the tube was cooled down to room temperature, 8.5 mg of octylglucopyranoside was added followed by 4 µL of PNGase F. The mixture was then incubated at 37 °C for 16 h. A Glycoclean^{TM} R Cartridge was used to remove the protein, peptides and detergent. The resulting glycans were subjected to a derivatization with 2-aminobenzamide (2-AB) (see next section) at 72 °C for 24 h. The excess 2-AB was removed by a Glycoclean^{TM} S Cartridge. The eluent from the Glycoclean^{TM} S Cartridge was then concentrated by a SpeedVac to obtain a final volume of 200 µL (see Fig. 2).

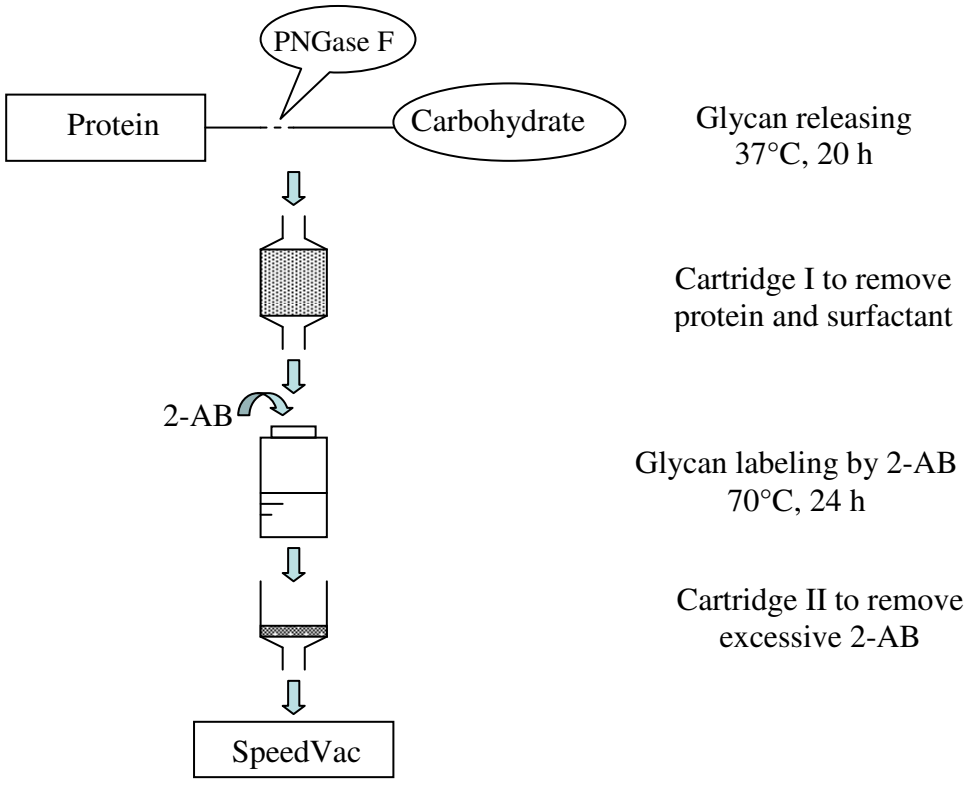

Figure 2. *Major steps involved in the preparation of N-glycans from glycoproteins.*

Derivatization of Carbohydrates with 2-AB

The 2-AB derivatization was performed according to a previously published reductive amination procedure [33-35]. Briefly, 200 µL of 0.25 M 2-AB in 1:1 water:methanol pH 5.0 (adjusted with acetic acid) was added and mixed with 30 µl of 1.0 M $NaBH_3CN$ in a 1.0 mL reaction vial. A 40 µL of 1.4 M aqueous saccharide solution or 50 µL concentrated glycan solution were then added to the vial and mixed well. The vials were sealed and put in a dry-bath, which was previously set at 72 °C. The derivatization reaction was allowed to proceed for 24 h. Figure 3 shows an example of the derivatization reaction between 2-AB and glucose as a typical reducing saccharide.

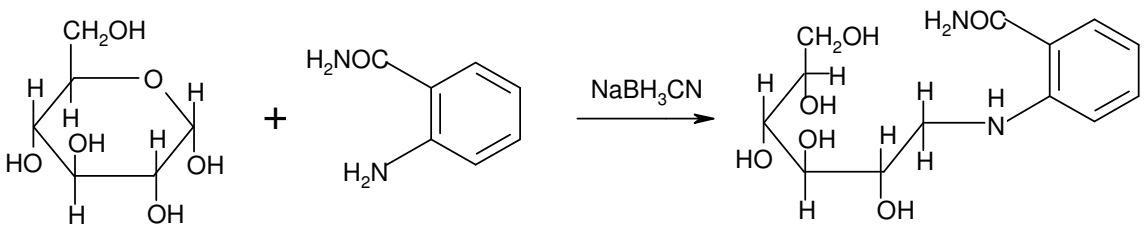

Figure 3. *Schematic of carbohydrate derivatization with 2-AB.*

Results and Discussion

Effect of Composition of Polymer Precursors and Mesopore Treatment on Silica Monolithic Column Performance

In our previous studies [1, 28, 33], it was found that the ratio of TMOS, PEG and solvent water affected the pore morphology of the monolith to a great extent. Also, the treatment time and temperature of the ammonium hydroxide to make mesopores along the monolithic piece had an effect on the surface area and thus affected the column separation efficiency.

Since silica can be dissolved by basic solution, ammonium hydroxide was usually employed to generate mesopores. In our experiment, with the treatment of ammonium hydroxide at 120 °C for 1 h, the surface area of the silica monolith was increased from 784 m^2/g to 840 m^2/g. Monolith with TMOS/PEG/HAc (3.750mL/0.3978g/11.250mL) has a surface area of 910 m^2/g, while the surface area of the monolith with TMOS/PEG/HAc (5.178mL/0.3978g/11.250mL) was 840 m^2/g. The reason for the decrease in the specific surface area with increasing the percentage of TMOS might be due to fewer macropores produced due to the high density of TMOS [36, 37]. Table 1

shows how the column performance changes with the changes of the TMOS/PEG/H_2O ratio as well as the concentrations and treatment time of ammonium hydroxide. The column performance was evaluated by a test sample mixture containing toluene, DMF, formamide and thiourea.

TABLE 1.

EFFECTS OF RATIO OF TMOS/PEG/H_2O AND CONCENTRATION AND TREATMENT TIME OF NH_4OH ON COLUMN PERFORMANCE

	TMOS/PEG/H_2O (g/g/ml)	NH_4OH Morality	Time	EOF (cm/min)	k'_{DMF}	$k'_{formamide}$	$k'_{thiourea}$
1	0.863/0.1989/1.875	0.01 M	1 h	5.04	0.102	0.210	0.301
2	0.863/0.1989/1.875	0.01 M	2 h	7.28	0.0910	0.200	0.301
3	0.937/0.1989/1.875	0.01 M	1 h	3.30	0.103	0.229	0.373
4	0.937/0.1989/1.875	0.01 M	2 h	4.71	0.0474	0.0994	0.162
5	0.937/0.1989/1.875	0.05 M	2 h	4.50	0.0900	0.169	0.223
6	0.937/0.2037/1.875	0.01 M	2 h	3.98	0.0632	0.142	0.234
7	0.937/0.2037/1.875	0.05 M	2 h	4.95	0.0920	0.202	0.307

Conditions: silica monolithic capillary column, 20/27 cm × 100 μm ID; mobile phase, hydroorganic solution made up of 5% v/v of 5 mM NH_4Ac (pH 6) and 95% v/v ACN; voltage, 20 kV; column temperature, 20 °C.

The monolith with TMOS/PEG/H_2O at 0.937g/0.1989g/1.875mL and treatment of ammonium hydroxide at 0.1 M for 2 h had a higher EOF of 4.76 cm/min, and a lower retention factor (k') of 0.249 for thiourea, compared to that under the treatment of ammonium hydroxide at 0.05 M for 2 h where the EOF was 4.41 cm/min and the k' of thiourea was 0.291. This indicates that the mesopores are easier to grow bigger and

finally into macropores with the high concentration of ammonium hydroxide [29]. The investigation also found that the percentage of PEG affected column performance.

Monolith 2 had a relatively high EOF of 7.28 cm/min after the mesopore treatment time with ammonium hydroxide was increased from 1 h to 2 h. This shows that the channels grew wider with treatment time and as a result the column had a higher EOF velocity. When the content of TMOS was increased from 0.863 g (Monolith 2) to 0.937 g (Monolith 4), the monolith became denser and this could lead to fewer macropores and smaller specific surface area as well, which was indicated by the lower EOF (4.71 cm/min) and retention factor. As the concentration of the ammonium hydroxide was increased from 0.01 M (Monolith 4) to 0.05 M (Monolith 5), more mesopores were generated and this resulted in higher retention factors and a slight decrease in EOF. Higher PEG percentage helped to produce more macropores and therefore the Monolith 6 had a higher EOF and lower retention factors than the monolith made using less PEG (Monolith 3).

Glycan Mapping by Capillary Electrophoresis

Capillary electrophoresis (CE) was used as a well-established separation process to monitor the cleavage of glycans from glycoproteins and their subsequent derivatization with 2-AB. The 2-AB-derivatized glycans were derived from ovalbumin, α_1-acid glycoprotein, transferrin and avidin by the method described in the Experimental section.

The identification of the 2-AB-derivatized glycans was based on the UV spectrum identification that the CE instrument produces in real time *via* its diode array detector

(DAD). Figure 4 shows the UV spectra of 2-AB and the 2-AB-derivatized maltose. The standard maltose was selected as a typical saccharide that may mimic the behavior of some of the neutral glycans as far as the characteristic of their UV spectra are concerned. Free 2-AB label exhibited a spectrum in DAD that had three maximum absorbance wavelengths (λ_{max}) at 210 nm, 245 nm and 320 nm while the 2-AB-derivatized maltose yielded a DAD spectrum with λ_{max} at 220 nm, 255 nm and 340 nm. The shift of the λ_{max} shows that the specific absorbance wavelength of the 2-AB had a red shift when it was attached to the reducing end of the maltose. The set of three λ_{max} values (i.e., 220 nm, 255 nm and 340 nm or a higher number set) was used to identify the existence of the glycans in the CE and CEC profiles of the 2-AB derivatized glycans.

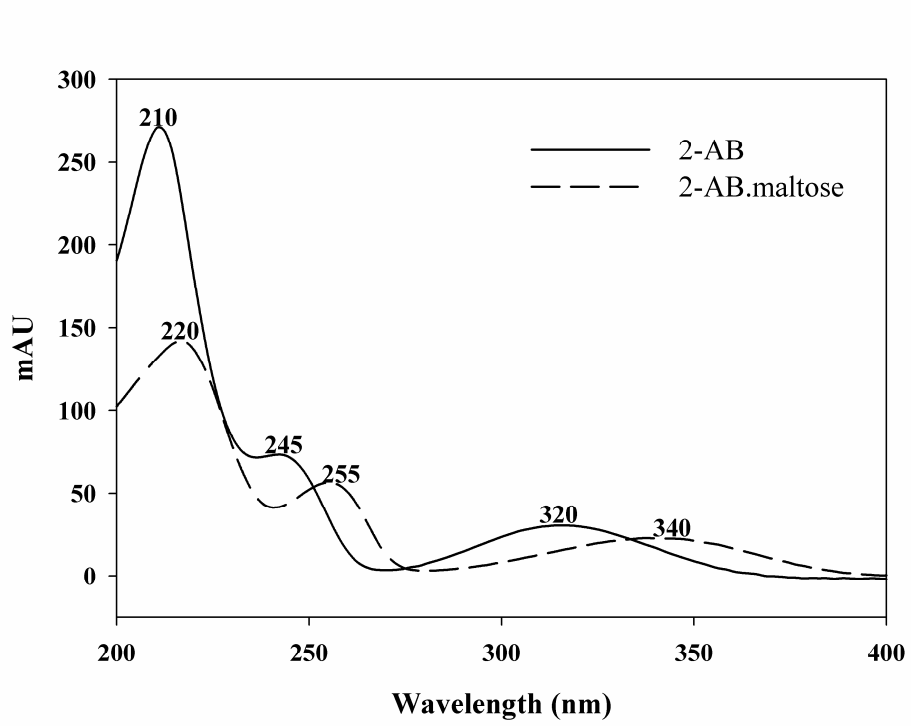

Figure 4. *UV Spectra of 2-AB and 2-AB-maltose obtained by the DAD of the CE/CEC/nano-LC instrument used in this study.*

Figures 5 to 8 show the CE profiles of the 2-AB-derivatized glycans derived from each glycoprotein using an open capillary with a running electrolyte solution containing 0.05 M borate at pH 9.5. Figure 5b and Figure 6b show the *N*-glycans derived from the ovalbumin and the α_1-acid glycoprotein separated by an open tube without the addition of borate. As can be seen in Figure 5b and Figure 6b, in the absence of borate, the 2-AB derivatized glycans migrate with little or no separation. Therefore, it was necessary to add borate to the running electrolyte solution in order to transform the neutral or slightly charged 2-AB glycans into charged complexes through the well-known complexation between the polyols of the carbohydrates and the hydroxyl groups of the tetrahydroxy borate anion [$B(OH)_4^-$] at alkaline pH and thus to improve separation [38].

Figure 5a shows the CE profile of the 2-AB-derivatized *N*-glycans derived from ovalbumin using borate as the running electrolyte at alkaline pH. Ovalbumin is a glycoprotein found in egg white with a molecular weight of 45 kDa and pI of 4.7. Its glycans account for 4% of the total glycoprotein weight and they are high mannose type and hybrid type *N*-glycans that share the same glycosylation site at Asn (asparagine) -292. The structures of these known major *N*-glycans are listed in Table 2 [39]. As can be seen in Table 2, there are at least 8 known glycan structures that have 7 to 11 monosaccharide residues. Due to steric hindrance, the sugar residues most likely to complex with tetrahydoxyborate ions are those residues that are peripheral at the non-reducing end. GlcNAc does not complex as strongly with borate as mannose [38], and therefore the hybrid type *N*-glycans are thought to have lower charge-to-mass ratio than the high mannose type *N*-glycans, and consequently, the former *N*-glycans may have

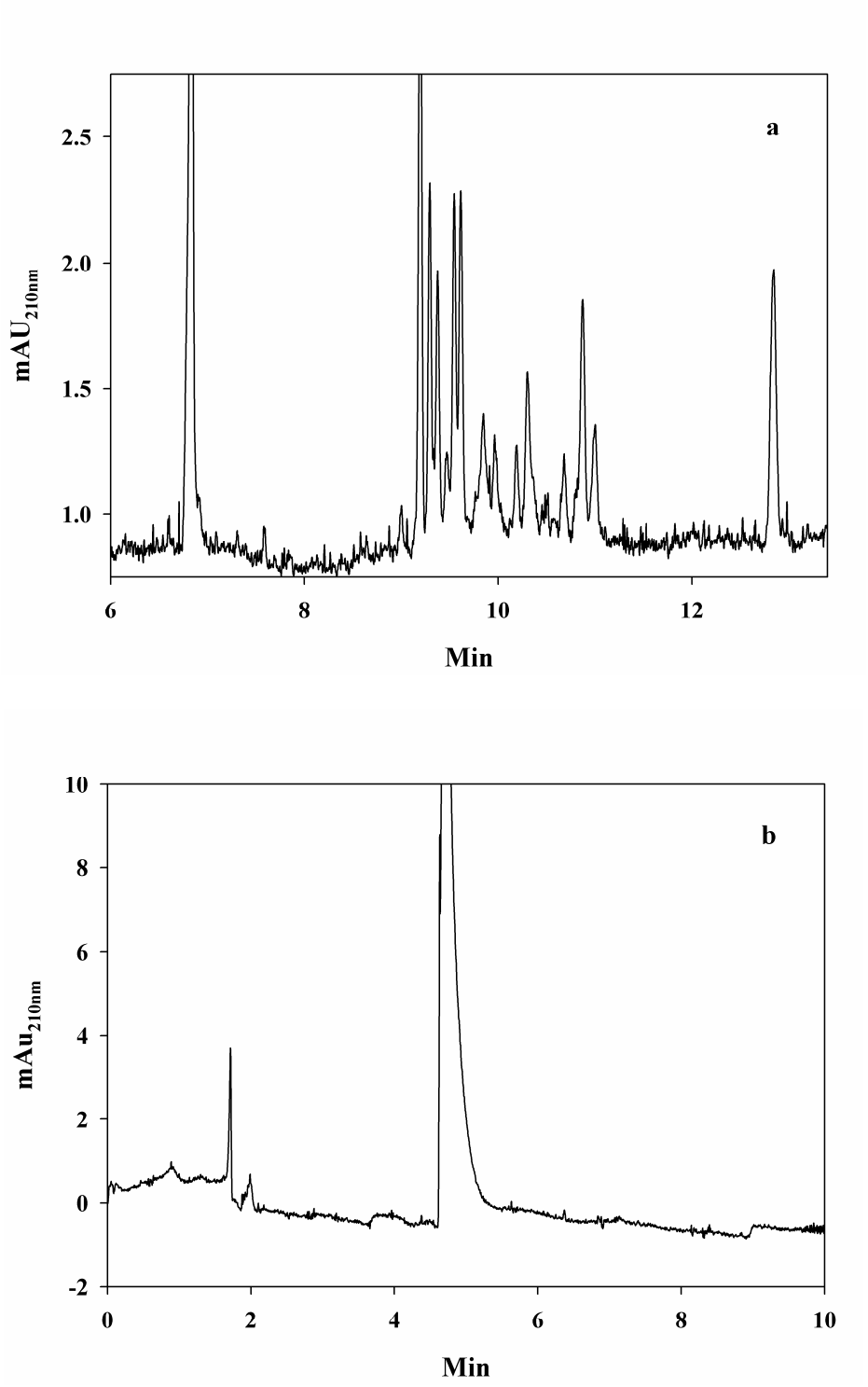

Figure 5. *Electropherograms of 2-AB-derivatized N-glycans derived from ovalbumin. Conditions: open tube, 50/58 cm×50 µm ID; voltage, 20 kV; column temperature, 20 °C; running electrolyte solution, (a) 0.05M borate, pH 9.5, (b) 0.001 M NH_4Ac, pH 6.*

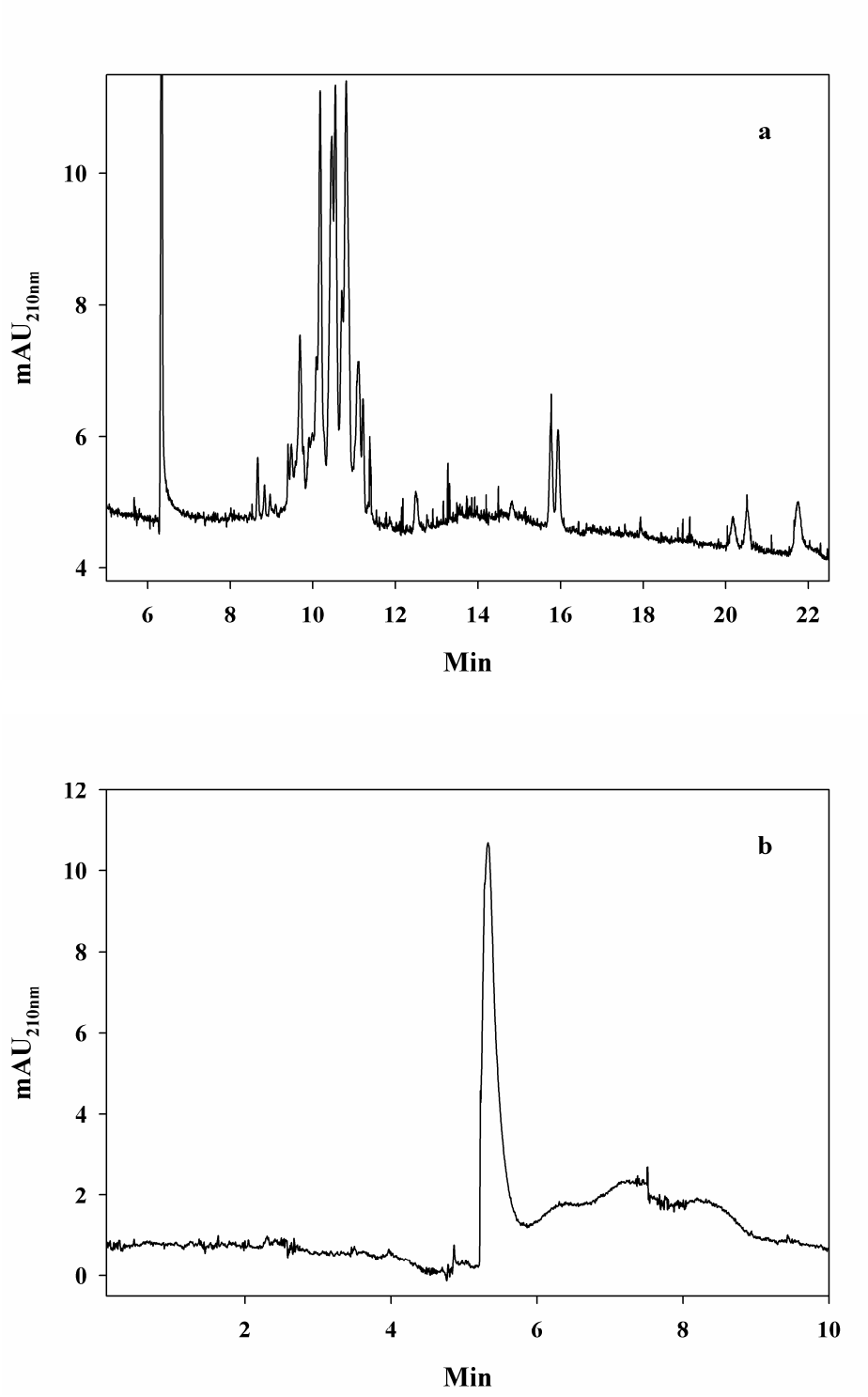

Figure 6. *Electropherograms of 2-AB-derivatized N-glycans derived from α_1-acid glycoprotein. Conditions are the same as in Figure 5.*

TABLE 2.

MAJOR *N*-GLYCANS DERIVED FROM OVALBUMIN [39]

(1)

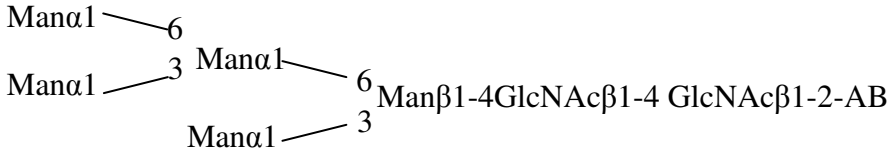

(2)

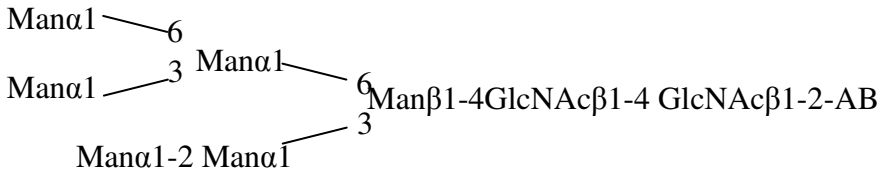

(3)

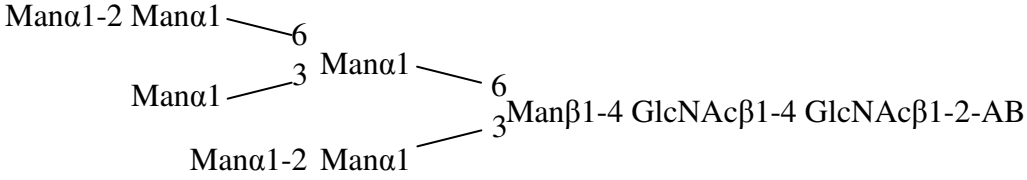

(4)

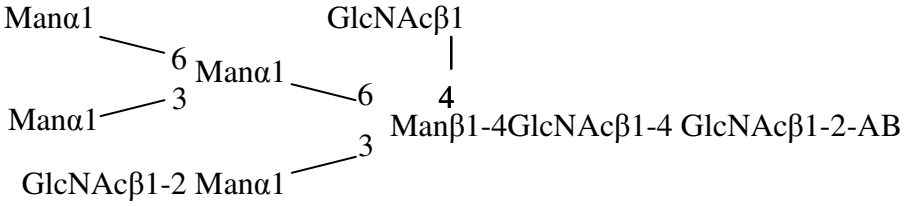

(5)

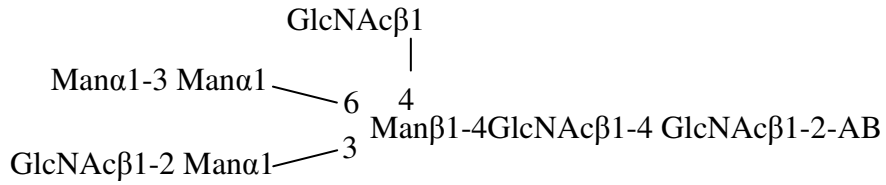

(6)

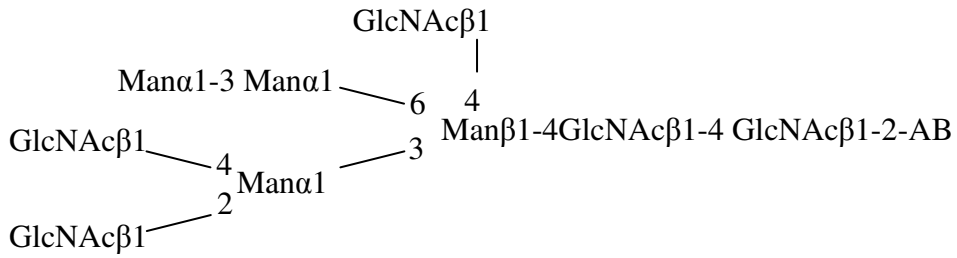

(7)

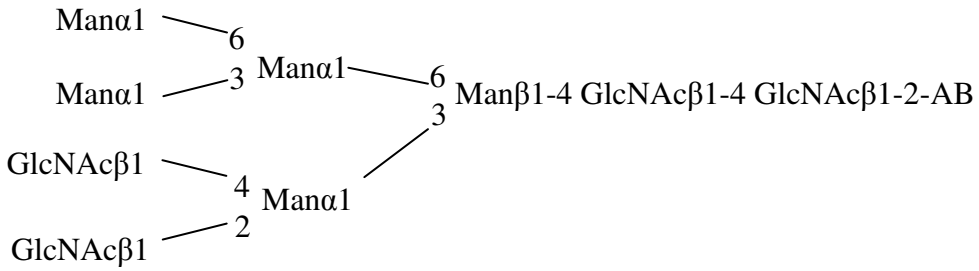

(8)

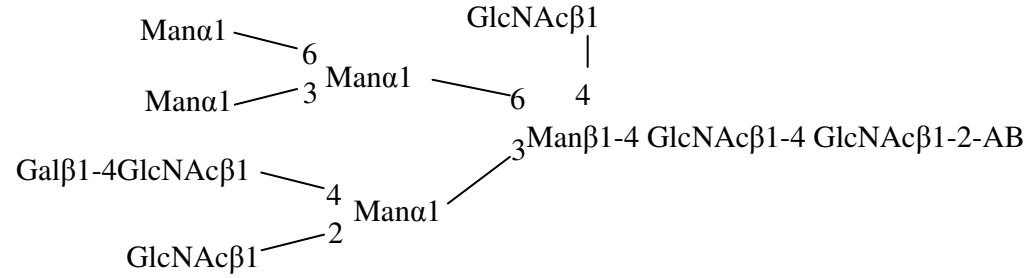

---

been the glycans that migrate first in the 8.5 – 10 min time interval whereas the latter *N*-glycans (i.e., high mannose type *N*-glycans) are those that migrate in the time interval 10.5-13.5 min. Most likely the last migrating peak in Figure 5a is that of structure 1 (or Man 6) in Table 2 due to its highest charge-to-mass ratio.

To gain insight into the nature of the migrating peaks, the DAD spectra of the peaks eluting in time interval 8.5 – 10 min displayed some of the characteristics of the 2-AB maltose with an additional band at 210 nm running on a somewhat steep slope. This may be the contribution of the presence of GlcNAc residues in the hybrid type *N*-glycans

[40]. On the other hand, the late migrating peaks in the time interval of 10.5 to 13.0 min have more or less the same characteristic absorbance than 2-AB maltose spectra with λ_{max} at 215 nm, 250 nm and 340-350 nm. These peaks are believed to belong to the high mannose type *N*-glycans.

α_1-Acid glycoprotein is one of the most important and also best-characterized plasma glycoproteins. α_1-Acid glycoprotein contains about 40% carbohydrates, most of which are sialylated. The glycosylation sites were found to be at Asn-15, Asn-38, Asn-54, Asn-75 and Asn-85. To these five glycosylation sites various complex di-, tri- and tetraantennary glycans are usually attached and the structures of these N-glycans are listed in Table 3 [41, 42].

Figure 6a shows the CE profile of the *N*-glycans derived from α_1-acid glycoprotein where one can see several peaks migrating over a very narrow time interval between 9 and 11 min, and some other minor peaks migrating over a wide time interval between 11.5 and 22 min. Examining the DAD spectra of the major peaks revealed UV characteristics that combine those of 2-AB and GlcNAc/sialic acid [43] with λ_{max} at ~210 nm, ~220 nm, ~255 nm and 340-350 nm.

Transferrin is a serum glycoprotein for iron ion delivery. It has a molecular weight of ~ 80 kDa and a pI of ~ 6. Human transferrin is composed of about 6% carbohydrates. The structures of the known *N*-glycans are listed in Table 4. The di-, tri-, or tetraantennary glycans of the *N*-acetyllactosamine type are attached to the two glycosylation sites, i.e., Asn-413 and Asn-611 [44]. Figure 7 shows the CE profile of the sialylated glycans form transferrin. Again, the DAD spectra show UV characteristics for *N*-glycans that are believed to be sialylated at different degree with λ_{max} at ~208 nm,

TABLE 3.

MAJOR *N*-GLYCANS DERIVED FROM α_1-ACID GLYCOPROTEIN [41, 42]

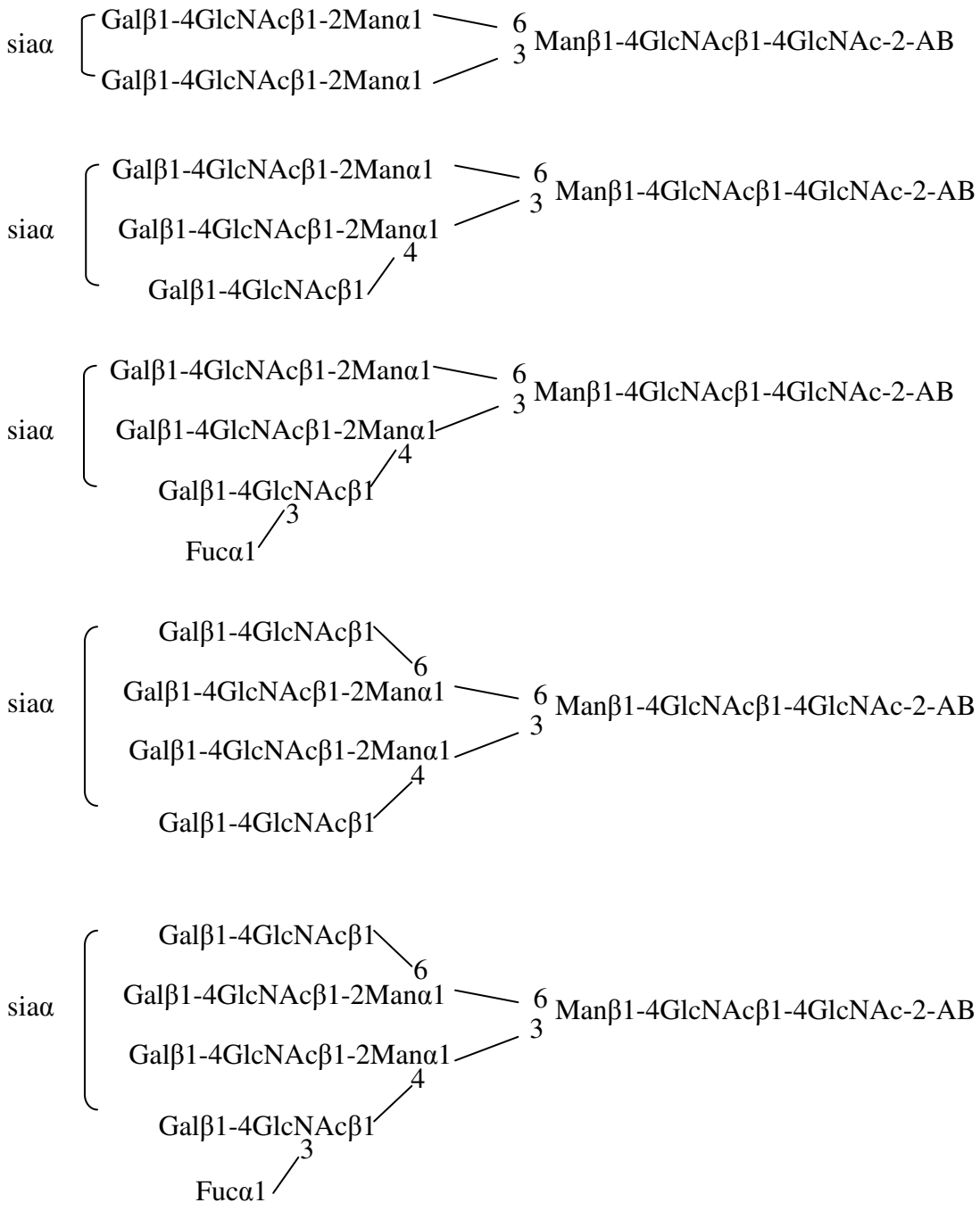

TABLE 4.

MAJOR N-GLYCANS DERIVED FROM TRANSFERRIN [45]

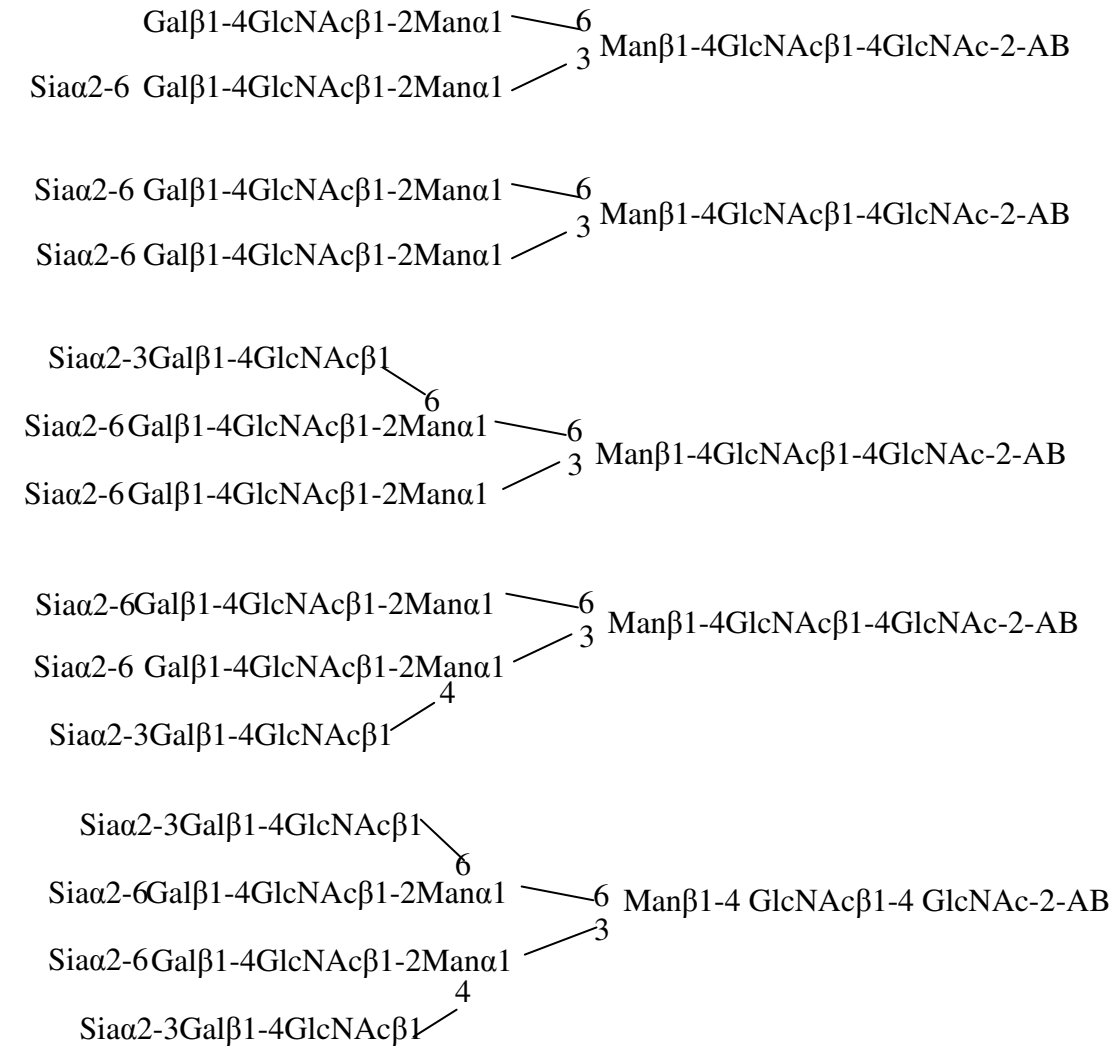

~215 nm, ~240 nm and 300-320 nm for some of the peaks and with λ_{max} at ~206 nm, ~220 nm, ~255 nm and ~340 nm for other peaks. These spectra are believed to combine the spectrum of 2-AB with the spectrum of GlcNAc/sialic acid sugar residues in the glycans under investigation.

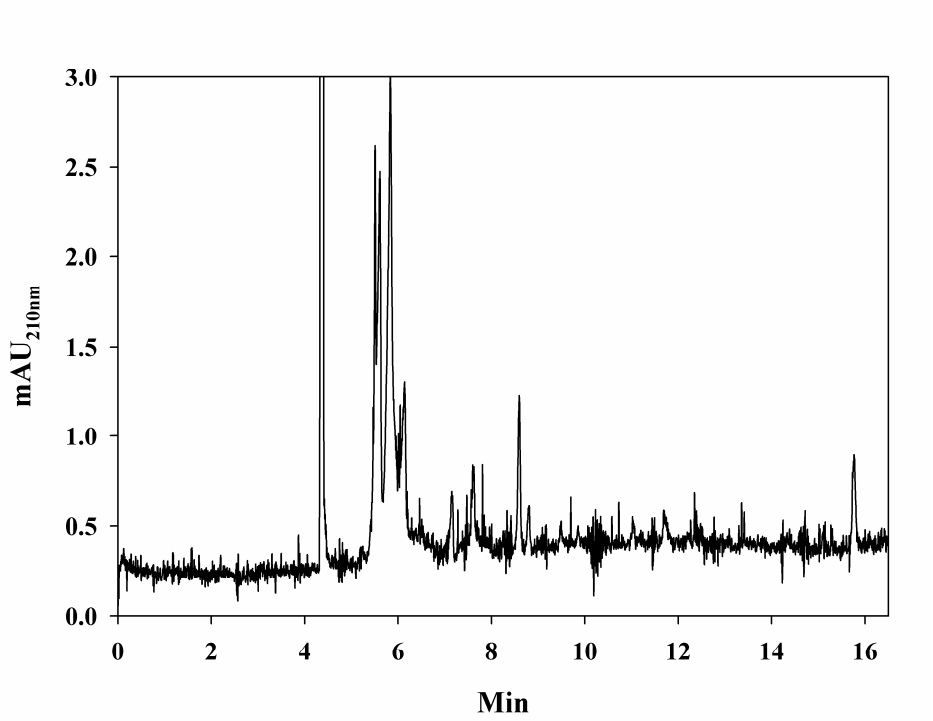

Figure 7. *Electropherogram of 2-AB-derivatized N-glycans derived from transferrin. Conditions are the same as in Figure 5.*

Avidin is a glycoprotein from egg white, which has a molecular mass of ~ 67 kDa and a pI of ~ 10.5 [46]. Avidin contains about 7-10 % carbohydrate that were reported to be constituted of four to five mannose and three *N*-acetylglucosamine residues per unit, which are attached to Asp-17 [47, 48]. The proposed *N*-glycans of avidin are listed in Table 5 [49, 50]. There are five hybrid type *N*-glycans versus only 2 high mannose type *N*-glycans. Figure 8 shows the CE profile of the *N*-glycans derived from avidin. Borate

is believed to complex more strongly with high mannose sugar chains (migrating between 8 and 12.5 min) than with hybrid type glycans (migrating between 4.5 and 6.5 min). The late migrating peaks (i.e., high mannose) yielded DAD spectra similar to those found for the late migrating glycans of ovalbumin (i.e., high mannose type glycans).

TABLE 5

PROPOSED N-GLYCANS DERIVED FROM AVIDIN [49, 50]

High mannose glycans: $Man_6GlcNAc_2$ (see structure (2) in Table 2),

$Man_7GlcNAc_2$ (see structure (3) in Table 2)

Bisected hybrid glycans: $Man_4GlcNAc_5$ (see structure (6) in Table 2),

$Man_5GlcNAc_5$ (similar to structure (8) in Table 2),

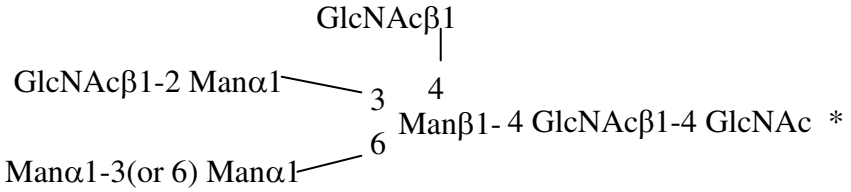

Non-bisected hybrid glycans: $Man_5GlcNAc_4$ (see structure (7) in Table 2),
$Man_6GlcNAc_4$

Note: the subscripted numbers are the numbers of the carbohydrate units;
*: adapted from reference [50]

In summary, this study has established that the use of CE for fast profiling of various 2-AB derivatized *N*-glycans derived from different types of glycoproteins combined with on-line DAD spectra is essential to assess the extent of the enzymatic cleavage (or deglycosylation) as well as their subsequent pre-column derivatization with

2-AB. The method established here should be applicable to the deglycosylation of other glycoproteins.

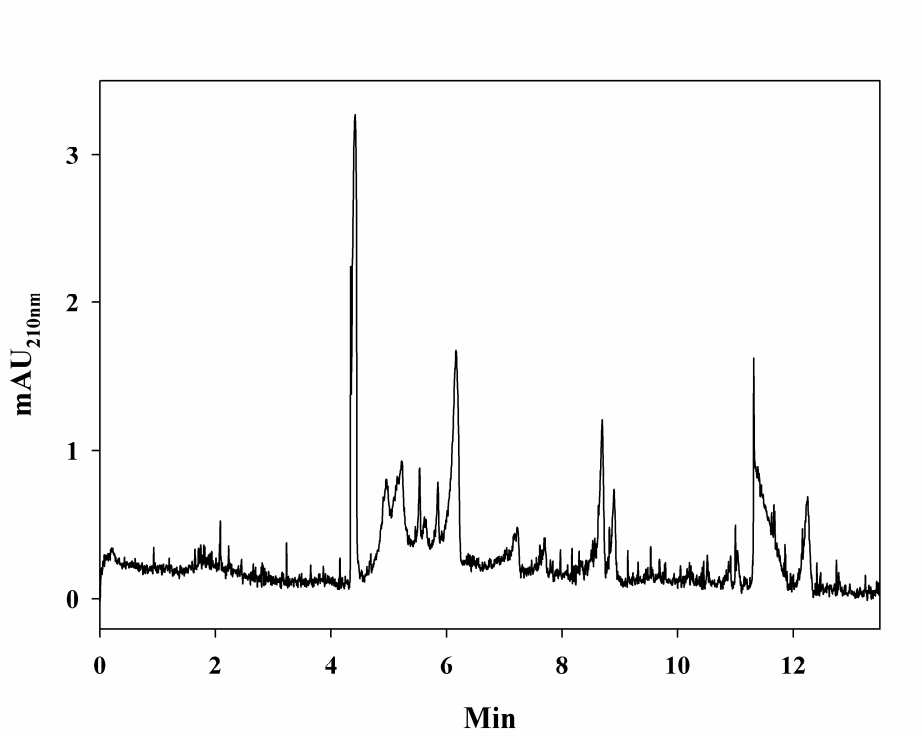

Figure 8. *Electropherogram of 2-AB-deivatized N-glycans derived from avidin. Conditions are the same as in Figure 5.*

2CN-OH Silica-Based Monolith for the Separation of *N*-Glycans by CEC and Nano - LC

CEC profiling of 2-AB derivatized *N*-glycans In principle, CEC gives more selectivity for separation than CE due to the presence of the additional chromatographic partitioning in the stationary phase for solutes [51]. In this investigation, the separation of the *N*-glycans on the 2CN-OH silica monolithic column was studied. Figure 9 shows the electrochromatogram of the *N*-glycans derived from α_1-acid glycoprotein obtained on the 2CN-OH monolith using a running electrolyte containing sulfated β-cyclodextrin (β-

CD) as a modifier/selectivity selector to improve separation. β-CD is constituted of seven glycopyranoside units and has a toroid shape (Figure 10). The primary and secondary hydroxyl groups are located at the openings of the toroid and this spatial arrangement makes the exterior of the toroid hydrophilic while the interior is hydrophobic. When the 2-AB-derivatized glycans meet the sulfated β-CD, the hydrophobic aromatic rings enter the hydrophobic cavity of the β-CD. However, the interaction of the aromatic ring and the β-CD is affected by the size, structure and polariry of the glycan attached (Figure 11). This kind of interaction provides more

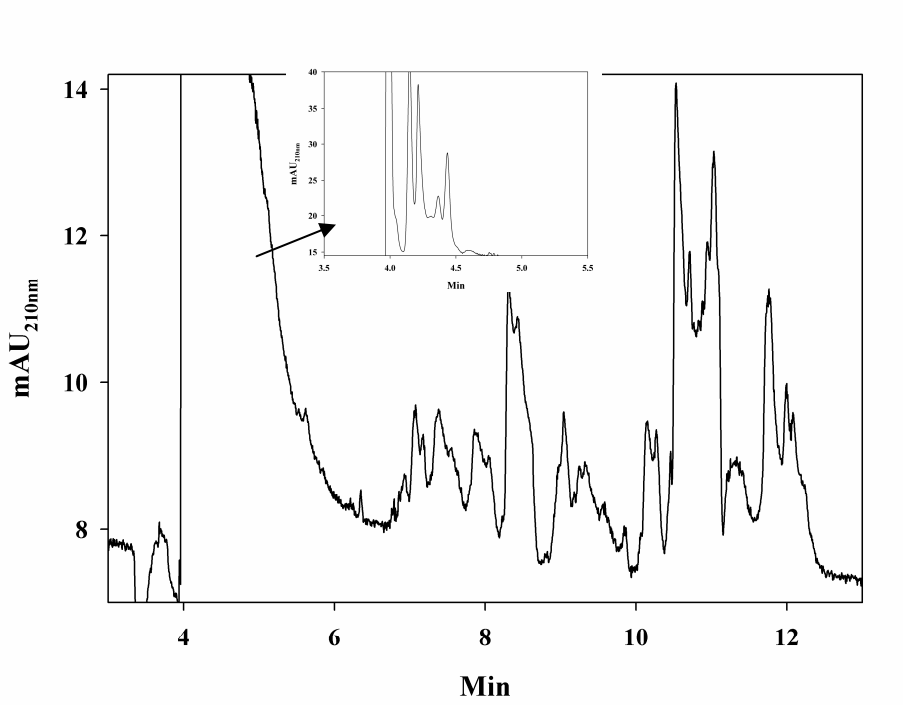

Figure 9. *Electrochromatogram of N-glycans derived from α_1-acid glycoprotein. Conditions: 2CN-OH monolithic capillary column, 25/33 cm × 100 μm ID. Mobile phase, hydro-organic solution made up of 65% v/v ACN, 35% v/v of 1 mM NH_4Ac (pH 6.0) and 1 mM sulfated β-CD; separation voltage, 20 kV; column temperature, 20 °C.*

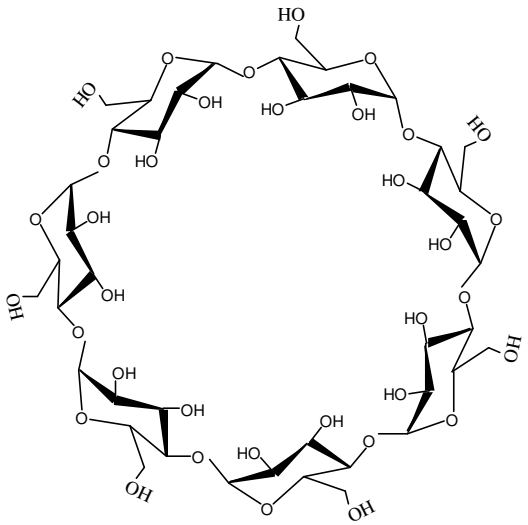

Figure 10. *Schematic structure of β-CD.*

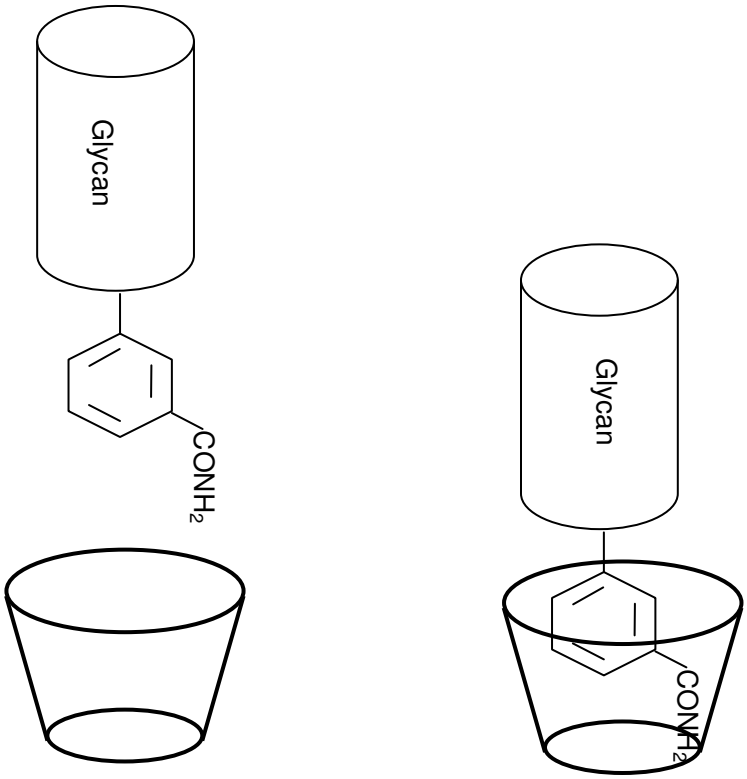

Figure 11. *Schematic of interaction between 2-AB derivatized glycans and β-CD.*

selectivity for different glycans and as a result more glycans were separated (Figure 9) when compared to CE (Figure 6a).

Figure 9 and Figures 12a and 12b and show the effect of the sulfated β-CD concentration on the CEC separation of the *N*-glycans derived from α_1-acid glycoprotein. When 1 mM sulfated β-CD was added to the mobile phase, more early eluting peaks were resolved (Figure 9) as compared to the results obtained in the absence of sulfated β-CD in the mobile phase (Figure 12a), and the peaks with longer retention time were more retarded in the presence of sulfated β-CD. This effect was more pronounced as the concentration of the sulfated β-CD was increased to 2 mM (Figure 12b). The glycans with short retention time at 4-6 min were separated completely while those at the higher retention time coeluted with each other when the concentration of the sulfated β-CD was increased to 2 mM. Thus, and for the remainder of the study, the concentration of sulfated β-CD in the mobile phase was kept at 1 mM.

Figures 13, 14 and 15 show the electrochromatograms of the 2-AB derivatized *N*-glycans derived from ovalbumin, avidin and transferrin, respectively, on the 2CN-OH silica-based monolithic column. As expected, the retention and separation selectivity of the glycans is largely affected by the concentration of acetonitrile (ACN) in the mobile phase, compare Figure 13a to Figure 13b. At 75% v/v ACN (Figure 13b), some of the early eluting peaks shifted to higher retention and separated from each other when compared to 65% v/v ACN (Figure 13a). However, it is believed that some of the late eluting peaks at 65% ACN were not eluted when operating the column at 75% ACN. So, as a compromise and for profiling the whole glycan mixture derived from a given

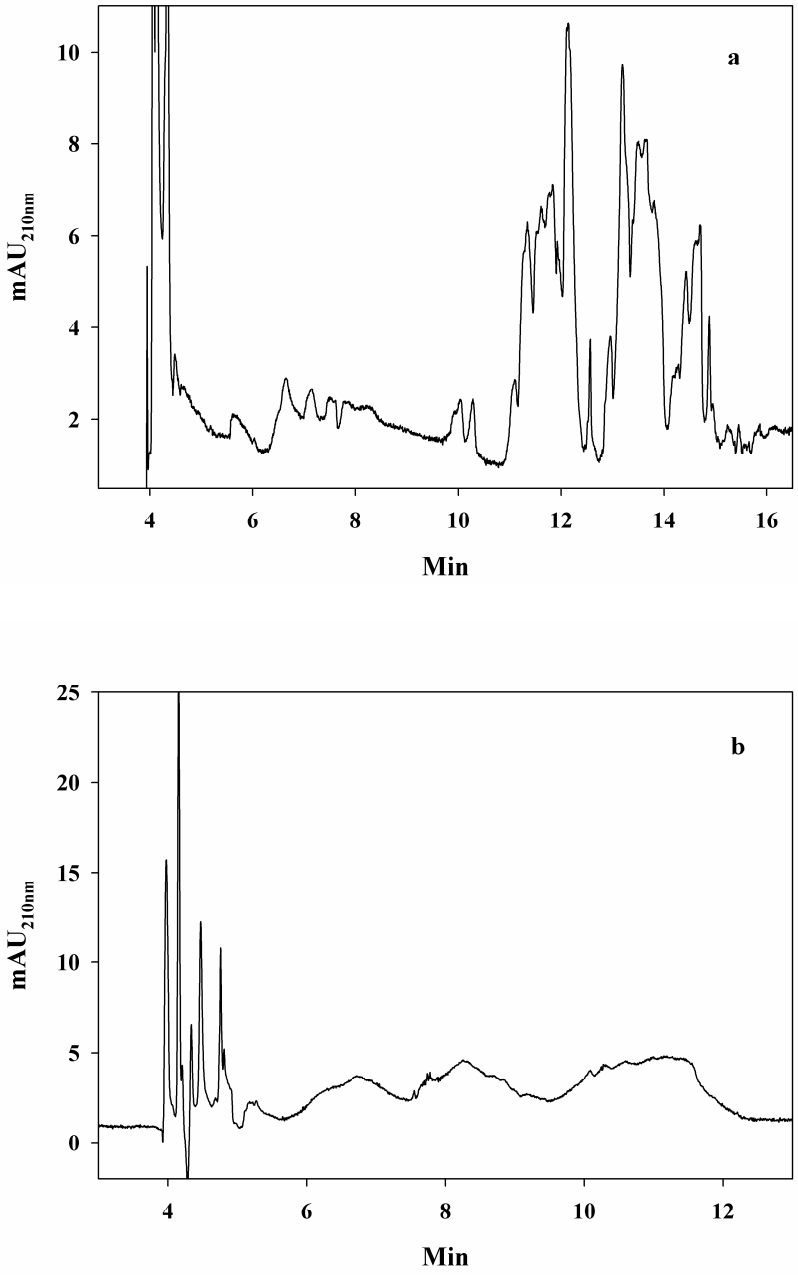

Figure 12. *Electrochromatograms of N-glycans derived from α_1-acid glycoprotein with different concentrations of sulfated β-CD in the running electrolyte solution. Conditions: 2CN-OH monolithic capillary column, 25/33 cm × 100 µm ID. Mobile phase, hydro-organic solution made up of 65% v/v ACN, 35% v/v of 1 mM NH_4Ac (pH 6.0) and 0 mM in (a) and 2 mM in (b) sulfated β-CD; separation voltage, 20 kV; column temperature, 20 °C.*

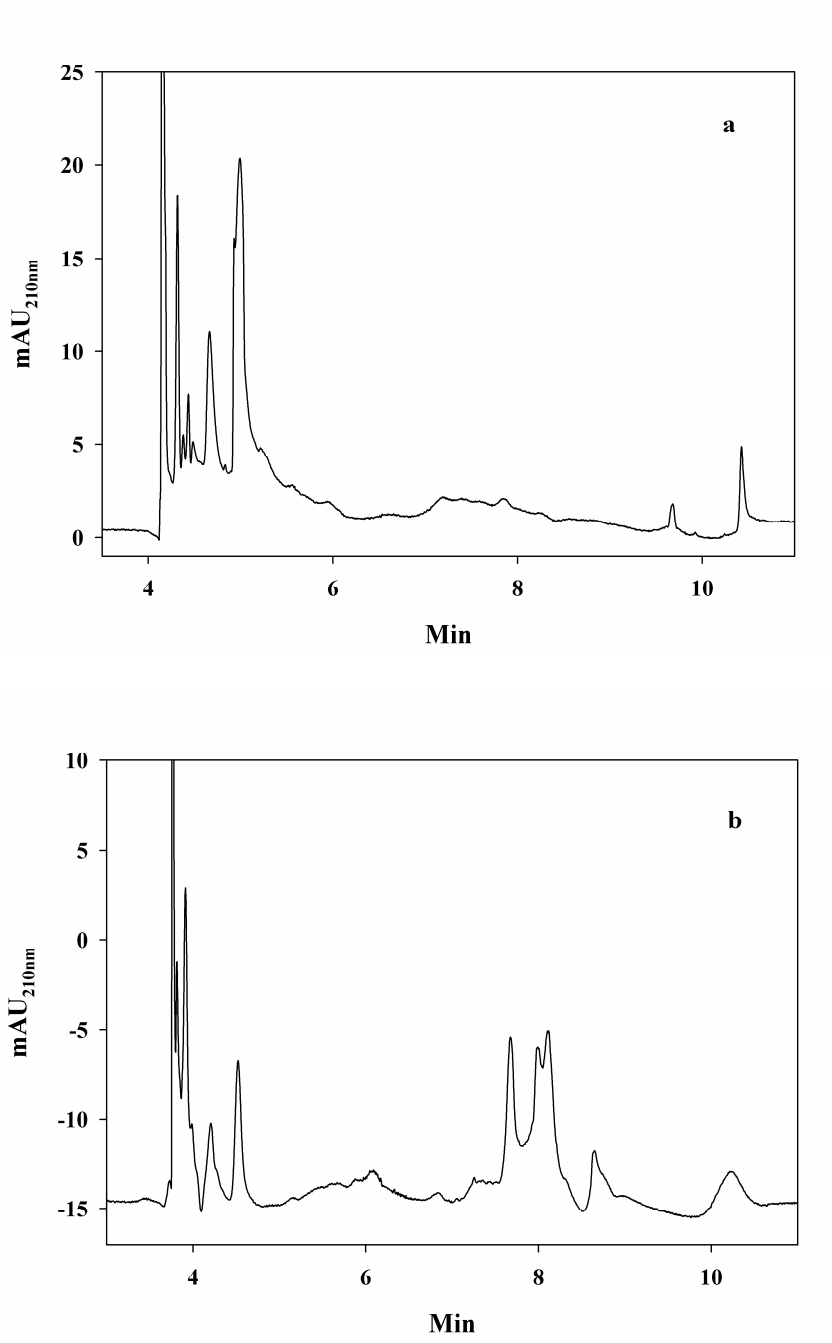

Figure 13. *Electrochromatograms of N-glycans derived from ovalbumin. Conditions: 2CN-OH monolithic capillary column, 25/33 cm × 100 µm ID. Mobile phase, hydro-organic solution made up of (a) 65% v/v ACN, 35% v/v of 1 mM NH_4Ac (pH 6.0) and 2 mM sulfated β-CD, (b) 75% v/v ACN, 25% v/v of 1 mM NH_4Ac (pH 6.0) and 1 mM sulfated β-CD; separation voltage, 20 kV; column temperature, 20 °C.*

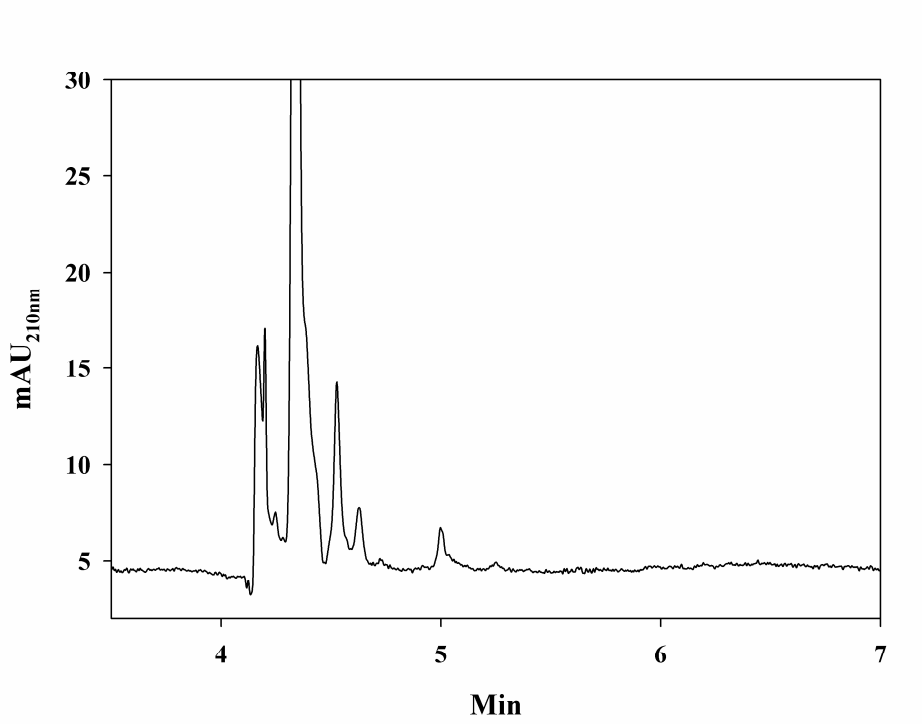

Figure 14. *Electrochromatogram of N-glycans derived from transferrin. Conditions: 2CN-OH monolithic capillary column, 25/33 cm × 100 µm ID. Mobile phase, hydro-organic solution made up of 65% v/v ACN, 35% v/v of 1 mM NH_4Ac (pH 6.0) and 2 mM sulfated β-CD; separation voltage, 20 kV; column temperature, 20 °C.*

glycoprotein, a mobile phase at 65% v/v ACN was preferred, and was used in the remainder of the study. The strong dependence of glycan retention on small changes in the ACN content of the mobile phase in CEC using polar stationary phases such as 2CN-OH monolith calls for gradient elution in normal phase CEC. Unfortunately, there are no commercially available CEC instruments yet on the market with gradient elution capability.

Figure 14 shows the CEC profiling of the 2-AB derivatized glycans derived from transferrin. As can be seen in this figure, the majority of glycans seem to co-elute in a

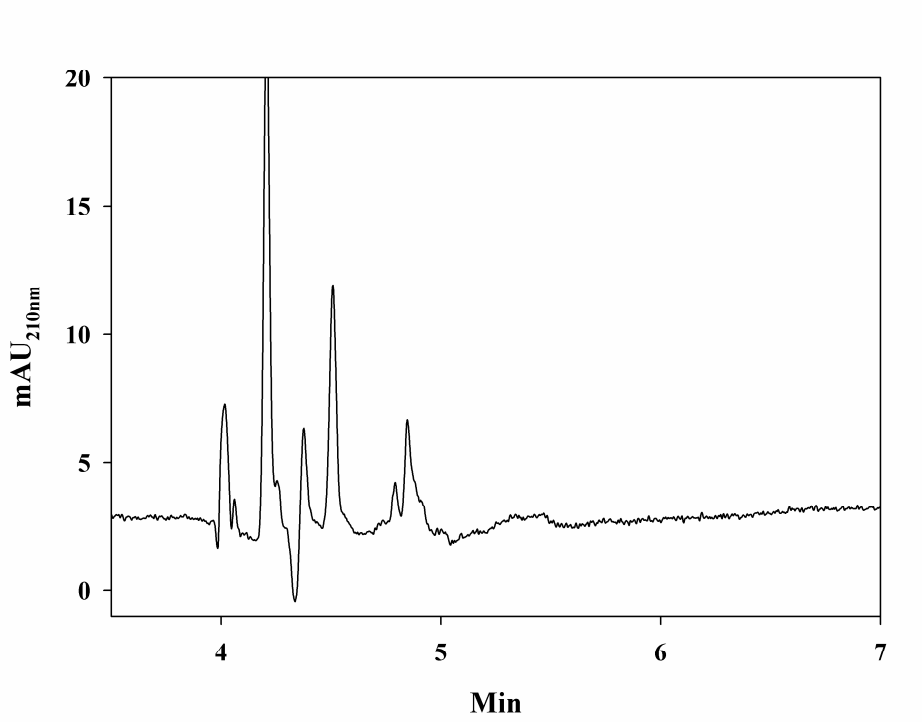

Figure 15. *Electrochromatogram of N-glycans derived from avidin. Conditions are the same as in Figure 14.*

large peak at about 4.4 min. In this regard, CE seems to give a better profiling for the glycans derived from transferrin than normal phase CEC, compare Figure 14 to Figure 7. On the other hand, CEC seems to give a much faster profiling than CE for the 2-AB derivatized *N*-glycans derived from avidin, compare Figure 15 to Figure 8.

In summary, to exploit the full potentials of CEC using polar stationary phases such as 2-CN-OH Monolith in profiling glycans, CEC instruments with gradient elution capability are badly needed. It seems that CEC work much better for glycans profiling than CE in cases where the glycans are neutral such as those derived from ovalbumin and avidin.

Nano-LC separation of *N*-glycans To further demonstrate the usefulness of the 2CN-OH silica based monolith, the 2-AB derivatized *N*-glycans derived from α_1-acid glycoprotein were chromatographed on the 2CN-OH monolith using nano-LC, and the results are shown in Figure 16. As expected nano-LC provided different selectivity than CEC under otherwise the same mobile phase conditions, compare Figure 16 to Figure 9. One important finding was that the presence of sulfated β-CD in the mobile phase was not as effective in modifying the separation selectivity as in CEC. This fact is apparent in Figure 17a and Figure 17b, where one can see that upon addition of sulfated β-CD to the mobile phase (Figure 17b) not much change was observed in profiling the 2-AB

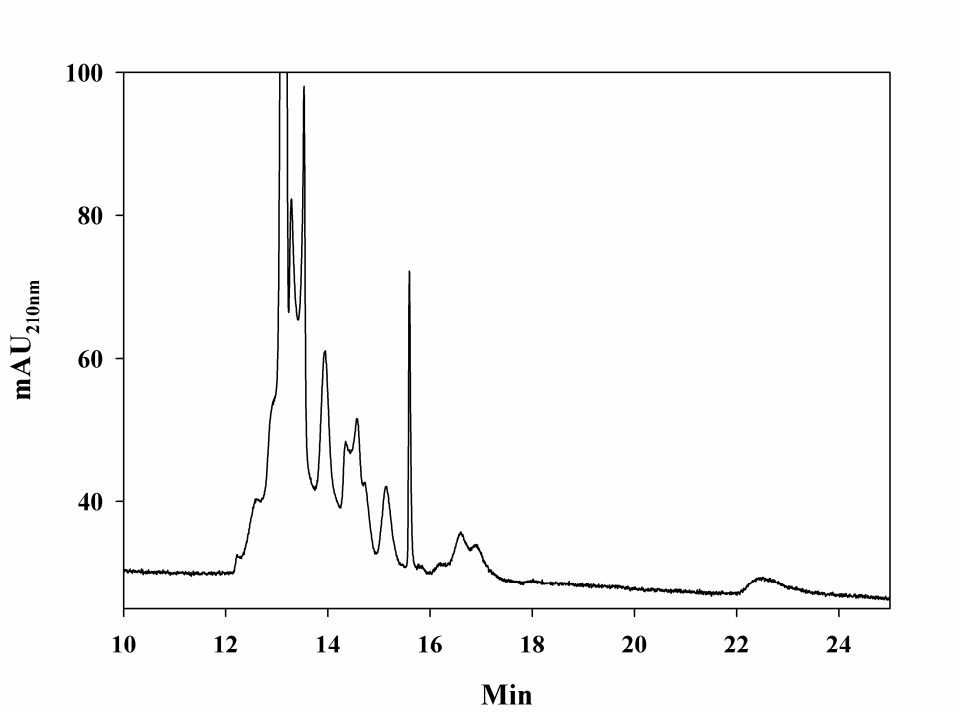

Figure 16. *Chromatogram of N-glycans derived from α_1-acid glycoprotein. Conditions: 2CN-OH monolithic capillary column, 25/33 cm × 100 μm ID; Mobile phase, hydro-organic solution made up of 65% v/v ACN, 35% v/v of 1 mM NH_4Ac (pH 6.0) and 1 mM sulfated β-CD; separation pressure, 10 bars; column temperature, 20 °C.*

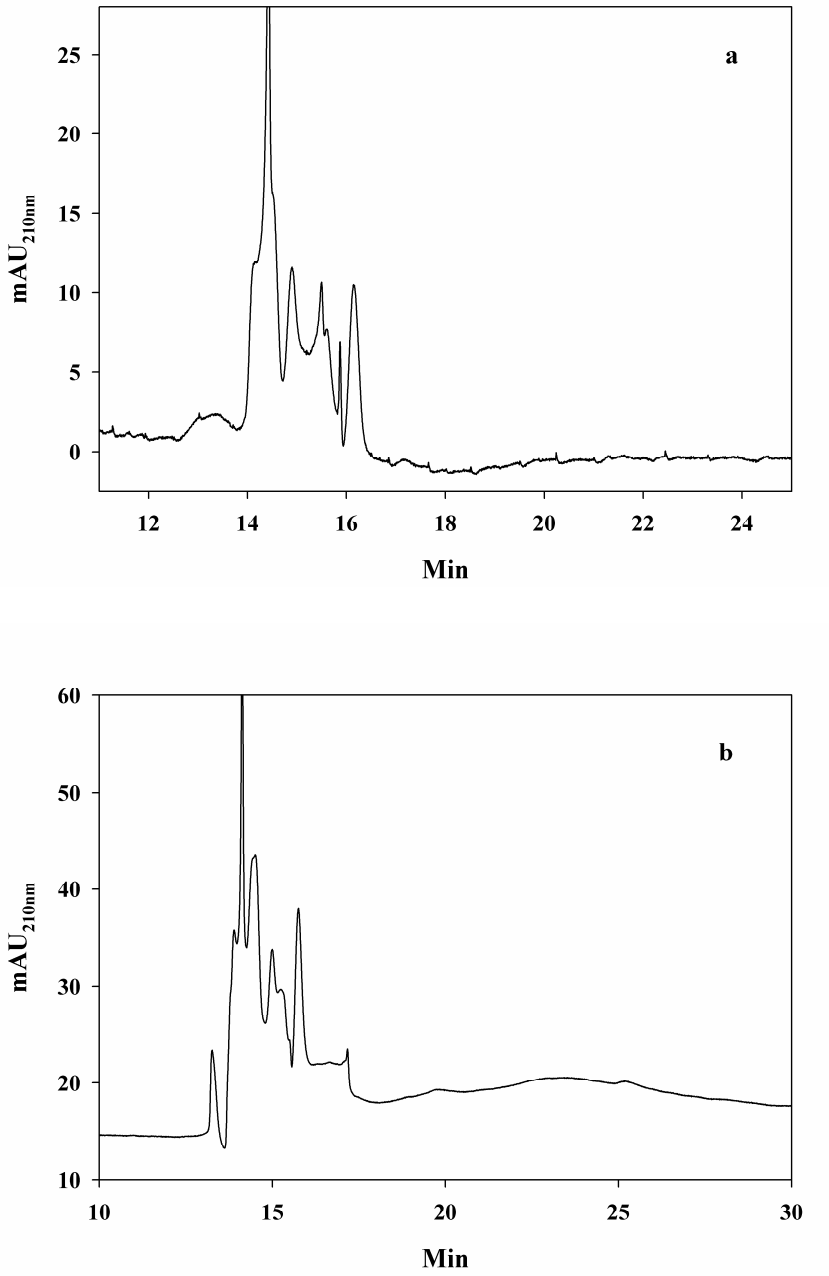

Figure 17. *Chromatogram of N-glycans derived from ovalbumin. Conditions: 2CN-OH monolithic capillary column, 25/33 cm × 100 µm ID; Mobile phase, hydro-organic solution made up of 65% v/v ACN, 35% v/v of 1 mM NH_4Ac (pH 6.0) and (a) 0 mM sulfated β-CD, (b) 2 mM sulfated β-CD; separation pressure, 10 bars; column temperature, 20 °C.*

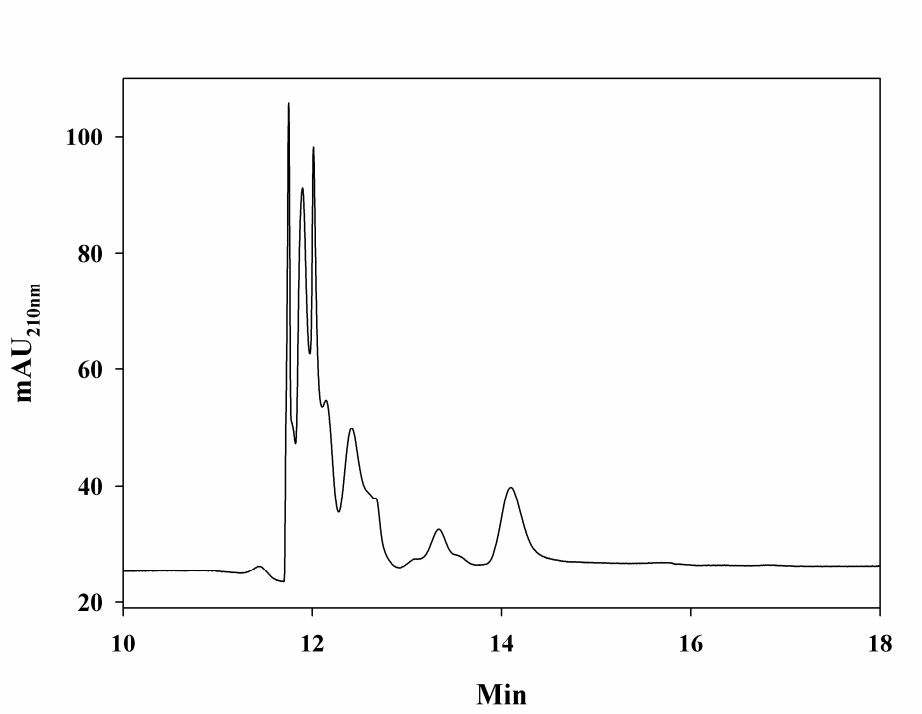

Figure 18. *Chromatogram of N-glycans derived from ovalbumin. Conditions: 2CN-OH monolithic capillary column, 25/33 cm × 100 μm ID. Mobile phase, hydro-organic solution made up of 75% v/v CAN, 25% v/v of 1 mM NH_4Ac (pH6.0) and 1 mM sulfated β-CD; separation pressure, 10 bars; column temperature, 20 °C.*

derivatized *N*-glycans derived from ovalbumin. It seems that the ACN content of the mobile phase has more impact on the nano-LC separation of glycans than the inclusion of sulfated β-CD in the mobile phase. In fact, when the organic content in the mobile phase was increased to 75%, higher resolution was observed for the early eluting solutes, see Figure 18.

In summary, nano-LC with 2CN-OH monolith yielded less selectivity toward *N*-glycans under otherwise that same mobile phase conditions. The higher selectivity and resolution observed in CEC may be due the differential binding of sulfated β-CD to

various glycans as well as the presence of sialic acids in some of the glycans [38] which impart the glycans with different charge-to-mass ratios thus inducing differential electromigration and finally better separation.

Conclusions

Sol-gel process was applied for the fabrication of silica-based monoliths. Factors affecting the pore morphology, the specific surface area and the column separation efficiency include the ratio of the functional monomer, porogen and solvent as well as the subsequent mesopore treatment (i.e., pore tailoring by ammonium hydroxide treatment). Fine pore tailoring is important to obtain a silica monolithic column with high separation efficiency.

The 2CN-OH silica-based monolith was useful in the separation of *N*-glycans by both CEC and nano-LC modes, with the CEC mode providing more selectivity and resolution toward closely related *N*-glycans. Modifiers such as sulfated β-CD added to the mobile phase in small amounts improved the CEC separations of *N*-glycans.

REFERENCES

[1] Zhong, H., El Rassi, Z., *J. Sep. Sci.* **2006**, *29*, 2031.

[2] Ikegami, T., Fujita, H., Horie, K., Hosoya, K., Tanaka, N., *Anal. Bioanal. Chem.* **2006**, *386*, 578.

[3] Horie, K., Ikegami, T., Horie, K., Saad, N., Fiehn, O., Tanaka, N., *J. of Chromatogr. A* **2007**, *1164*, 198.

[4] Ikegami, T., Horie, K., Jaafar, J., Hosoya, K., Tanaka, N., *J. Biochem. Biophys. Methods* **2007**, *70*, 31.

[5] Vinas, P., Soler-Romera, M. J., Hernandez-Cordoba, M., *Talanta* **2006**, *69*, 1063.

[6] Taylor, M. E., Drickamer, K., *Introduction to Glycobiology*, Oxford University Press **2003**.

[7] Cooper, A. C., Wilkins, M. R., Williams, K. L., Packer, N. H., *Electrophoresis* **1999**, *20*, 3589.

[8] Merkle, R. K., Cummings, R. D., *J. Biol. Chem.* **1987**, *282*, 8179.

[9] Tsuji, T., Irimura, T., Osawa, T., *J. Biol. Chem.* **1981**, *256*, 10497.

[10] Rademacher, T. W., Parekh, R. B., Dwek, R. A., *Ann. Rev. Biochem.* **1988**, *57*, 785.

[11] El Rassi, Z., Nashabeh, W., *High Performance capillary electrophoresis of carbohydrates and glycoconjugates*, in: El Rassi, Z. (Ed.), *Carbohydrate Analysis: High Performance Liquid Chromatography and Capillary Electrophoresis*, Elsevier, Amsterdam **1995**, pp. 267.

[12] Chen, F. T. A., Evangelista, R. A., *Anal. Biochem.* **1995**, *230*, 273.

[13] Mechref, Y., Ostrander, G. K., El Rassi, Z., *J. Chromatogr. A* **1995**, *695*, 83.

[14] El Rassi, Z. (Ed.), *Carbohydrate Analysis by Modern Chromatography and Electrophoresis*, Elsevier, Amsterdam **2002**.

[15] El Rassi, Z. (Ed.), *Carbohydrate Analysis*, Elsevier, Amsterdam **1995**.

[16] Zhang, M., El Rassi, Z., *Electrophoresis* **1998**, *19*, 2068.

[17] Zhang, R., Z., Z., Liu, G., Hidaka, Y., Shimonish, Y., *J. Chromatogr.* **1993**, *646*, 45.

[18] Strydom, D. J., *J. Chromatogr. A* **1994**, *678*, 17.

[19] El Rassi, Z., Tedford, D., An, J., Mort, A., *Cargohydr. Res.* **1991**, *215*.

[20] Simms, P. J., Haines, R. M., Hicks, K. B., *J. Chromatogr.* **1993**, *648*, 131.

[21] Amstrong, D. W., Jin, H. L., *J. Chromatogr.* **1989**, *462*, 219.

[22] Kitahata, S., Hara, K., Fujita, K., Nakano, H., Kuwahara, N., Koizumi, K., *Biosci. Biotechnol. Biochem.* **1992**, *56*, 1386.

[23] Stefansson, M., Lu, B., *Chromatographia* **1993**, *35*, 61.

[24] Bonn, G., *J. Chromatogr.* **1985**, *322*, 411.

[25] Knudsen, P. J., Eriksen, P. B., Fenger, M., Florentz, K., *J. Chromatogr.* **1980**, *187*, 373.

[26] Koizumi, K., Utamura, T., Kuroyanagi, T., Hizukuri, S., Abe, J. I., *J. Chromatogr.* **1986**, *360*, 397.

[27] Cummings, R. D., Kornfeld, S., *J. Biol. Chem.* **1982**, *257*, 1235.

[28] Zhong, H., *Polar Bonded Stationary Phases Consisting of Silica-Based Monoliths for Normal Phase Capillary Electrochromatography,* Oklahoma State University, Stillwater, **2005**, 71 pp

[29] Allen, D., El Rassi, Z., *Electrophoresis* **2003**, *24*, 408.

[30] Minakuchi, H., Nakanishi, K., Soga, N., Ishizuka, N., Tanaka, N., *Anal. Chem.* **1996**, *68*, 3498.

[31] Chen, F. T. A., Evangelista, R. A., *Electrophoresis* **1998**, *19*, 2639.

[32] Guttman, A., Chen, F. T. A., Evangelista, R. A., *Electrophoresis* **1996**, *17*, 412.

[33] Zhong, H., El Rassi, Z., *J. Sep. Sci.* **2006**, *29*, 2023.

[34] Bigge, J. C., Patel, T. P., Bruce, J. A., Goulding, P. N., Charles, S. M., Parekh, R. B., *Anal. Biochem.* **1995**, *230*, 229.

[35] Zhang, M., Melouk, H. A., Chenault, K., El Rassi, Z., *J. Agric. Food Chem.* **2001**, *49*, 5265.

[36] Nakanishi, K., *J. Porous Mater.* **1997**, *4*, 67.

[37] Nakanishi, K., Minakuchi, H., Ihizuka, N., Soga, N., Tanaka, N., *Sol-GelSynthesis and Processing*, American Ceramic Soceity, Westerville **1998**, pp. 139.

[38] El Rassi, Z., *High Performance Caillary Electrophoresis of Carbohydrates*, Beckman Instruments, Inc., Fullerton **1996**.

[39] Honda, S., Makino, A., Suzuki, S., Kakehi, K., *Anal. Biochem.* **1990**, *191*, 228.

[40] Liu, D., Wei, Y., Yao, P., Jiang, L., *Carbohydr. Res.* **2006**, *341*, 782.

[41] Okanda, F. M., *Non-polar and affinity monolithic stationary phases for biopolymer separations by capillary electrochromatography and nano-liquid chromatography,* Oklahoma State Unviersity, Stillwater, OK, **2006**, 175 pp

[42] Treuheit, M. J., Costello, C. E., Halsall, H. B., *Biochem. J.* **1992**, *283*, 105.

[43] Dong, X., Xu, Y., Lin, B., *Chromatographia* **2000**, *52*, 14.

[44] Montreuil, J., Vliegenthart, J. F. G., Schachter, H., *Glycoproteins II*, Elsevier Science B.V. **1997**.

[45] Montreuil, J., Spik, G., Mazurier, J., *Transferrin superfamily*, in: Montreuil, J. (Ed.), *Glycoproteins II*, Elsevier, Amsterdam **1997**, pp. 203.

[46] Hiller, Y., Gershoni, J. M., Bayer, E. A., Wilchek, M., *Biochem. J.* **1987**, *248*, 167.

[47] DeLange, R. J., *J. Biol. Chem.* **1970**, *245*, 907.

[48] Green, N. M., Toms, E., *Biochem. J.* **1970**, *118*, 67.

[49] Lee, B., Krishnanchettiar, S., Lateef, S. S., Lateef, N. S., Gupta, S., *Rapid Commun. Mass Spectrom.* **2005**, *19*, 2629.

[50] Bruch, R., White, H. B., *Biochemistry* **1982**, *21*, 5334.

[51] Krull, I. S., Stevenson, R. L., Mistry, K., Swartz, M. E., *Capillary Electrochromatography and Pressurized Flow Capillary Electrochromatography*, HNB Publishing, New York **2000**.

CHAPTER IV

LECTIN AFFINITY CHROMATOGRAPHY AND ELECTROCHROMATOGRAPHY ON MONOLITHIC SILICA CAPILLARY COLUMNS

Introduction

Affinity chromatography is a separation technique that is based on the specific biological interactions between the analytes and the stationary phase affinity ligands. These bio-interactions include enzyme and substrate, antigen and antibody and receptor and ligand.

Lectins are plant proteins that bind to their specific sugar moieties including glycoproteins, and therefore they can be used to isolate, purify or enrich any species that have the specific carbohydrate structures. Monolithic columns offer the advantages of good mass transfer ability, low backpressure and easy fabrication compared to the particle packing columns. While silica-based and organic polymer-based monoliths can be used as the support materials to produce affinity columns, silica monolith has its own unique feature that distinguish it from other kinds of monoliths, i.e., high surface area, which provides more sites for ligand immobilization and also for solute and stationary phase interactions [1]. Thus far, penicillin G acylase [2], trypsin [3], β-glucoronidase [4] and α_1-acid glycoprotein [5, 6] have been used in the fabrication of silica-based

monolithic affinity columns. Lectins have been immobilized on particulate silica support [7-11], magnetic beads[12], acrylate-based monoliths [13, 14], gold foils [15] and affinity membranes [8, 16]. However, attempts to use silica-based monoliths for lectin affinity column fabrications have not been reported so far (for detailed discussion and background, see Chapter II). Thus, it is the aim of this study to develop silica-based monolithic lectin affinity columns for glycoconjugate fractionation and purification. In this investigation, the optimized silica monolith (see Chapter III) has been employed as the support material for lectin (e.g. Concancavalin A (Con A) and wheat germ agglutinin (WGA)) immobilization. The separation of the monosaccharides and the affinity interaction behaviors of the glycoproteins on the silica-based lectin columns were also studied.

Experimental

Instrumentation

The instruments used are the same as those described in Chapter III.

Reagents and Materials

ortho-Nitrophenyl (*oNP)-N*-acetyl-α-D glucosaminide, *para*-nitrophenyl (*pNP)-N*-acetyl-α-D glucosaminide, *pNP-N*-acetyl-β-D glucosaminide, Con A, ovalbumin, human α_1-acid glycoprotein and human transferrin were from Sigma-Aldrich Fine

Chemicals (St. Louis, MO, USA). WGA was from Vector Laboratories Inc. (Burlingame, CA, USA). The rest of chemicals and materials are as the same as those described previously. The structures of *pNP-N*-acetyl-β-D-glucosaminide, *pNP-N*-acetyl-α-D-glucosaminide and *oNP-N*-acetyl-α-D-glucosaminide, are shown in Figure 1.

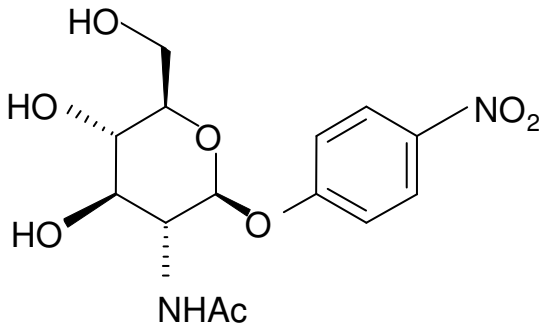

(1)

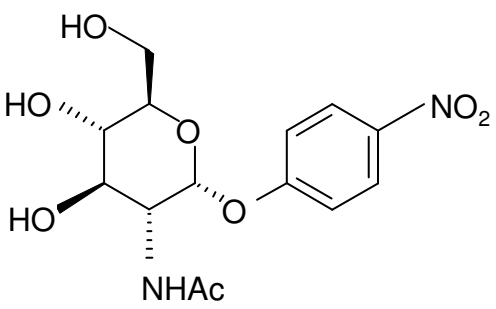

(2)

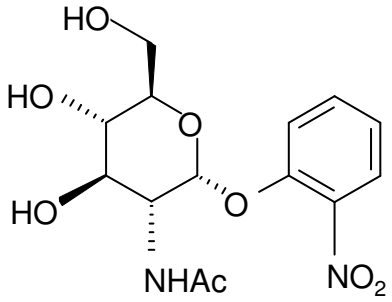

(3)

Figure 1. *Structures of pNP-N*-acetyl-β-D-glucosaminide (1), *pNP-N*-acetyl-α-D-glucosaminide (2) and *oNP-N*-acetyl-α-D-glucosaminide (3).

Lectin Immobilization

The silica-based monolithic column prepared as described in Chapter III and, after its subsequent reaction with γ-glycidoxypropyltrimethoxysilane, was rinsed with ACN

followed by water. Then a 0.2 M sulfuric acid solution was introduced into the column, which was then incubated at 60 °C for 3 h. After the column was washed with water, it was filled with a 0.1 M $NaIO_4$ and the reaction was allowed to proceed at room temperature for 1 h. The resulting column was washed with water before filled with 5 mg/mL Lectin in 0.1 M sodium acetate (NaAc), pH 6.4, 0.05 M sodium cyanoborohydride ($NaBH_3CN$), 0.1 M hapten monosaccharide and a metal cation if needed. For the Con A immobilization, 0.3 mM Ca^{2+}, 0.3 mM Mg^{2+}, 0.3 mM Mn^{2+} and methyl α-D-mannopyranoside (i.e., the hapten sugar) were added to the mixture. *N*-Acetyl-D-glucosamine (GlcNAc) was used as the hapten sugar for WGA immobilization. In all cases the hapten sugar was added during lectin immobilization to protect the lectin's carbohydrate binding site.

Results and Discussion

Separation of Monosaccharide Anomers and Isomers on Lectin Affinity Silica Monolith

Effect of concentration of hapten sugar on separation WGA is a plant protein with a molecular weight of ~ 36 kDa and a pI of ~ 9. The sugar ligand for WGA is *N*-acetylglucosamine (GlcNAc). WGA can bind oligosaccharides with structures containing terminal *N*-acetylglucosamine or chitobiose. In this investigation, the WGA-immobilized silica monolith was used for the separation of monosaccharide anomers and isomers. It was found that the pH and concentration of the hapten sugar in the mobile phase affected the separation. As shown in Figure 2, when the concentration of the hapten sugar GlcNAc

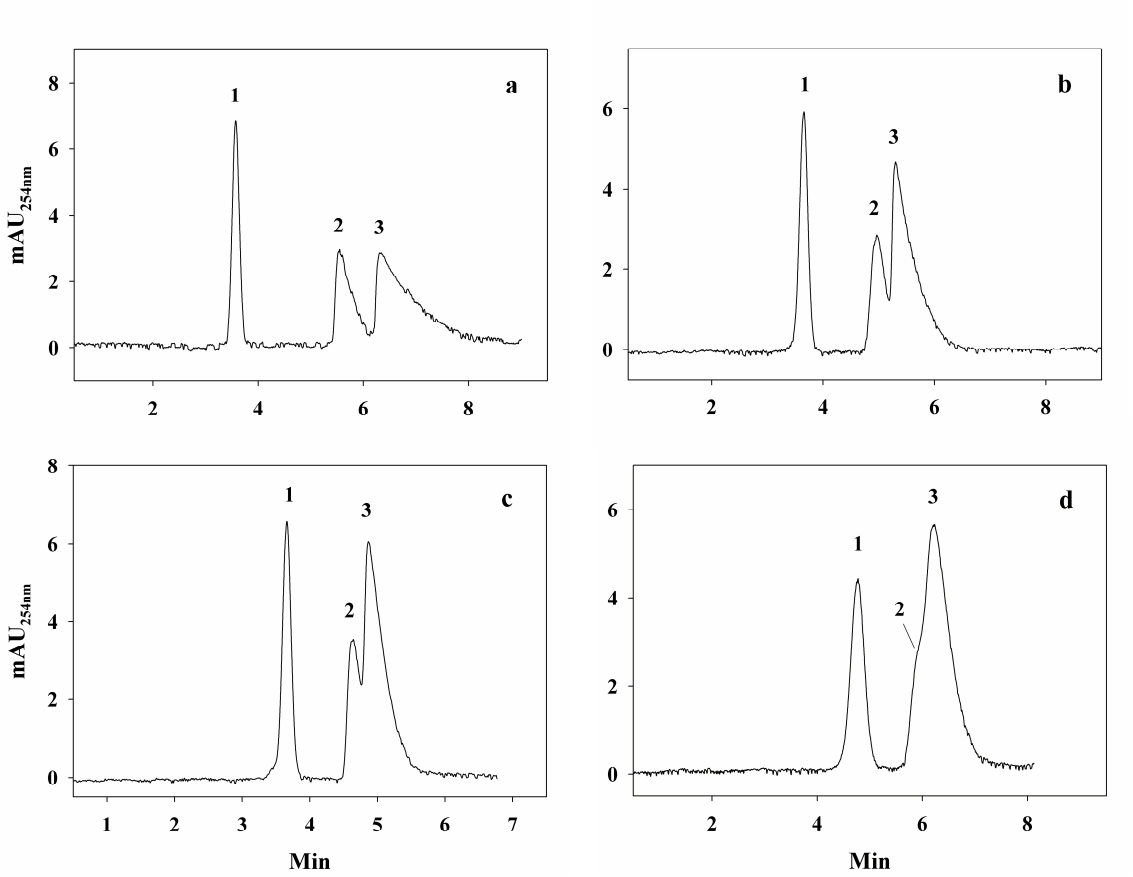

Figure 2. *Effect of concentration of hapten sugar on the separation of pNP-N-acetyl-α-D glucosaminide and pNP-N-acetyl-β-D-glucosaminide. Conditions: WGA immobilized silica-based monolithic column, 20/27 cm ×100 μm ID; voltage, 20 kV; column temperature, 20 °C; mobile phase, 5 mM BisTris, pH 6.0, 5 mM NaCl, 0.1-0.4 M GlcNAc: a. 0.1 M, b. 0.2 M, c. 0.3 M and d. 0.4 M; Solutes: 1, uracil; 2, pNP-N-acetyl- β-D glucosaminide; 3, pNP-N-acetyl- α-D-glucosaminide*.

in the mobile phase was 0.1 M, the *pNP-N*-acetyl-α-D-glucosaminide and *pNP-N*-acetyl-β-D-glucosaminide were separated from each other. As the concentration of the hapten sugar GlcNAc was increased to 0.2 M, the peaks of the two solutes overlapped partially and even further at 0.3 M GlcNAc. When the concentration of the hapten sugar went up

to 0.4 M GlcNAc, the anomers co-eluted. This indicates that the interaction of the *pNP* monosaccharides with WGA is based solely on specific interactions, and nonspecific interactions are virtually absent. It was also found that k' decreased rapidly when the concentration of the hapten sugar was increased from 0.1 M to 0.2 M, and then decreased slowly afterwards (see Figure 3). Thus, a concentration of 0.2 M of the hapten sugar was selected for the eluting mobile phase.

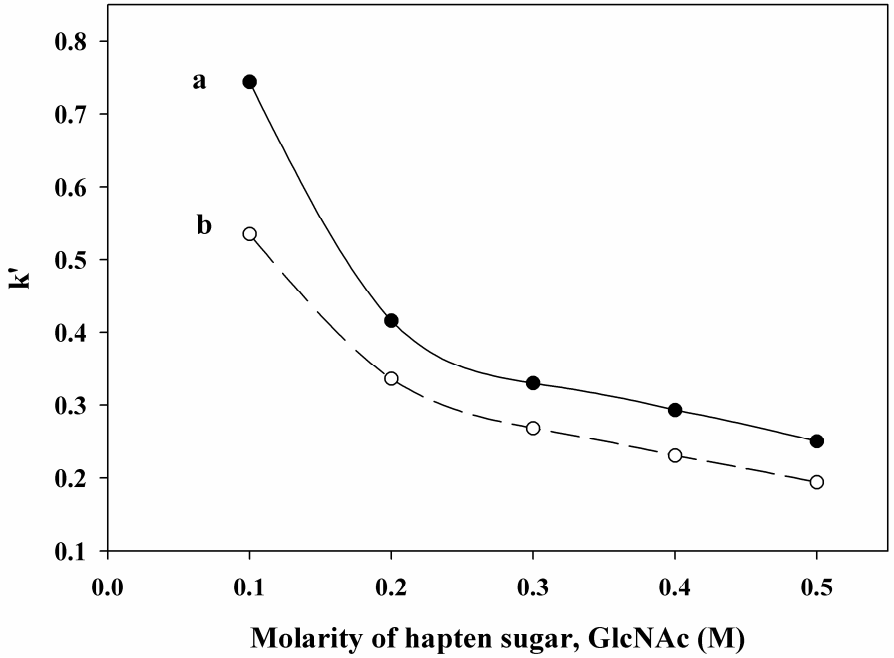

Figure 3. *Dependence of k' of pNP monosaccharides on the molarity of the hapten sugar in the mobile phase. Conditions: WGA immobilized silica-based monolithic column, 20/27 cm ×100 μm ID; voltage, 20 kV; column temperature, 20 °C; mobile phase, 5 mM BisTris, 5 mM NaCl, 0.1-0.5 M GlcNAc; solutes: a. pNP-N-acetyl-α-D-glucosaminide, b. pNP-N-acetyl-β-D-glucosaminide.*

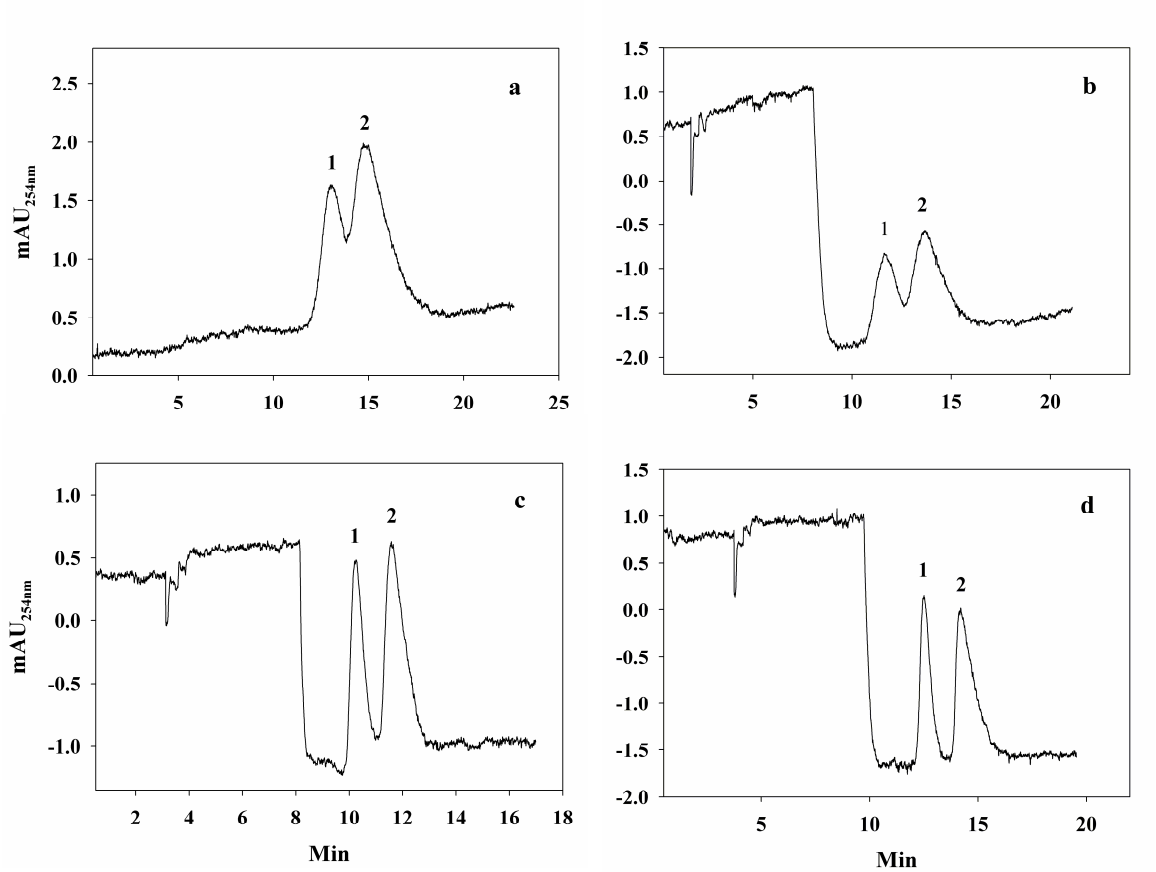

Figure 4. *Effect of concentration of hapten sugar on the separation of pNP-N-acetyl-α-D-glucosaminide and pNP-N-acetyl-β-D-glucosaminide. Conditions: WGA immobilized silica-based monolithic column, 20/27 cm ×100 μm ID; voltage, 20 kV; column temperature, 20 °C; binding mobile phase, 5 mM BisTris, 5 mM NaCl, pH 6; eluting mobile phase, 0.2 M GlcNAc in the binding mobile phase; a. 100 % eluting mobile phase; b. 0-3min, binding mobile phase, after 3 min, eluting mobile phase; c. 0-5min, binding mobile phase, after 5 min, eluting mobile phase; d. 0-6min, binding mobile phase, after 6 min, eluting mobile phase; solutes: 1, pNP-N-acetyl-β-D-glucosaminide; 2, pNP-N-acetyl-α-D-glucosaminide.*

In order to further understand the dependence of separation and elution of monosaccharides under investigation on the hapten sugar concentration in the mobile phase, a series of experiments involving a step gradient were conducted. The delay of applying the step gradient with the hapten sugar affected the resolution of the two-monosaccharide anomers (Figure 4). With an eluting mobile phase containing 0.2 M GlcNAc, the peaks of the anomers overlapped extensively (see Figure 4a). They separately eluted when the eluting mobile phase was applied at 3 min after equilibrating the WGA column with the binding mobile phase (see Figure 4b). The resolution became much higher when the eluting mobile phase was applied at 5 min and reached 100% at 6 min (see Figure 4c and 4d).

Effect of pH on separation Figure 5 shows the effect of pH of the mobile phase on the separation of the *pNP*-monosacharride anomers (i.e., *pNP*-*N*-acetyl-β-D glucosaminide and *pNP*-*N*-acetyl-α-D-glucosaminide) under investigation. WGA is positively charged at an acidic pH due to its high pI value of 9. At low pH, a negative polarity voltage was needed to elute the *pNP*-monosaccharides from the WGA immobilized monolithic column. On the other hand, at pH 6.0 or higher the net positive charge of immobilized WGA decreased and a positive polarity voltage was applied to elute the *pNP*-monosaccharides under investigation. Figure 5 shows the electrochromatograms obtained at various pH. As can be seen in this figure, pH 5.0 yielded an optimum resolution between the two anomers. Figure 6 represents the dependence of k' on pH. It seems that the optimum activity of the WGA toward the

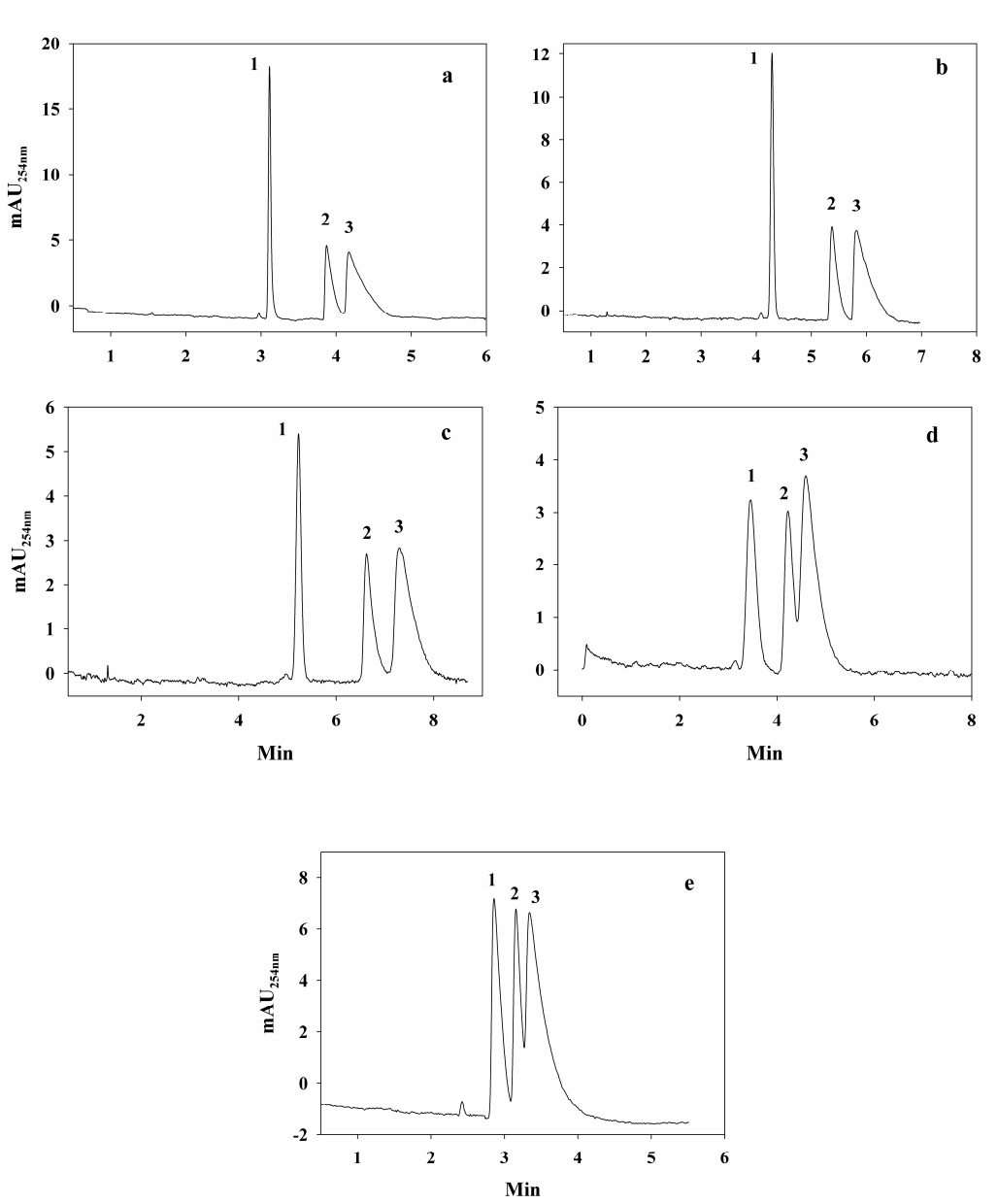

Figure 5. *Effect of pH on the separation of pNP-N-acetyl-α-D glucosaminide and pNP-N-acetyl-β-D glucosaminide. Conditions: WGA immobilized silica-based monolithic column, 20/27 cm ×100 μm ID; voltage, 20 kV; column temperature, 20 °C; mobile phase, 5 mM BisTris, 5 mM NaCl, 0.2 M GlcNAc; a. pH 3.5, b. pH 4, c. pH 5, d. pH 6, e. pH 7; solutes: 1, uracil; 2, pNP-N-acetyl-β-D-glucosaminide; 3, pNP-N-acetyl-α-D-glucosaminide.*

monosacharides under investigation is at around pH 5.0. This is manifested by a maximum in the k' values at around pH 5.0 (see Figure 6).

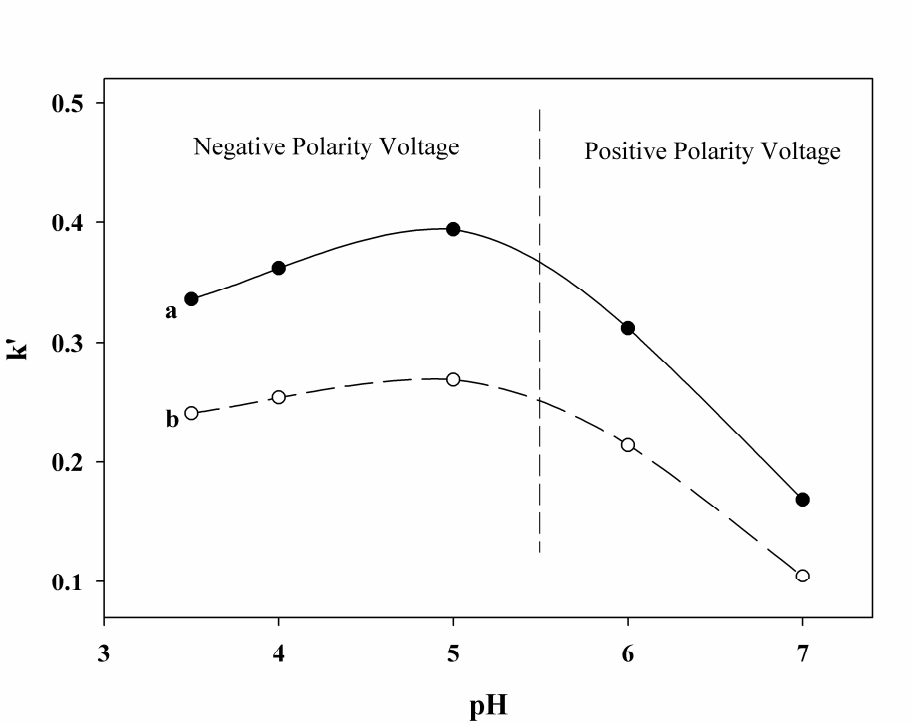

Figure 6. *Effect of pH on the retention factors of the pNP*-monosaccharides. *Conditions are the same as in Figure 3. a, pNP-N-acetyl-α-D-glucosaminide; b, pNP-N-acetyl-β-D-glucosaminide.*

Simultaneous separation of monosaccharide isomers and anomers Under the optimized separation conditions (as described in Figure 7), *oNP-N*-acetyl-α-D-glucosaminide, *pNP-N*-acetyl-α-D-glucosaminide and *pNP-N*-acetyl-β-D-glucosaminide (structures are shown in Figure 1) were separated from each other on the WGA immobilized silica monolith in the CEC mode. Glucosamine has weak affinity to WGA, and the affinity becomes stronger with a nitro group attached to the para position of the benzene ring [13, 14]. The affinity is the strongest when the nitro group is attached to the

ortho position. This is illustrated by the last peak of the *oNP-N*-acetyl-α-D-glucosaminide on the electrochromatogram.

It should be noted that in the nano-LC mode, *pNP-N*-acetyl-α-D glucosaminide and *pNP-N*-acetyl-β-D glucosaminide co-eluted.

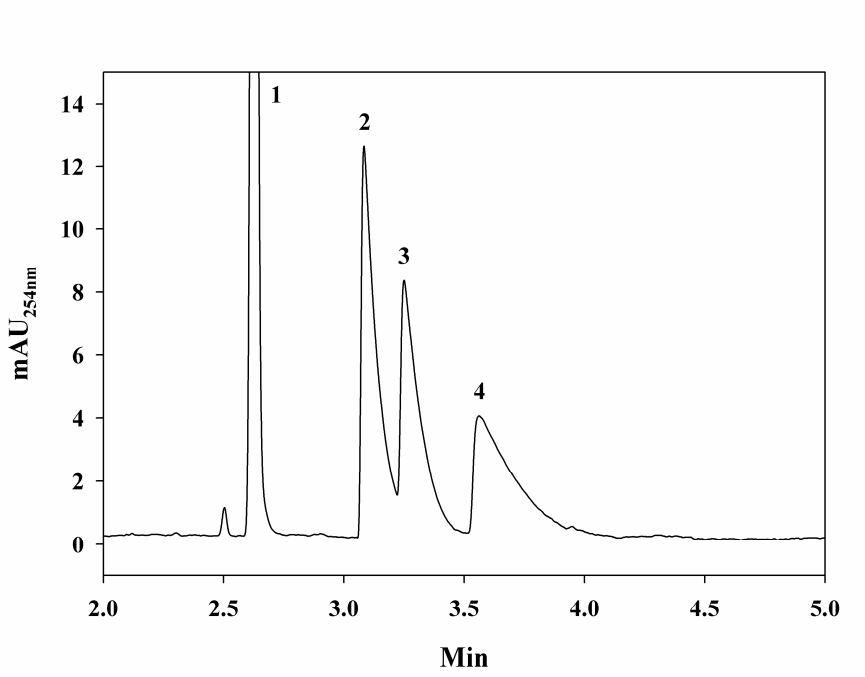

Figure 7. *Separation of pNP-N-acetyl-α-D-glucosaminide, pNP-N-acetyl-β-D-glucosaminide and oNP-N-acetyl-α-D-glucosaminide on the WGA immobilized silica monolith. Conditions: column size, 20/27 cm × 100 μm ID; voltage, 20 kV; column temperature, 20 °C; mobile phase, 5 mM BisTris, pH 5, 5 mM NaCl, 0.2 M GlcNAc; solutes: 1, uracil; 2, pNP-N-acetyl-α-D-glucosaminide; 3, pNP-N-acetyl-β-D-glucosaminide; 4, oNP-N-acetyl-α-D-glucosaminide.*

Characterization of the Silica-Based Lectin Affinity Monoliths with Glycoproteins

Con A immobilized silica monolith Con A exists as a dimer of two identical subunits of ~ 26 kDa at pH 4.5-5.6 and predominantly a tetramer at pH 7 or higher. Con A recognizes α-mannose, which is a common constituent for many glycoproteins such as serum and membrane glycoproteins. α-Methyl-D-glucopyranoside is a competitive inhibitor to Con A [17] called hapten sugar. The binding of the carbohydrates requires two metal ions, Ca^{2+} and a transition metal, usually Mn^{2+} [18]. The specificity of Con A toward oligosaccharides is shown in Figure 8.

Glycoproteins such as transferrin, ovalbumin, α_1-acid glycoprotein, glucose oxidase and ribonuclease B were employed to study the affinity interactions with the Con A immobilized on the silica monolith. The information about the structures of the *N*-glycans derived from transferrin, ovalbumin and α_1-acid glycoprotein are included in Chapter III.

The *N*-glycans of the human transferrin are di-, tri-, and tetraantennary glycans of complex type glycans with a high degree of sialylation on the outer-branch residues. As shown in Figure 9, almost all of the transferrin was retained on the Con A column. Since tri- and tetraantennary complex type glycans that are bound to transferrin (see Chapter III) have a very weak affinity to Con A (see Figure 8), and the fact that all the transferrin was retained on the Con A column indicates that the two possible glycosylation sites of transferrin (Asn 413 and Asn 611) in the majority of transferrin molecules are mostly populated by the biantennary complex *N*-glycans that have stronger affinity to Con A than the tri- and tetraantennary complex glycans.

1. Structures exhibiting strong binding and requiring 0.2 M methyl-α-D-mannopyranoside for elution

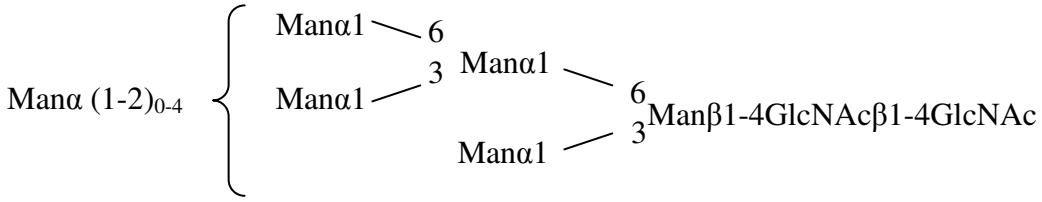

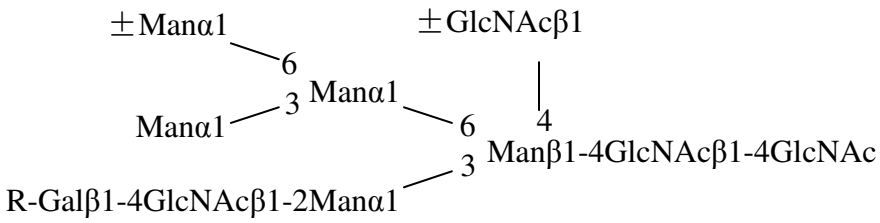

2. Structures possessing weak binding and requiring 0.005 M methyl-α-D-mannopyranoside for elution

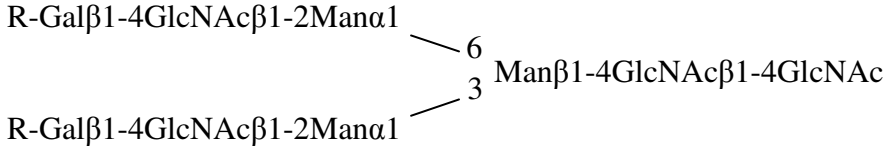

(+: With the residue; -: without the residue; R: H or sugar residue)

Figure 8. *Specificity of Con A toward N-glycans [19].*

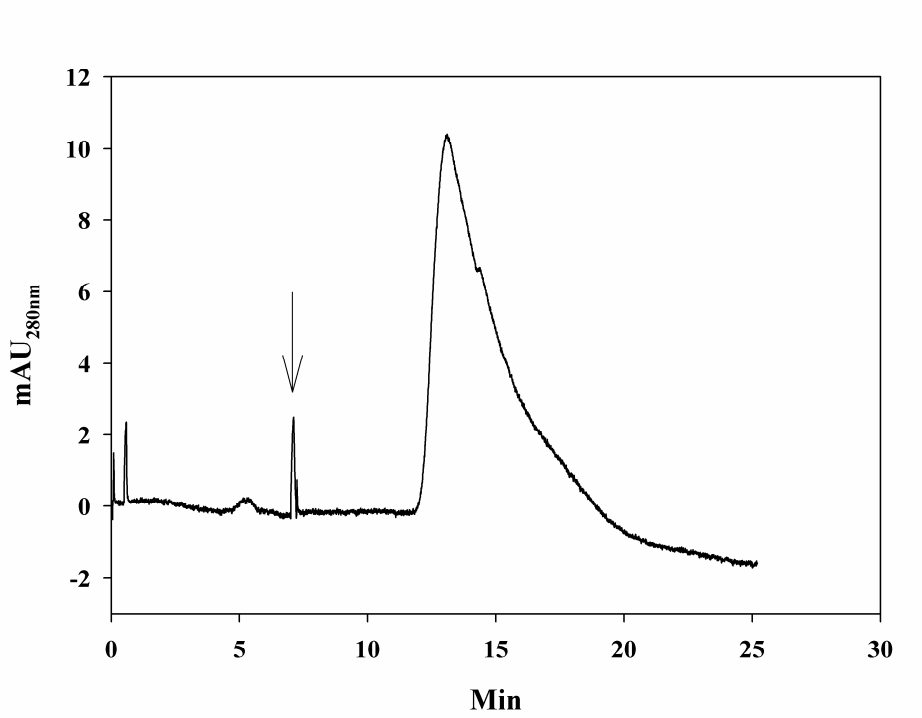

Figure 9. *Chromatogram of transferrin on the Con A immobilized silica monolithic column. Conditions: Con A silica monolithic column, 25/33 cm × 100 μm ID; arrow indicates the change to the eluting mobile phase. Binding mobile phase: 20 mM BisTris, pH 6.0, containing 100 mM NaCl, 1 mM Ca^{2+}, 1 mM Mn^{2+} and 1 mM Mg^{2+}; eluting mobile phase: 0.2 M Methyl α-D-manopyranoside in the binding mobile phase, introduced at 7.0 min as indicated by the arrow; separation pressure, 10 bar; column temperature, 20°C.*

Ovalbumin that has a single glycosylation site at Asn 292 to which various hybrid type and high mannose type *N*-glycans can be attached (see Chapter III) [20, 21], gave two peaks when chromatographed on the Con A column (Figure 10). One of the peaks eluted with the binding mobile phase while the elution of the second peak necessitated a stepwise elution with the hapten sugar. This may indicate that the first peak is mostly

ovalbumin molecules populated with hybrid type *N*-glycans that are not reactive with Con A.

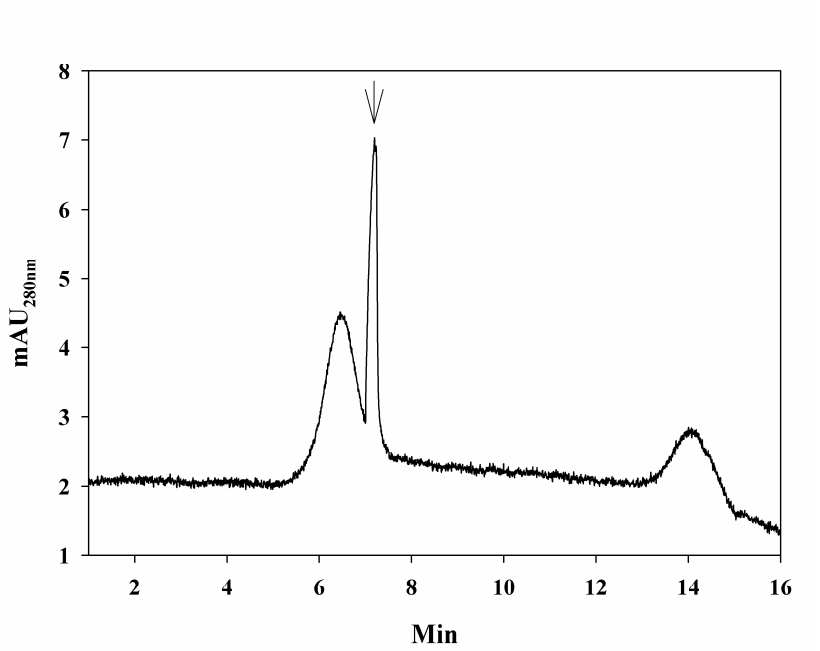

Figure 10. *Chromatogram of ovalbumin on the Con A immobilized silica monolithic column. Conditions are the same as in Figure 9.*

The intense peak of the non-retained α_1-acid glycoprotein on the Con A immobilized column (see Figure 11) might be explained by the fact that the glycosylation site of the majority of α_1-acid glycoprotein molecules are populated mostly by sialylated tri- and tetra-antennary complex type glycans which are not reactive with Con A while the small, retained peak may be attributed to the α_1-acid glycoprotein molecules that have biantennary complex type *N*-glycans that are weakly reactive with Con A.

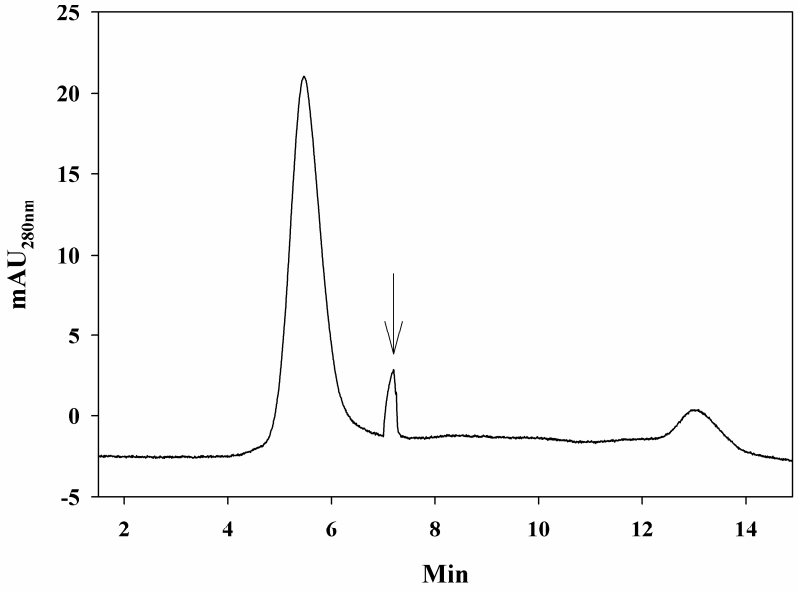

Figure 11. *Chromatogram of α_1-acid glycoprotein on the Con A-immobilized silica monolithic column. Conditions are the same as in Figure 9.*

WGA immobilized silica monolith This investigation studied the affinity interaction of α_1-acid glycoprotein, ovalbumin and κ-casein with the immobilized WGA. The specificity of WGA toward oligosaccharides is shown in Figure 12.

As shown in Figure 13, the majority of the α_1-acid glycoprotein glycoforms were retained by the WGA column and yielded an intense peak that eluted by a stepwise elution with GlcNAc hapten sugar. Only a very small fraction of α_1-acid glycoprotein eluted with the binding mobile phase in the dead volume of the column. Most likely, the high degree of sialylation of the *N*-glycans as well as the presence of repeating lactosamine blocks are responsible for the affinity of α_1-acid glycoprotein to the immobilized WGA.

1. Structures exhibiting strong binding and requiring 0.1 M GlcNAc for elution

GlcNAcβ1-4GlcNAc

GlcNAcβ1-4Manβ1-4GlcNAcβ1-4GlcNAc

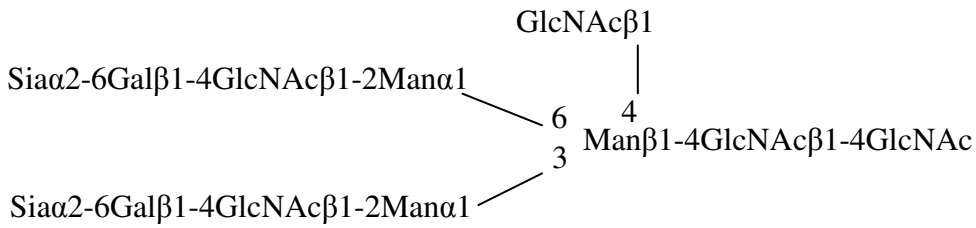

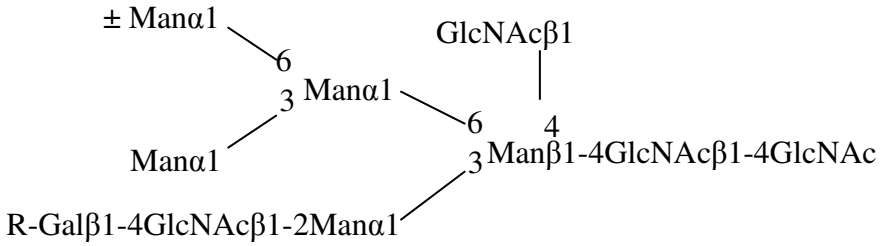

Cluster of sialic acid residues

2. Structures possessing weak binding

Poly-N-acetyllactosamine chains (R: H or sugar residue)

Figure 12. *Specificity of WGA toward N-glycans [19].*

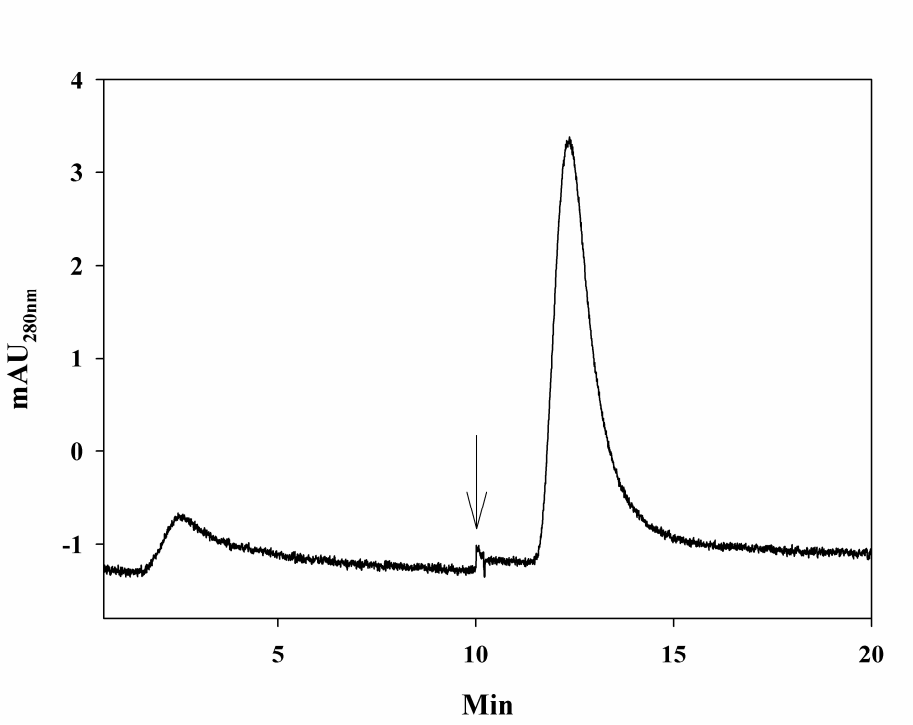

Figure 13. *Chromatogram of α_1-acid glycoprotein on the WGA immobilized silica monolithic column. Conditions: WGA silica monolithic column, 25/33 cm × 100 μm ID; arrow indicates the change to the eluting mobile phase. Binding mobile phase: 20 mM BisTris, pH 6.0, containing 100 mM NaCl; eluting mobile phase: 0.2 M GlcNAc in the binding mobile phase; separation pressure, 10 bar; column temperature, 20°C.*

Ovalbumin is a glycoprotein, which has various high mannose type and hybrid type *N*-glycans. The ovalbumin molecules bearing hybrid type *N*-glycans bind to the WGA and are thus retained on the column and eluted with the hapten sugar. The molecules of ovalbumin with high mannose type *N*-glycans have no affinity with WGA and therefore eluted first in the dead volume of the column with the binding mobile phase (Figure 14).

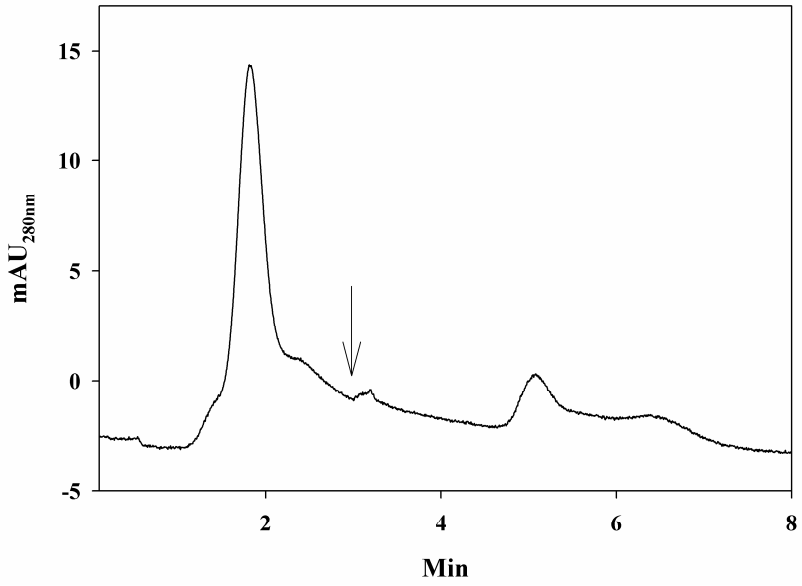

Figure 14. *Chromatogram of ovalbumin on the WGA immobilized silica monolithic column. Conditions are the same as in Figure 13.*

κ-Casein is the glycoprotein in bovine milk, whose *N*-glycans possess three different monosaccharides, i.e., galactose, *N*-acetylgalactosamine and *N*-acetylneuraminic acid. The *O*-glycans of the κ-casein identified are GalNAc, Gal-GalNAc disaccharide, NeuAc-Gal-GalNAC trisaccharide, Gal-(NeuAc)GalNAc trisaccharide and NeuAc-Gal-(NeuAc)GalNAc [2]. It is believed that the sialylated residues of the glycans of the κ-casein were bound to the WGA. The bound fraction of κ-casein that contains the molecules with sialylated glycans was eluted by the step gradient with GlcNAc, while the unretained fraction which eluted at the dead volume of the column with the binding mobile phase has the κ-casein molecules without the glycans that are reactive with WGA (see Figure 15).

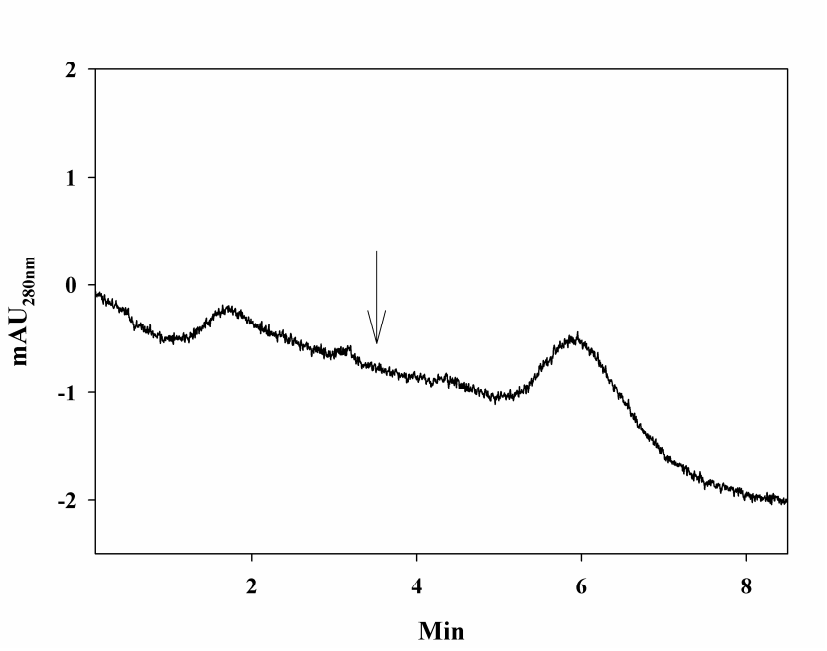

Figure 15. *Chromatogram of κ-casein on the WGA immobilized silica monolithic column. Conditions are the same as in Figure 13.*

Conclusions

In summary, through reductive amination reaction, lectins such as Con A and WGA were successfully immobilized onto the surface of silica monolith. While lectin affinity chromatography and electrochromatography using silica monolithic support was very useful for affinity separation of some monosaccharides as well as some acidic glycoproteins (e.g., tranferrin, ovalbumin, α_1-acid glycoprotein), the use of monolithic silica was not suitable for lectin affinity chromatography or electrochromatography of basic glycoproteins such as ribonuclease B (pI = 8.9). Basic glycoproteins are thought to undergo electrostatic interactions (i.e., non-specific interactions) with the negatively charged residual silanols at the surface of the lectin silica monolith. These nonspecific

interactions may have contributed to the strong binding of basic proteins and subsequently their low recovery from the lectin affinity monolithic silica column. These observations have led us to investigate acrylate-based monoliths, which are the subject of the next two chapters (i.e., Chapters V and VI).

REFERENCES

[1] Mallik, R., H., X., Hage, D. S., *J. Chromatogr. A* **2007**, *1149*, 294.

[2] Calleri, E., Massolini, G., Lubda, D., Tmporini, C., Loiodice, F., Caccialanza, G., *J. Chromatogr. A* **2004**, *1031*, 93.

[3] Calleri, E., Temporini, C., Perani, E., Stellam, C., Rudaz, S., Lubda, D., Mellerio, G., Veuthey, J. L., Caccialanza, G., Massolini, G., *J. Chromatogr. A* **2004**, *1045*, 99.

[4] Calleri, E., Marrubini, G., Massolini, G., Lubda, D., de Gaziio, S. S., Furlanetto, S., Wainer, I. W., Manzo, L., Caccialanza, G., *J. Pharmaceut. Biomed. Anal.* **2004**, *35*, 1179.

[5] Xuan, H., Hage, D. S., *Anal. Biochem.* **2006**, *346*, 300.

[6] Xuan, H., Hage, D. S., *J. Sep. Sci.* **2006**, *29*, 1412

[7] Madera, M., Mechref, Y., Klouckova, I., Novotny, M. V., *J. Chromatogr. A* **2006**, *845*, 121.

[8] Madera, M., Mechref, Y., Novotny, M. V., *Anal. Chem.* **2005**, *77*, 4081.

[9] Xiong, L., Andrews, D., Regnier, F., *J. Proteome Res.* **2003**, *2*, 618.

[10] Cartellieri, S., Hamer, O., Helmholz, H., NIiemeyer, B., *Biotechnol. Appl. Biochem.* **2002**, *35*, 83.

[11] Honda, S., Suzuki, S., Nita, T., Kakehi, K., *J. Chromatogr.* **1988**, *438*, 73.

[12] Krogh, T. N., Berg, T., Hojrup, P., *Anal. Biochem.* **1999**, *247*, 153.

[13] Bedair, M., El Rassi, Z., *J. Chromatogr. A* **2005**, *1079*, 236.

[14] Okanda, F., El Rassi, Z., *Electrophoresis* **2006**, *27*, 1020.

[15] Bundy, J. L., Fenselau, C., *Anal. Chem.* **1999**, *71*, 1460.

[16] Bundy, J. L., Fenselau, C., *Anal. Chem.* **2001**, *73*, 751.

[17] Goldstein, I., Hollerman, C., Smith, E., *Biochem* **1965**, *4*, 876.

[18] Grimaldi, J., Sykes, B., *J. Biol. Chem.* **1975**, *250*, 1618.

[19] Fukuda, M., Kobata, A., *Glycobiology A Practical Approach*, Oxford University Press, New York **1993**.

[20] An, H. J., Peavy, J. L., Hedrick, J. L., Lebrilla, C. B., *Anal. Chem.* **2003**, *75*, 5628.

[21] Ohyama, Y., Kasai, K., Nomoto, H., Inoue, Y., *J. Biol. Chem.* **1985**, *260*, 6882.

CHAPTER V

DEVELOPMENT OF NOVEL POLAR ORGANIC POLYMER MONOLITHS FOR NORMAL PHASE NANO LIQUID CHROMATOGRAPHY AND CAPILLARY ELECTROCHROMATOGRAPHY OF POLAR SPECIES

Introduction

Ever since the concept of the rigid monolithic stationary phase based on methacrylate ester was introduced by Svec and Frechet in the 1990's [1, 2], and Hjerten et al announced the preparation of the highly crosslinked acrylamide-based continuous bed for use in CEC in 1995 [3], the polymer-based monoliths have been developed and applied rapidly to LC and CEC separations in reverse phase chromatography, normal phase chromatography including HILIC, affinity chromatography and ion-exchange chromatography (IC). As described in Chapter II, in addition to the nonpolar (or hydrophobic) polymer monoliths, many papers have been published on the development and application of the hydrophilic polymer monoliths for uses in IC, affinity chromatography and NPC including the chiral separation and HILIC. However, there were only a few papers about the polar polymer monolith used in HILIC [4-7]. In this regard, this investigation is to develop a new polar polymer monolith that is useful in the

HILIC. Also, it is expected that this monolith is applicable to the further protein modification *via* the Schiff base reaction due to its vicinal hydroxyl groups.

Hydrophilic and the hydrophobic polymer monoliths can be prepared by the direct synthesis [8] and by indirect synthesis that involves post-modifications of the parent monoliths to introduce the desired ligands [9]. In the direct synthesis, monomers that possess the desired functionalities were selected and subjected to a one-step copolymerization. The preparation is very straightforward and convenient, and the functionalities are readily available in the monolith formed. Different monoliths can be obtained by changing the monomers, crosslinkers, porogens and the reaction conditions such as temperature and reaction time. In the indirect synthesis, a parent monolith was firstly produced followed by a post-modification. The indirect synthesis has the advantage of more controllability on the monolith structure [10].

The most popular functional monomer that is used for indirect synthesis of the acrylate-based polymer monolithic stationary phases is the GMA [11, 12]. The advantage of using GMA is that it has an epoxy group for subsequent ring opening to generate vicinal hydroxyl groups (or 1,2-diols) for further surface modification reactions. However, the ring opening reaction requires sulfuric acid treatment under high temperature. This may cause the problem of corrosion when stainless steel is employed in column fabrication. Thus, it is the aim of this investigation to develop an organic polymeric monolith which is friendly to the column material and at the same time provides sufficient surface area and high column efficiency for separation, and which can also be used as the polar stationary phase in the normal phase chromatography (NPC) or

normal phase capillary electrochromatography (NP-CEC) as well as supporting material for affinity chromatographic columns.

The preparation of the organic monoliths is generally based on radical polymerization that is a kinetically controlled process [13]. The factors that affect the kinetic polymerization process also influence the pore morphology of the monoliths. These factors include the varieties and concentrations of the functional monomer, the crosslinker, the porogen solvent and the initiator, the temperature, dose and dose rate, etc [14]. This study focused on the effects of the monomer, the crosslinker and the porogen solvent on the column performance.

In the fabrication of the acrylate-based monolith, EDMA is one of the most widely used crosslinkers [15, 16]. Trimethylolpropane trimethacrylate (TRIM) that has three methacrylate functions per molecule can be an alternative to EDMA. To study the effect of different crosslinkers on the properties of the acrylate-based monolith, column performance of the DIOL monolith and GMA monolith using EDMA and TRIM as the crosslinkers were investigated. As will be shown in this chapter, the monolith, which employed glycerol monomethacrylate as the functional monomer was found to be a polar stationary phase for NPC and NP-CEC, and a good parent monolith for further protein immobilization to produce columns for affinity chromatography.

Experimental

Instrumentation

The instrument used in this study was the same as the one described in Chapter III.

Chemicals and Materials

Glyceryl monomethacrylate was from Monomer-Polymer & Dajac Labs, Inc. (Feasterville, PA, USA). Glycidyl methacrylate, ethylene glycol dimethacrylate, 2, 2'-azobis(isobutyronitrile) (AIBN), trimethylolpropane trimethacrylate and 1-dodecanol were from Aldrich (Milwaukee, WI, USA). Cyclohexanol, acetonitrile (HPLC grade) were from Fisher Scientific (Fair Lawn, NJ, USA). Sodium periodate was from Fluka Chemical Corp. (Milwaukee, WI, USA). The rest of the chemicals used in this Chapter were the same as those in Chapter III.

Column Preparation

Column pretreatment A fused-silica capillary (33 cm × 100 μm) was filled with 1.0 M sodium hydroxide and kept for 30 min, then a 0.1 M hydrochloric acid was pushed into the column for 30 min. It was then rinsed with water followed by acetone. The inner wall of the capillary was allowed to react with a 50% (v/v) of 3-

(trimethoxysilyl)propyl methacrylate in acetone for 2 h for inner wall vinylization. The capillary was rinsed with acetone and then dried with a stream of nitrogen.

Fabrication of GMA monolith A polymer precursor solution weighing 2 g was prepared by mixing 0.360 g GMA, 0.240 g EDMA, 1.176 g cyclohexanol, 0.224 g dodecanol and 0.006 g AIBN with a Vortex. The resulting solution was sonicated for 1 min and then degassed by a stream of nitrogen gas for 5 min before it was introduced into the dry and vinylized capillary described in the previous section. The ends of the capillary were connected with a Teflon tube, and the capillary was heated in a water bath at 50 °C for 24 h. The resulting monolith with the surface epoxy functionalities was rinsed with ACN and water and then used for further reactions. To open the epoxy ring, a solution of 0.2 M H_2SO_4 was introduced into the column and the column was heated at 80 °C for 3 h (Figure 1). Finally the column was rinsed with water and used for further reactions.

Fabrication of DIOL monolith A polymerization solution was prepared by mixing 0.500 g glyceryl monomethacrylate, 0.350 g EDMA (or TRIM), 0.269 g cyclohexanol, 1.123 g dodecanol and 0.008 g AIBN. The mixture was mixed by a Vortex, sonicated for 1 min and finally degassed by a stream of nitrogen gas for 5 min before it was introduced into a dry and vinylized capillary. The ends of the capillary were connected with a Teflon tube, and the capillary was heated in a water bath at 50 °C for 24 h. The resulting column was rinsed with ACN and used as a polar stationary phase with bonded hydroxyl functionalities (Figure 1).

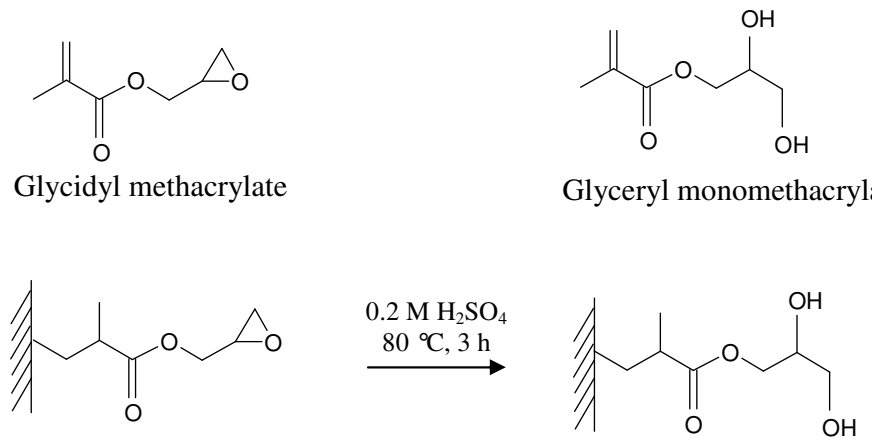

Figure 1. *Structures of the monomers used for the GMA monolith and the DIOL monolith and the schematic of the conversion from the GMA monolith to the DIOL monolith.*

Specific Surface Area Measurement by BET

The method used here is the same as that described in Chapter III.

Preparation of Glycans

The method used to prepare glycans is the same as that described in Chapter III.

Derivatization of Carbohydrates with 2-AB

The method used for precolumn derivatization of glycans is the same as that described in Chapter III.

Results and Discussion

Chromatographic Characterization of the Polar Monolith

Polymer precursor solutions were prepared by mixing 0.500 g GMA or glyceryl monomethacrylate (DIOL), 0.350 g EDMA or TRIM, 0.990 g cyclohexanol, 0.990 g dodecanol and 0.008 g AIBN. The monoliths with different functional monomers and different crosslinkers were prepared following the procedures described in the Experimental section.

DIOL monolith with EDMA or TRIM as the crosslinker The monolith with DIOL as functional monomer and EDMA (or TRIM) as crosslinker was prepared by the method described above (see Experimental). The column performance was evaluated by a test sample mixture containing toluene, DMF, formamide and thiourea in the modes of both nano-LC and CEC (see Figures 2-5). The column dead time t_0, EOF, column efficiency and retention factor k' of DMF, formamide and thiourea were calculated and compared (Tables 1 and 2).

In the nano-LC mode, the DIOL monolith with EDMA as crosslinker (hereafter denoted as DIOL-EDMA), when compared to the DIOL monolith with TRIM as crosslinker (denoted as DIOL-TRIM) had longer t_0, slightly lower k' and lower column efficiency, while in the CEC mode, it had higher EOF, lower k' and higher column efficiency. The solubility parameters of EDMA and TRIM are 18.2 and 18.5 $MPa^{1/2}$, respectively [14]. Therefore, the effects of the solubility of EDMA and TRIM on

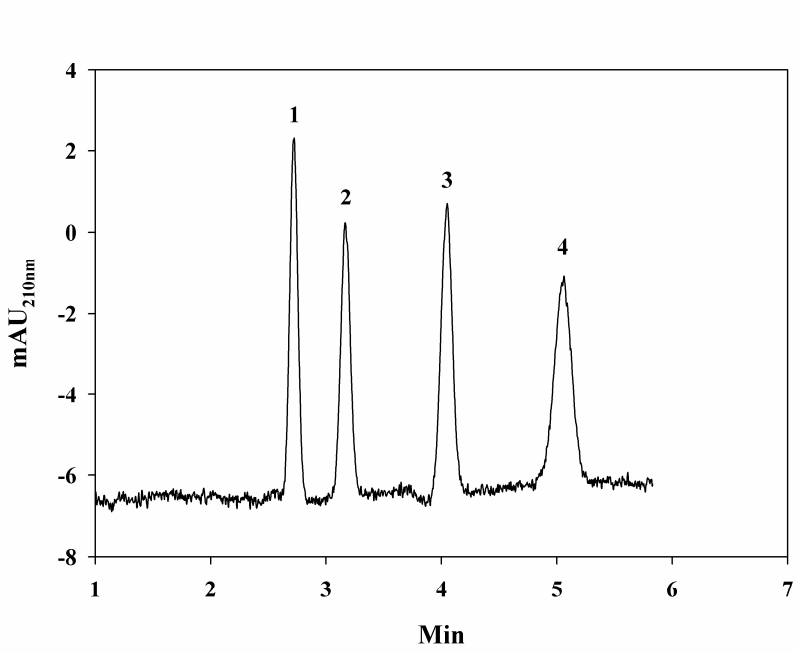

Figure 2. *Chromatogram of the test mixture on DIOL-EDMA column in the nano-LC mode. Conditions: column size, 25/33 cm × 100 μm ID; mobile phase, hydro-organic solution made up of 95% v/v ACN, 5% v/v of 5 mM NH_4Ac (pH 6.0); separation pressure, 10 bars; column temperature, 20 °C. Solutes: 1, toluene; 2, DMF; 3, formamide; 4, thiourea.*

the morphology of the monolith are about the same. On the other hand, EDMA (FW = 198.22) has a higher fraction of methacrylate groups available for polymerization than TRIM (FW = 338.40). High content of crosslinker is helpful to obtain monoliths with large surface area but at the cost of limited permeability to liquids because of the highly developed surface area [11]. This explains why DIOL-EDMA had a higher t_0 (2.35 min) than DIOL-TRIM (1.60 min) in the mode of nano-LC (Table 1). The high retention factors of the solutes on the DIOL/TRIM monolith imply that the TRIM helped to

produce the monolith with smaller pore size in the specific polymerization system described above.

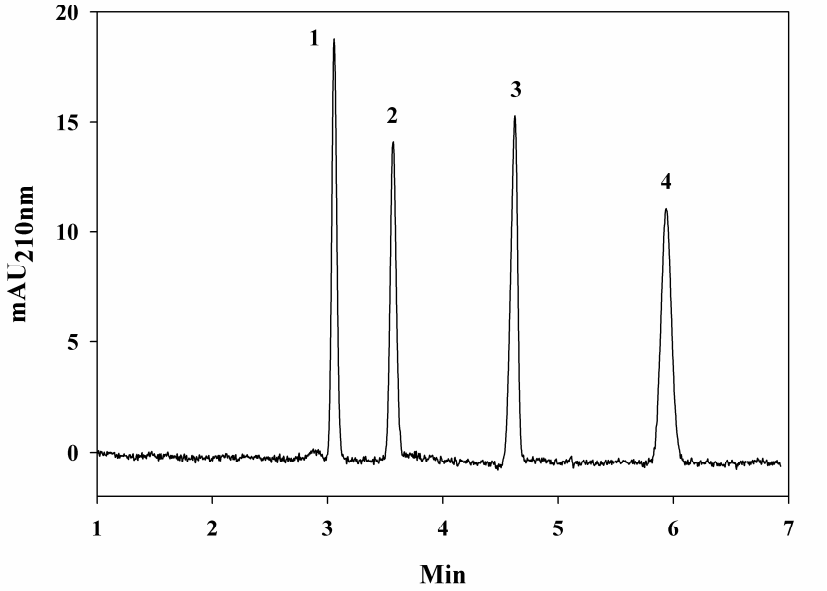

Figure 3. *Electrochromatogram of the test mixture on DIOL-EDMA column in the CEC mode. Conditions: column size, 25/33 cm × 100 μm ID; Mobile phase, hydro-organic solution made up of 95% v/v ACN, 5% v/v of 5 mM NH_4Ac (pH 6.0); voltage, 20 kV; column temperature, 20 °C. Solutes: 1, toluene; 2, DMF; 3, formamide; 4, thiourea.*

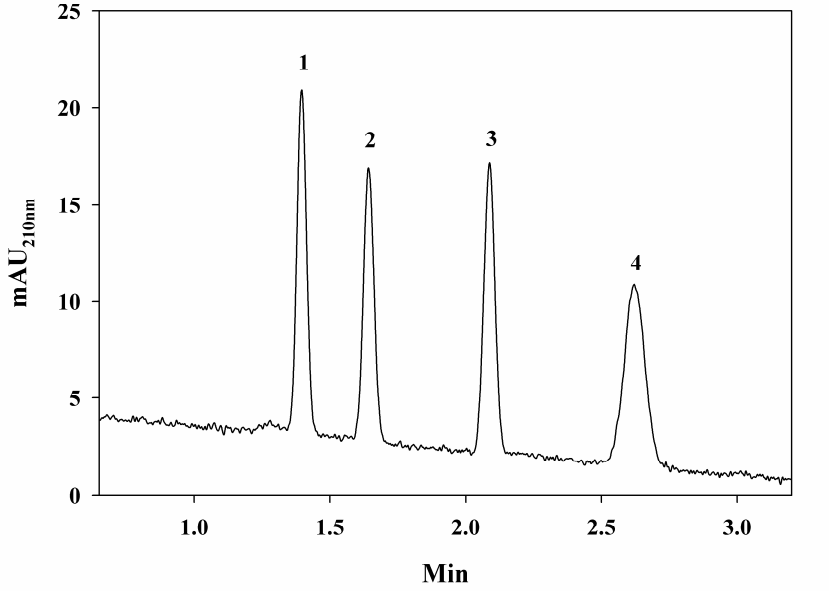

Figure 4. *Chromatogram of the test mixture on DIOL-TRIM column in the nano-LC mode. Solutes: 1, toluene; 2, DMF; 3, formamide; 4, thiourea. Conditions are the same as in Figure 2.*

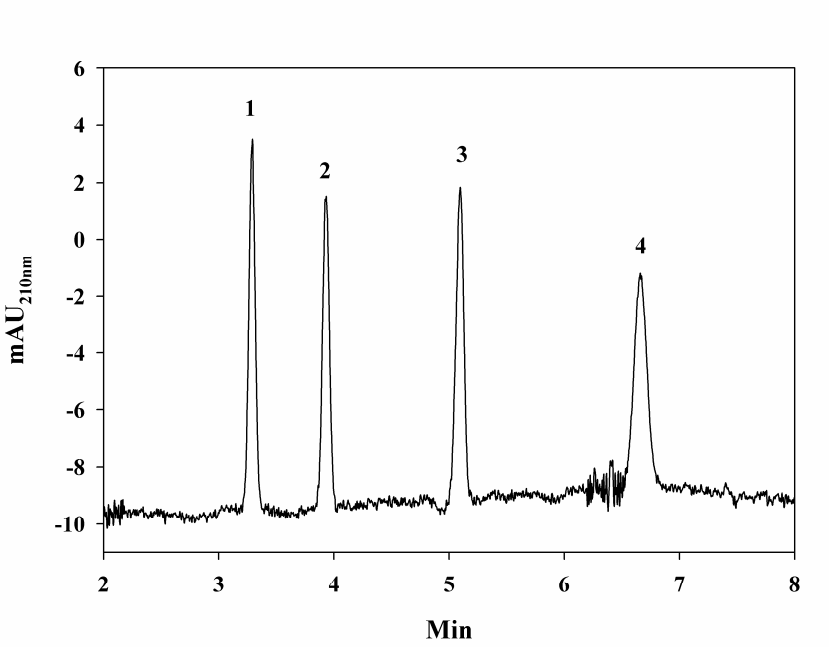

Figure 5. *Electrochromatogram of the test mixture on DIOL-TRIM column in the CEC mode. Solutes: 1, toluene; 2, DMF; 3, formamide; 4, thiourea. Conditions are the same as in Figure 3.*

TABLE 1.

COMPARISION OF COLUMN PERFORMANCES OF DIOL-EDMA AND DIOL-TRIM MONOLITHS IN THE NANO-LC MODE

Crosslinker	t_0 (min)	k'_{DMF}	$k'_{Formamide}$	$k'_{Thiourea}$	Average Plate Number Per Meter
EDMA	2.35	0.165	0.491	0.854	25,900
TRIM	1.60	0.179	0.499	0.884	33,500

Conditions are the same as in Figure 2. Values are average of two measurements.

TABLE 2.

COMPARISION OF COLUMN PERFORMANCES OF DIOL-EDMA AND DIOL-TRIM MONOLITHS IN THE CEC MODE

Crosslinker	EOF(mm/sec)	k'_{DMF}	$k'_{Formamide}$	$k'_{Thiourea}$	Average Plate Number Per Meter
EDMA	1.37	0.168	0.510	0.933	94,200
TRIM	1.26	0.191	0.537	0.996	78,300

Conditions are the same as in Figure 2. Values are average of two measurements.

Opened epoxy ring GMA monolith with EDMA/TRIM as crosslinker The monolith with GMA as the functional monomer and EDMA (or TRIM) as crosslinker was prepared by the method described above (see Experimental). The column performance was evaluated with a test sample mixture containing toluene, DMF, formamide and thiourea in nano-LC and CEC modes (see Figures 6-9). The column dead time t_0, EOF, column efficiency and retention factor k' of DMF, formamide and thiourea were calculated and compared (Tables 3 and 4).

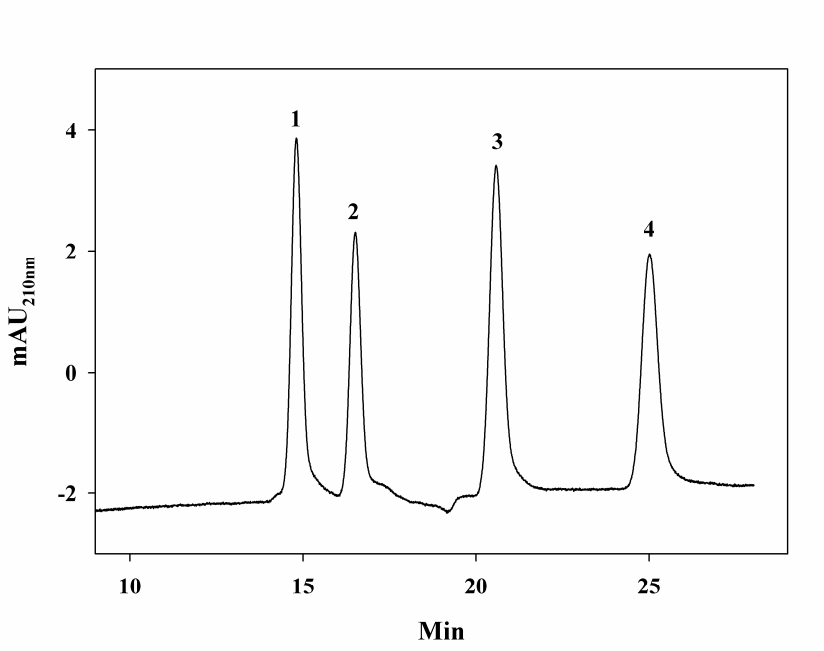

Figure 6. *Chromatogram of the test mixture on epoxy-opened GMA-EDMA column in the nano-LC mode. Solutes: 1, toluene; 2, DMF; 3, formamide; 4, thiourea. Conditions are the same as in Figure 2.*

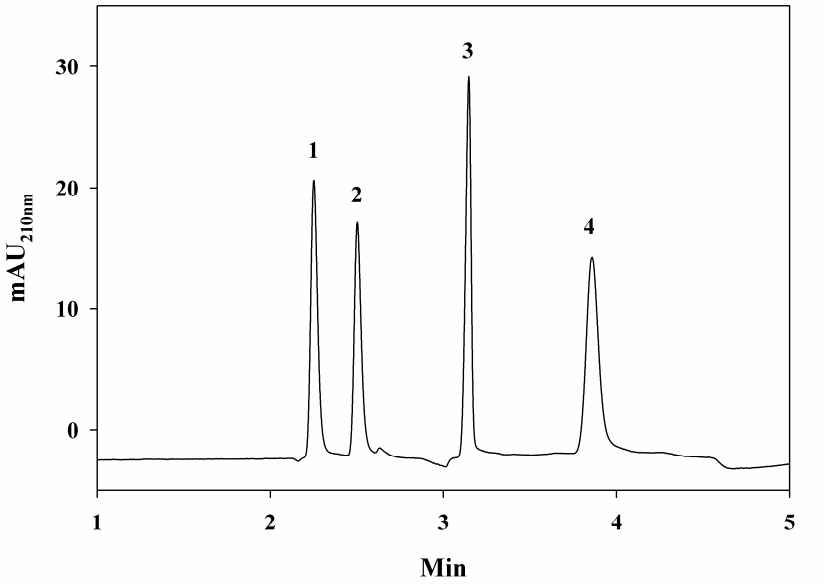

Figure 7. *Electrochromatogram of the test mixture on epoxy-opened GMA-EDMA column in the CEC mode. Solutes: 1, toluene; 2, DMF; 3, formamide; 4, thiourea. Conditions are the same as in Figure 3.*

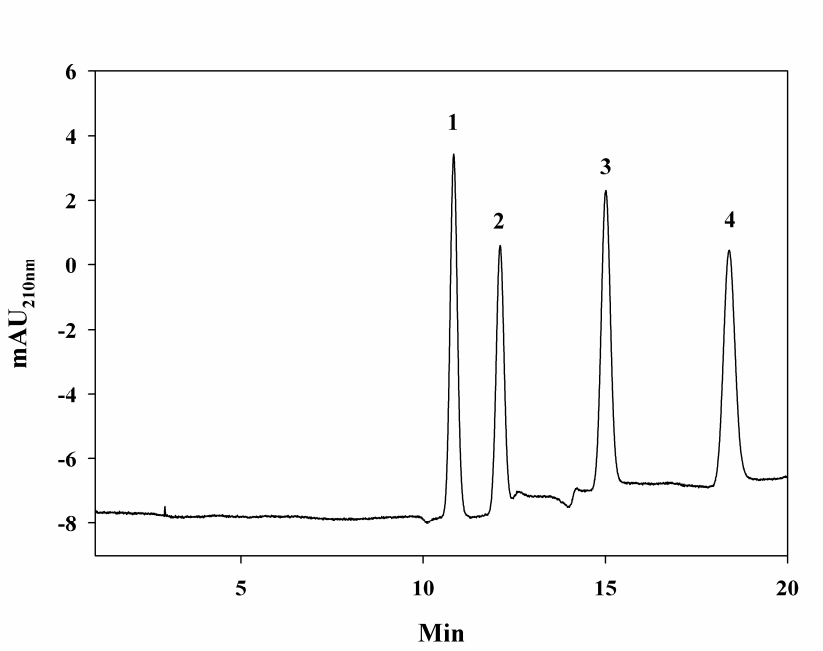

Figure 8. *Chromatogram of the test mixture on epoxy-opened GMA-TRIM column in the nano-LC mode. Solutes: 1, toluene; 2, DMF; 3, formamide; 4, thiourea. Conditions are the same as in Figure. 2.*

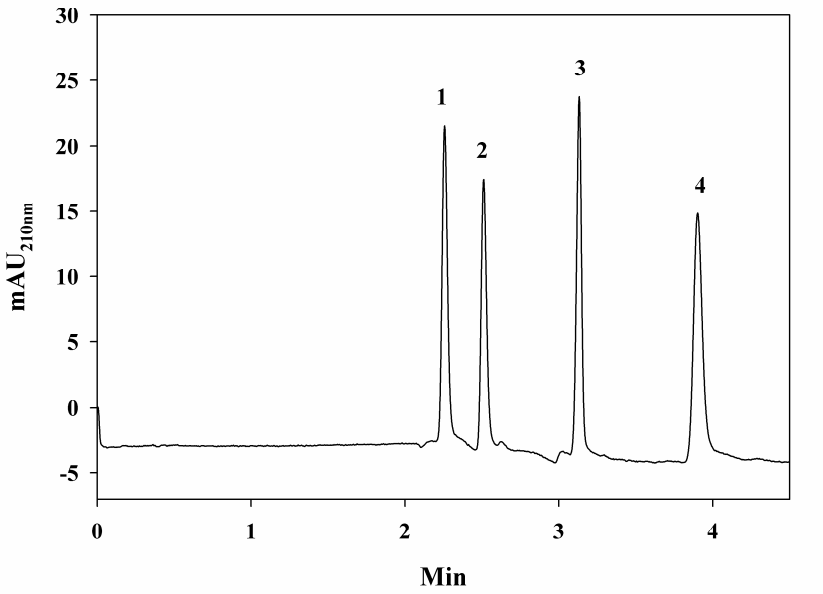

Figure 9. *Electrochromatogram of the test mixture on epoxy-opened GMA-TRIM column in the CEC mode. Solutes: 1, toluene; 2, DMF; 3, formamide; 4, thiourea. Conditions are the same as in Figure 3.*

TABLE 3.

COMPARISION OF COLUMN PERFORMANCES OF GMA-EDMA AND GMA-TRIM MONOLITHS IN THE NANO-LC MODE

Crosslinker	t_0 (min)	k'_{DMF}	$k'_{Formamide}$	$k'_{Thiourea}$	Average Plate Number Per Meter
EDMA	14.80	0.116	0.387	0.690	50,700
TRIM	10.76	0.116	0.387	0.699	59,800

Conditions are the same as in Figure 2. Values are average of two measurements.

TABLE 4.

COMPARISION OF COLUMN PERFORMANCES OF GMA-EDMA AND GMA-TRIM MONOLITHS IN THE CEC MODE

Crosslinker	EOF(mm/sec)	k'_{DMF}	$k'_{Formamide}$	$k'_{Thiourea}$	Average Plate Number Per Meter
EDMA	1.85	0.112	0.396	0.713	97,500
TRIM	1.84	0.112	0.386	0.728	123,000

Conditions are the same as in Figure 3. Values are average of two measurements.

In the CEC mode, the EOF and the retention behaviors of the solutes on the GMA monolith with TRIM as crosslinker (denoted as GMA-TRIM) were nearly identical to those on the GMA monolith with EDMA as crosslinker (denoted as GMA-EDMA). In the nano-LC mode, similar to the DIOL monoliths, the GMA-EDMA monolith had higher t_0 than the GMA-TRIM monolith. This can be explained by the fact discussed above that the relatively high content of crosslinker resulted in a larger surface area but

poorer permeability to liquid. In CEC, since EOF is a plug-like flow, the change of the pore structure does not affect the flow of both solvent and solutes, therefore similar results were obtained for both columns. Conversely to DIOL-TRIM, GMA-TRIM had higher column efficiency than GMA-EDMA in the CEC mode. The high plate number of the GMA-TRIM monolith resulted from the relatively low retention factors.

The GMA monolith fabricated under the selected optimum conditions has a specific surface area of 20 m^2/g, while the DIOL monolith prepared under the same conditions has a surface area of 5.7 m^2/g. The low surface area indicates the large pore structure of the DIOL monolith fabricated under the selected conditions. This explains why the GMA monoliths had very high t_0 compared to that of the DIOL monoliths. It can be expected that the DIOL monolith prepared under optimum conditions will exhibit higher column efficiency in separations of polar species. For producing DIOL monolith with higher specific surface area, refer to Table 5.

Compared to the DIOL monolith that was prepared with the same concentration and procedures, the GMA monolith exhibited less permeability and weaker retentivity toward the polar solutes.

Column Performance of GMA Monolith Without Epoxy Ring Opening Treatment

A monolithic column was prepared by a method similar to fabricate the GMA-EMDA monolith but without the epoxy ring opening reaction. The column performance was evaluated by the same test sample mixture in the nano-LC mode. As shown in Figure 10, the elution order and the retention of the solutes were different from those on

the DIOL-TRIM/EDMA and the GMA-TRIM/EDMA monoliths. The difference might be originated from the nature of the less polar epoxy groups on the surface of the monolith.

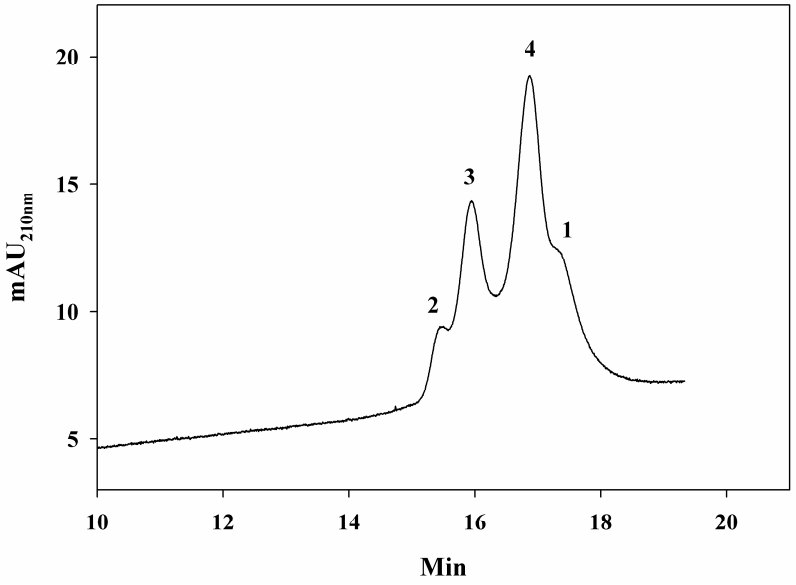

Figure 10. *Chromatogram of the test mixture on GMA column in the nano-LC mode. Solutes: 1, toluene; 2, DMF; 3, formamide; 4, thiourea. Conditions are the same as in Figure 2.*

Effect of the Porogen Composition on the Specific Surface Area of the Monolith

The most important factors that affect the porous structure of the organic monolith are the property of the porogenic solvents and their proportion to the monomers [11]. The porogenic solvent causes the change of the porous structure of the monolith through the "solvation of the polymer chains in the reaction medium during the early stages of the polymerization" [17]. The addition of a poor porogenic solvent leads to an early phase

separation of the polymer. The new phase swells with the monomers preferentially and thus the local density of the monomers in the swollen nuclei is higher than elsewhere in the solution. Also, the polymerization predominates in these swollen nuclei. The newly formed nuclei can be adsorbed by the large preglobules formed previously and as a result the size of the globules increases. This also causes larger voids in between the globules. As a contrast, a good porogenic solvent competes with the monomers in the solvation of the polymer. Therefore the local density of the monomers is low and the globules formed are small [17]. It was found that, the closer the solubility parameters of the monomer and the porogenic solvent, the smaller the pores of the monolith [18].

In this study, a combination of cyclohexanol and dodecanol was selected as the porogenic solvents for the DIOL monolith and the effect of the ratio of cyclohexanol to dodecanol on the specific surface area of the monolith was investigated. Table 5 shows the specific surface areas of the monoliths fabricated under different percentages of cyclohexanol and dodecanol with 0.500 g glyceryl monomethacrylate, 0.350 g EDMA and 0.008 g AIBN. It shows that the surface area of the monolith increased with an increased percentage of dodecanol in the mixture of the polymer precursor solution and with decreased percentage of cyclohexanol. The specific surface area increased linearly by increasing the ratio of the dodecanol to cyclohexanol. The solubility parameters of dodecanol and cyclohexanol are 20.5 and 23.3 $MPa^{1/2}$, respectively [19]. This implies that the solubility parameter of glyceryl monoacrylate is near or slightly below 20.5 $MPa^{1/2}$. The reason for the monolith no. 2 (see Table 5) to exhibit a specific surface area less than predicted by the curve in Figure 11 is that at the ratio of the two porogens equal to 1.00, the total percentage of the porogenic solvents (i.e. 69.8%) was higher than those

TABLE 5

EFFECT OF PERCENTAGES OF CYCOHEXANOL/DODECANOL ON

SPECIFIC SURFACE AREA

	Cyclohexanol		Dodecanol		Ratio	Specific Surface Area
Monolith	(g)	%	(g)	%	Dodecanol /Cyclohexanol	(m^2/g)
1	0.944	42.0	0.444	19.8	0.470	4.93
2	0.990	34.9	0.990	34.9	1.00	5.73
3	0.476	20.3	1.011	43.1	2.12	10.72
4	0.444	19.8	0.944	42.0	2.13	11.15
5	0.269	12.0	1.123	50.0	4.17	19.20

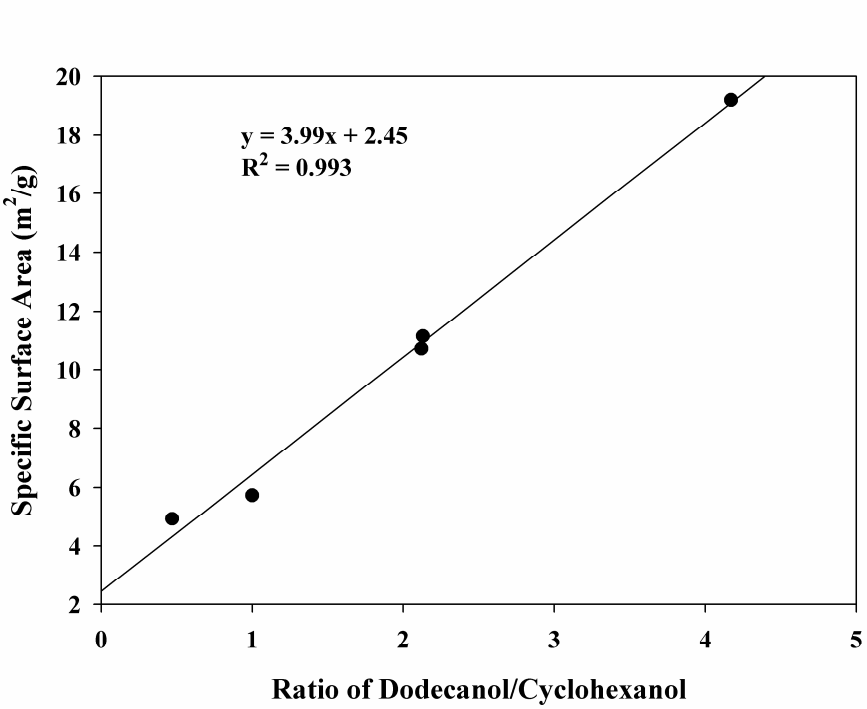

Figure 11. *Relationship between the specific surface area of the monolith and the ratio of dodecanol to cyclohexanol in the range studied.*

of the rest monoliths (~62%) (See Figure 11). The lower specific surface area of monolith no. 2 resulted from the larger pore formation due to the usage of larger amount of porogenic solvent.

Due to the favorably high specific surface area of monolith no. 5, which should yield higher retention for small solutes such as glycans, monolith no. 5 was used in the rest of the studies in this chapter as well as in lectin affinity chromatography of glycans in Chapter VI. On the other hand and for large protein molecules such as glycoproteins, monoliths of lower specific surface area such as monolith no. 2 was used in lectin affinity chromatography of glycoproteins in Chapter VI.

Profiling of Glycans on the DIOL Monolith

Nano-LC The DIOL monolith was tested in the profiling of glycans in the nano-LC mode. Figures 12a and 13a show the chromatograms of glycans derived from ovalbumin and α_1-acid glycoprotein, respectively, with a mobile phase containing 65 % ACN in the presence of 1 mM ammonium acetate (pH 6) and 1 mM sulfated β-CD. The increase of the ACN content in the mobile phase resolved more peaks for both kinds of glycan samples (see inserts in Figures 12b and 13b). Refer to Chapter III for the structures of glycans.

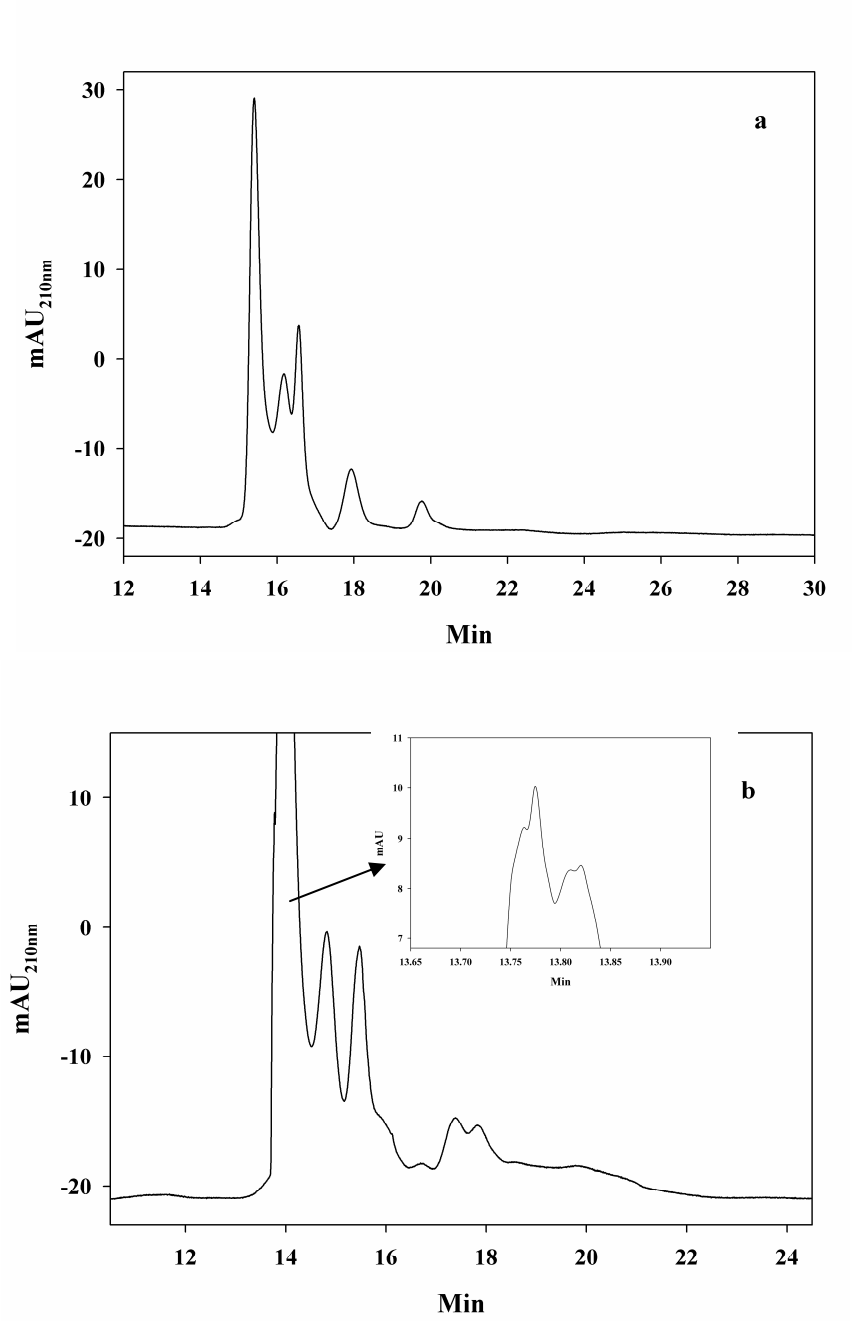

Figure 12. *Chromatograms of N-glycans derived from ovalbumin. Conditions: DIOL monolithic capillary column, 25/33 cm × 100 μm ID. Mobile phase, hydro-organic solution made up of 65% v/v ACN and 35% v/v of 1 mM NH_4Ac (pH 6.0) and 1 mM sulfated β-CD in (a) 75% v/v ACN and 25% v/v of 1 mM NH_4Ac (pH 6.0) and 1 mM sulfated β-CD in (b); separation pressure,10 bar; column temperature, 20 °C.*

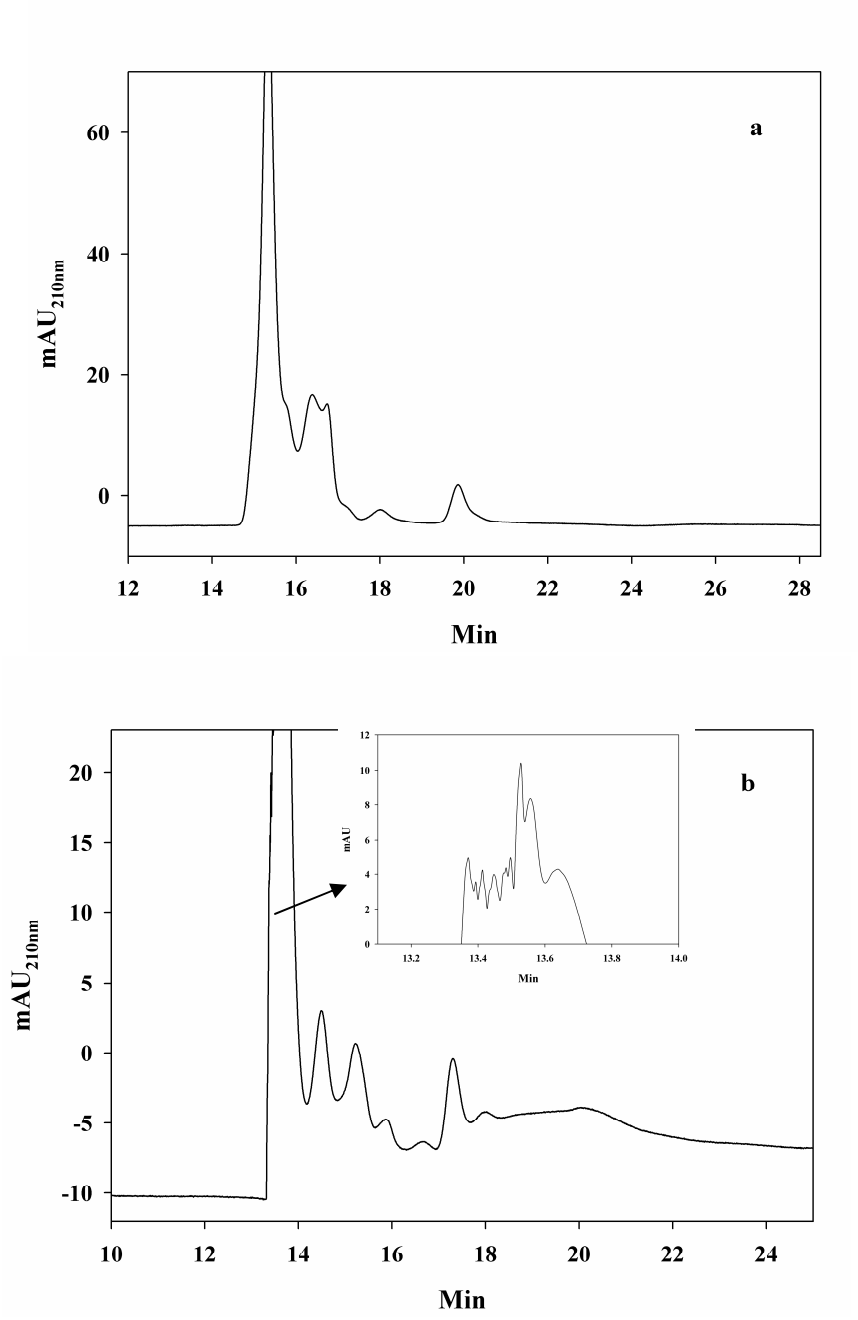

Figure 13. *Chromatogram of N-glycans derived from α_1-acid glycoprotein. Conditions are the same as in Figure 12.*

Returning to Figure 12, and analyzing the DAD spectra of the peaks revealed that the unresolved peaks eluting between 15 and 16 min (Figure 12a) or slightly resolved

peaks eluting between 13.5 and 14.5 min have UV characteristics of hybrid type glycans whereas the separated peaks eluting after 16 min in Figure 12a and after 14.5 min in Figure 12b displayed DAD spectra with UV characteristics of the high mannose type. This indicates that the hybrid type glycans are less polar than their counterpart high mannose type. In fact, high mannose glycans have mannose residues at the non reducing end while the hybrid type have mostly GlcNAc residues which are less polar than the mannose residues thus interacting less with the polar DIOL monolith.

As expected, the nano-LC profiling of the glycans derived from α_1-acid glycoprotein shown in Figure 13 yielded various peaks over a wide migration range. The glycans derived from α_1-acid glycoprotein are the complex type at different degree of sialylation. It is believed that the higher the degree of sialylation the more polar is the glycan and the higher is its retention on the polar DIOL monolith. In fact, the DAD spectra of the peaks in Figure 13a and 13b have UV characteristics of the sialylated complex type glycans.

CEC The CEC separation of the glycans on the DIOL monolith was also performed with the same running electrolyte solutions as those mobile phases used in the nano-LC mode. Figures 14 and 15 show the electrochromatograms of glycans derived from ovalbumin and α_1-acid glycoprotein, respectively, with an electrolyte solution containing 65 % ACN in the presence of 1 mM ammonium acetate (pH 6) and 1 mM sulfated β-CD. In the separation of the glycans from ovalbumin, a slightly better separation was achieved in nano-LC than in CEC, compare Figure 14 to Figure 12. Conversely, in the separation of the glycans from α_1-acid glycoprotein, most of the

solutes were eluted within 15 min in CEC with an improved resolution compared to that in nano-LC. The glycans from α_1-acid glycoprotein are sialylated and carry negative charges, a fact that favors CEC over nano-LC since the negatively charged glycans can undergo chromatographic partitioning as well as electrophoretic migration in CEC as opposed to chromatographic partitioning only in nano-LC.

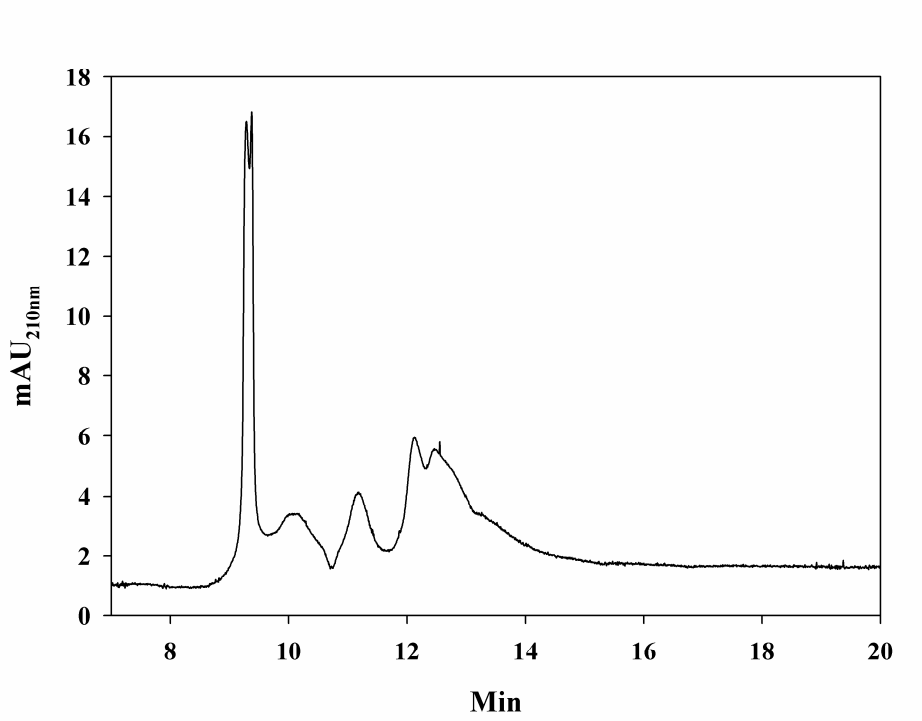

Figure 14. *Electrochromatogram of N-glycans derived from ovalbumin. Conditions: DIOL monolithic capillary column, 25/33 cm × 100 μm ID. Mobile phase, hydro-organic solution made up of 65% v/v ACN, 35% v/v of 1 mM NH_4Ac (pH 6.0) and 1 mM sulfated β-CD; voltage, 20 kV; column temperature, 20 °C.*

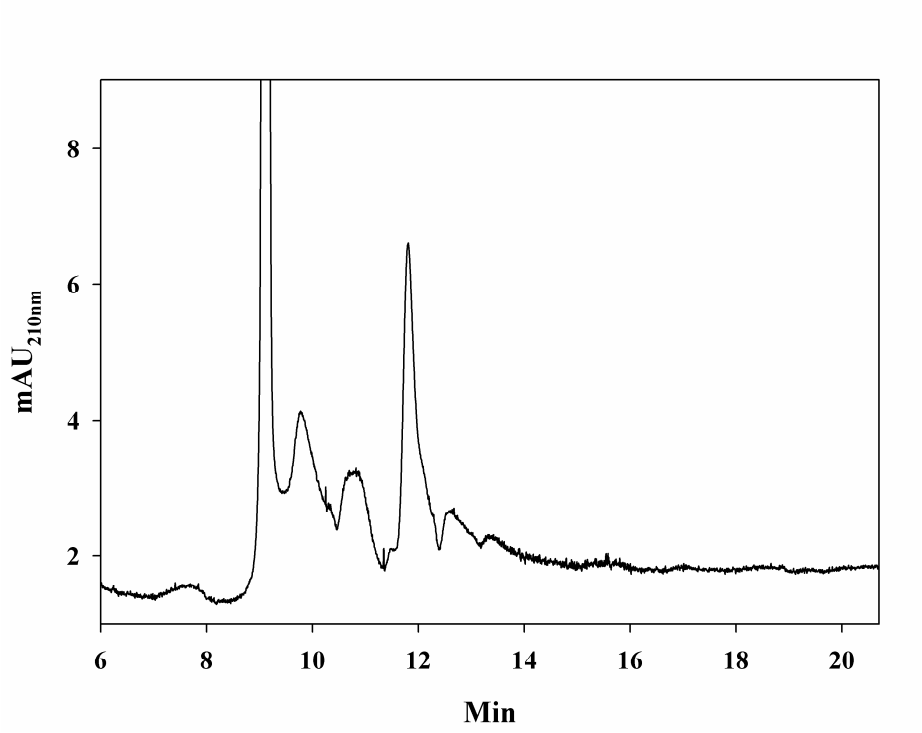

Figure 15. *Electrochromatogram of N-glycans derived from α_1-acid glycoprotein. Conditions are the same as in Figure 14.*

Conclusions

Monoliths incorporating TRIM as the crosslinker had higher flow rate than those with the EDMA crosslinker in nano-LC for both GMA-based and DIOL-based monoliths. With GMA as the functional monomer, the functions of the EDMA and TRIM were nearly identical except for the difference in the flow rate in nano-LC since they exhibited similar EOF in CEC and the same retention factor k' in both CEC and LC. In the case of DIOL used as the functional monomer, the DIOL-TRIM monolith had higher k' than the DIOL-EDMA monolith in both CEC and LC. The DIOL-EDMA monolith had a higher EOF than the DIOL-TRIM monolith in CEC. Fabricated with the same concentration

and procedures, DIOL monolith exhibited excellent permeability and strong retentivity compared to GMA monolith. The DIOL monolith was useful in the separation of the polar species including the glycans. It can be predicted that the DIOL monolith with the higher surface area will be an even more efficient stationary phase for NPC and NP-CEC.

REFERENCE

[1] Svec, F., Frechet, J. M. J., *Anal. Chem.* **1992**, *64*, 820.

[2] Svec, F., Frechet, J. M. J., *Science* **1996**, *273*, 205.

[3] Hjerten, S., Eaker, D., Elenbring, K., Ericson, C., Kubo, K., Liao, J., Zeng, C., Lidstrom, P. A., Lindh, A., Srichiayo, P., Valtcheva, L., Zhang, R., *Electrophoresis* **1995**, *39*, 105.

[4] Holdsvendova, P., Suchankova, J., Buncek, M., Backovska, V., Coufal, P., *J. Biochem. Biophys. Methods* **2007**, *70*, 23.

[5] Hosoya, K., Hira, N., Yamanoto, K., Nishimura, M., Tanaka, N., *Anal. Chem.* **2006**, *78*, 5729.

[6] Que, A. H., Konse, T., Baker, A. G., Novotny, M. V., *Anal. Chem.* **2000**, *72*, 2703.

[7] Que, A. H., Novotny, M. V., *Anal. Bioanal. Chem.* **2003**, *375*, 599.

[8] Gu, B., Chen, Z., Thulin, C. D., Lee, M. L., *Anal. Chem.* **2006**, *78*, 3509.

[9] Wieder, W., Bisjak, C. P., Huck, C. W., Pakry, R., Bonn, G. K., *J. Sep. Sci.* **2006**, *29*, 2478.

[10] Wu, R., Hu, L., Wang, F., Ye, M., Zou, H., *J. Chromatogr. A* **2008**, *1184*, 369.

[11] Vlakh, E. G., Tennikova, T. B., *J. Sep. Sci.* **2007**, *30*, 2801.

[12] Ponten, E., Viklund, C., Irgum, K., Bogen, S. T., Lindgren, A. N., *Anal. Chem.* **1996**, *68*, 4389.

[13] Li, W. H., Stover, H. D. H., *J. Appl. Polym. Sci. A* **1998**, *36*, 1543.

[14] Lai, J., Yang, M., Niessner, R., *Anal. Bioanal. Chem.* **2007**, *389*, 405.

[15] Hahn, R., Podgornick, A., Merhar, M., Schallaun, E., Jungbauer, A., *Anal. Chem.* **2001**, *73*, 5126.

[16] Yu, C., Xu, C., Svec, F., Frechet, J. M. J., *J. Polym. Sci. A: Polym. Chem.* **2002**, *40*, 755.

[17] Viklund, C., Svec, F., Frechet, J. M. J., *Chem. Mater.* **1996**, *8*, 744.

[18] Safrany, A., Beiler, B., Laszlo, K., Svec, F., *Polymer* **2005**, *46*, 2862.

[19] Jose, A. J., Ogawa, S., Bradley, M., *Polymer* **2005**, *46*, 2880.

CHAPTER VI

ACRYLATE-BASED LECTIN AFFINITY MONOLITHS AND THEIR APPLICATIONS TO GLYCOPROTEIN AND GLYCAN SEPARATIONS BY NANO LIQUID CHROMATOGRAPHY

Introduction

Monolithic stationary phases provide relatively low mass-transfer resistance compared to the conventional particle-based stationary phase materials [1], which is advantageous to minimize the problem of band spreading of macromolecules such as proteins. The monolithic materials that have been employed in affinity chromatography include GMA/EDMA (acrylate-based), agarose, cryogel, urea/formaldehyde and silica polymers [2]. Among these monoliths, GMA/EDMA is the most widely used polymer for affinity chromatography due to the fact that GMA/EDMA contains epoxy groups which can be later converted into vicinal hydroxyl groups via acidic hydrolysis for further immobilizations. As described in Chapter II, many papers have been published on the development and application of the polymer-based affinity monoliths. These monoliths have been applied to various kinds of affinity chromatography basing on interactions of enzyme affinity, immunoaffinity, lectin affinity, protein A affinity, protein

G affinity, immobilized metal affinity, sugar-based affinity and aptamer affinity, etc. However, there are only a few publications about the fabrication and application of the lectin affinity columns based on polymer monoliths [3-5]. Lectins are nonimmune system proteins that can recognize and bind certain carbohydrate residues [6]. They have been used to separate biomolecules that contain carbohydrate residues and to identify the types of the carbohydrates that have affinity interactions with a given biological agent. The investigation in this chapter seeks to expand the development and application of the lectin polymer-based monolith by developing a novel polymer monolith for lectin immobilization, and also by studying the interactions between the immobilized lectin and the carbohydrates and glycoconjugates. These lectin monoliths are expected to find future use in glycomics and proteomics studies. As will be shown in this chapter, the novel acrylate-based lectin affinity columns immobilized with Con A, WGA, RCA-I, jacalin and SNA, which were produced *via* a simplified and time efficient *in situ* polymerization method, exhibited strong interactions with particular glycoproteins and glycans. The mechanism of the affinity interactions between the ligand and the receptor will be illustrated.

According to the classification recently outlined by Kobata and Yamashita [7], lectins fall into three major categories: (i) lectins with specificities directed to the core portion of *N*-glycans, (ii) lectins which specifically interact with the non-reducing terminal moieties of outer chains and (iii) lectins with specificities involving the outer chain branching. Most lectins belong to categories (i) and (ii) and fewer to category (iii). To exploit the full potential of acrylate-based monoliths in lectin affinity chromatography (LAC), it was essential to select a few lectins that belong to the two major categories. In

this study, Con A and WGA were selected as typical lectins of category (i) while RCA-I and SNA were chosen as representative of category (ii). Furthermore, and to widen the usefulness of the monolithic columns developed in the framework of this study, jacalin lectin specific for *O*-glycans was selected to provide a complete set of LAC columns for the isolation and fractionation of a wide range of glycoconjugates, e.g., glycans and glycoproteins.

Experimental

Instrumentation

The instruments used in this chapter were the same as those described in Chapter III.

Chemicals and Materials

Elderberry Bark Lectin (SNA) and Jacalin were from Vector Laboratories Inc. (Burlingame, CA, USA). Avidin from egg white was from EMD Biosciences Inc. (San Diego, CA, USA). Fetal calf serum III fetuin, collagen type VI from human placenta, myoglobin, glucose oxidase and *pNP*-α-D-manopyranoside were from Sigma-Aldrich Fine Chemicals (St. Louis, MO, USA). The rest of chemicals and materials used in this chapter were the same as those described in previous chapters.

Preparation of the Monoliths

The monoliths were prepared following the methods described in Chapter V. The monolith with immobilized SNA was the GMA-EDMA type of monolith made by the method explained under the subtitle "Fabrication of GMA monolith" in the Experimental section of Chapter V. The rest of the monoliths used for other lectins immobilization were of the DIOL-EDMA type monoliths made using the fabrication conditions of the monolith no. 2 in Table 7 of Chapter V by the method described under the subtitle "Fabrication of DIOL monolith" in the Experimental section of Chapter V.

Immobilization of Lectin to the Surface of the Monolith

The GMA based monolithic column having EDMA as a crosslinker (denoted as GMA-EDMA monolith) whose epoxy groups were hydrolyzed to diols or the DIOL monolithic column (denoted DIOL-EDMA) was filled with a freshly prepared solution of 0.1 M $NaIO_4$ and the oxidation reaction was allowed to proceed for 1 h. The column was rinsed with water before it was filled with a solution containing the lectin to be immobilized. For Con A and WGA immobilization, the procedures described in Chapter III were followed. For RCA, jacalin and SNA immobilizations, solutions containing 5 mg/mL of lectin, 0.1 M NaAc (pH 6.4), 0.05 M $NaBH_3CN$ and 0.1 M galactose were used during lectin immobilization on the various monolithic columns (See Figure 1).

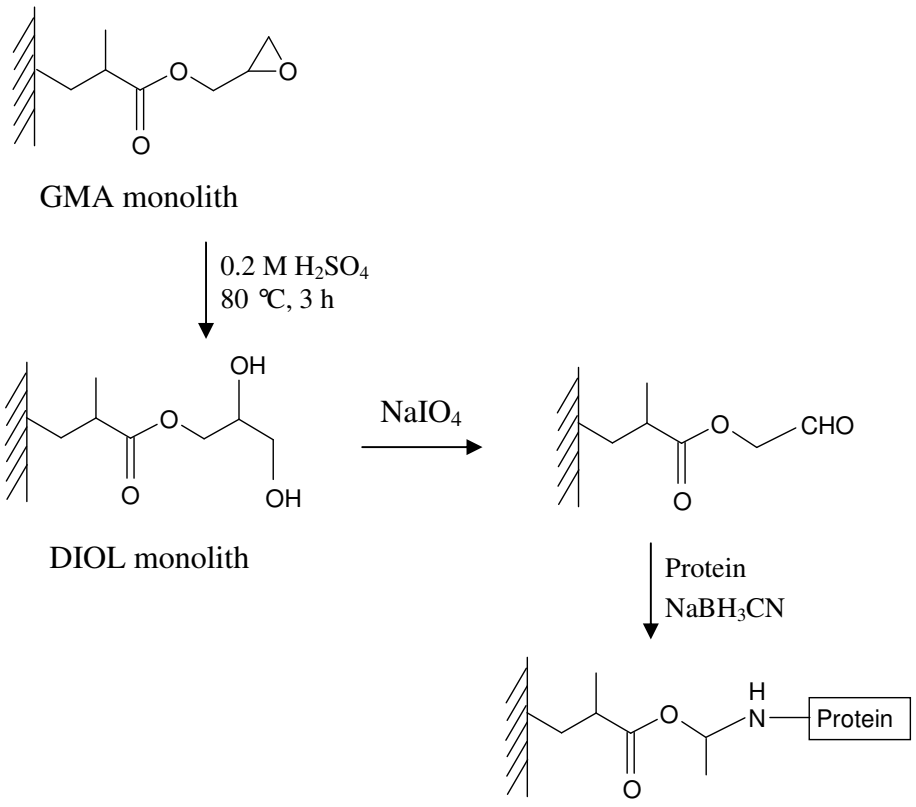

Figure 1. *Schematic of the reaction pathway to immobilize protein on the surface of the acrylate-based monolith.*

Preparation of Glycans

The method to prepare the glycans from the glycoproteins is the same as that described in Chapter III.

Derivatization of Glycans with 2-AB

The method used in this chapter to label the glycans with 2-AB is the same as that described in Chapter III.

Results and Discussion

Acrylate-Based Lectin Affinity Monoliths

The acrylate-based monoliths prepared by the polymerization of glyceryl monomethacrylate in the presence of EDMA crosslinker (i.e., DIOL-EDMA monoliths or simply DIOL monoliths) were subjected to lectin immobilization reactions. One exception involving SNA lectin, the monolith was based on copolymerization of GMA and EDMA (i.e, GMA-EDMA monolith). The resulting lectin affinity monoliths were evaluated with some specific standard glycoproteins. The lectins investigated included Con A, WGA, RCA, jacalin and SNA.

Con A-immobilized affinity monolith The affinity interactions between the immobilized Con A and *pNP*-α-D-mannopyranoside, transferrin, ribonuclease B and α_1-acid glycoprotein were studied. The information on the specificity of Con A toward *N*-glycans and the structures of the *N*-glycans attached to the three glycoproteins under investigation are provided in Chapters III and IV.

Figure 2 shows the chromatogram of the *pNP*-α-D-manopyranoside obtained on the Con A immobilized DIOL-EDMA monolithic column. Despite the use of the eluting mobile phase containing 0.2 M Me-α-D-Man (i.e., the hapten sugar), the *pNP*-α-D-manopyranoside was retained with a retention factor k' = 0.83 and eluted as a broad peak. In principle in the absence of nonspecific interaction and using the eluting mobile phase, the *pNP*-α-D-manopyranoside should yield a k' ~ 0. The fact that the *pNP*-α-D-manopyranoside was slightly retained (k' = 0.83) may indicate the presence of some

hydrophobic interactions, most likely between the benzene ring of the *pNP* and the acrylate backbone of the monolith. Being a small molecule, the *pNP*-α-D-manopyranoside can explore the surface of the monolith even in the presence of immobilized Con A on the monolith surface. The residual hydrophobic interaction with he acrylate backbone of the monolith was also observed with Con A-immobilized acrylate monolith based on GMA-EDMA where *pNP*-α-D-manopyranoside yielded a k' ~ 0.5.

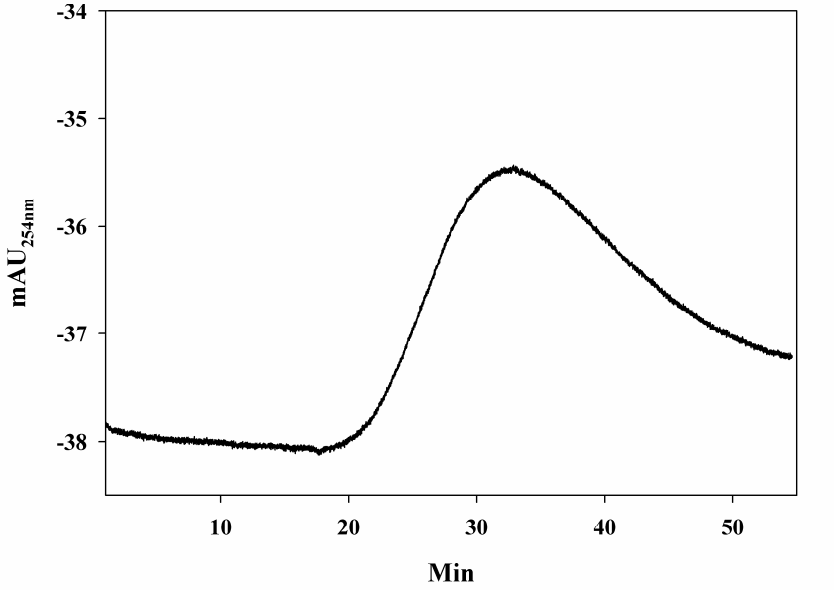

Figure 2. *Chromatogram of pNP-α-D-manopyranoside on the Con A-immobilized acrylate-based (DIOL-EDMA) monolithic column. Conditions: column size, 25/33 cm × 100 µm ID; mobile phase: 0.2 M Me-α-D-Man in 20 mM BisTris, pH 6.0 containing 100 mM NaCl; separation pressure, 10 bar; column temperature, 20 °C.*

Similarly to the Con A immobilized silica-based monolith (see Chapter IV), most of the transferrin was retained by the Con A-immobilized acrylate column and eluted

from the Con A column with the eluting mobile phase (see Figure 3). Ribonulease B and α_1-acid glycoprotein had similar interactions with the Con A immobilized acrylate column as shown in Figures 4 and 5, respectively. The ribonuclease B has only one single glycosylation site at Asn-34. The proposed *N*-glycans of ribonuclease B are listed in Table 1 [8]. While ribonuclease B behaved as expected on the Con A acrylate column it did not show a complete recovery from the Con A silica column, a behavior that can be explained by some electrostatic interaction of the basic protein with the residual surface silanols of the silica (see Chapter IV). Ribonuclease B has high mannose type *N*-glycans

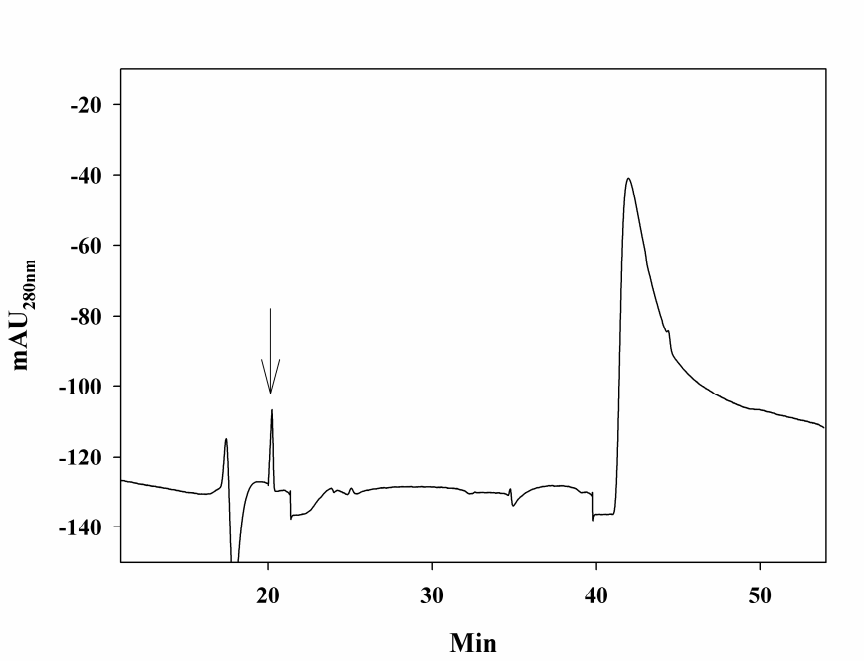

Figure 3. *Chromatogram of transferrin on the Con A-immobilized acrylate-based (DIOL-EDMA) monolithic column. Conditions: column size, 25/33 cm × 100 μm ID; arrow indicates the change to the eluting mobile phase. Binding mobile phase: 20 mM BisTris, pH 6.0, containing 100 mM NaCl, 1 mM Ca^{2+}, 1 mM Mn^{2+} and 1 mM Mg^{2+}; eluting mobile phase: 0.2 M Me-α-D-Man in the binding mobile phase; separation pressure, 10 bar; column temperature, 20 °C.*

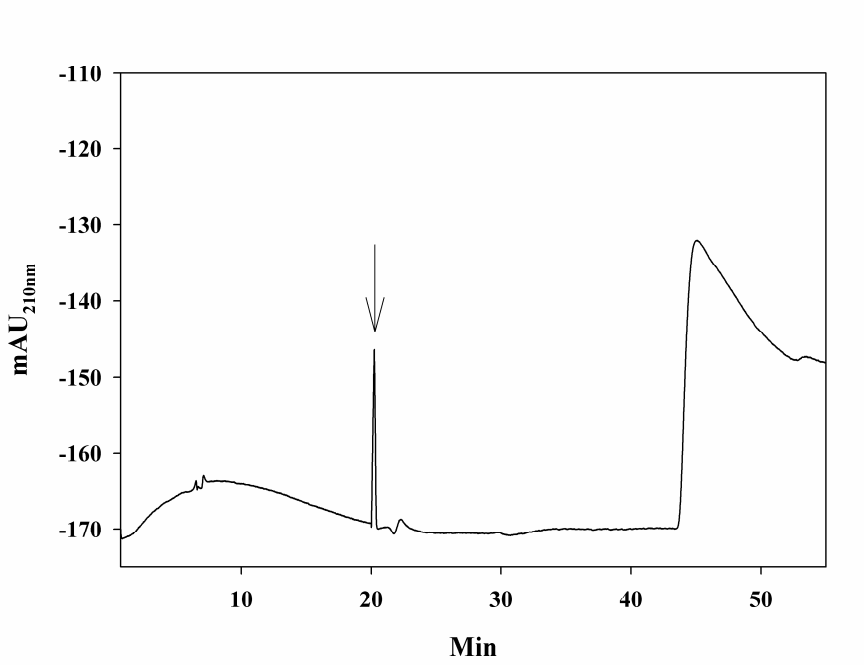

Figure 4. *Chromatogram of ribonuclease B on the Con A-immobilized acrylate-based (DIOL-EDMA) monolithic column. Conditions are the same as in Figure 3.*

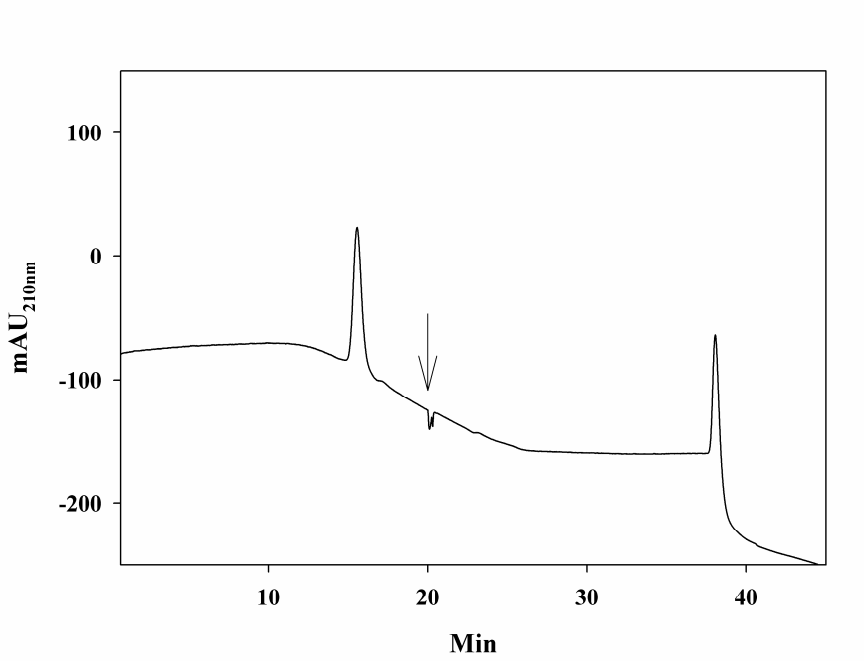

Figure 5. *Chromatogram of α_1-acid glycoprotein on the Con A-immobilized acrylate-based (DIOL-EDMA) monolithic column. Conditions are the same as in Figure 3.*

which are believed to be responsible for the full retention of the glycoprotein on the Con A acrylate column. Again, and similarly to the Con A silica based column (see Chapter IV), the Con A acrylate column retained only a fraction of the α_1-acid glycoprotein, which was eluted by a step gradient with the haptenic sugar, see Figure 5.

TABLE 1

PROPOSED *N*-GLYCANS DERIVED FROM RIBONUCLEASE B

$Man_5GlcNAc_2$ (see Table 2 (1) in Chapter III)
$Man_6GlcNAc_2$ (see Table 2 (2) in Chapter III)
$Man_7GlcNAc_2$ (see Table 2 (3) in Chapter III)
$Man_8GlcNAc_2$
$Man_9GlcNAc_2$

WGA immobilized affinity monolith WGA is known for its affinity to GlcNAc and glycoconjugates containing GlcNAc residues. Therefore, a quick evaluation for the WGA immobilized monolith is to test its affinity toward the *p*-nitrophenyl (*pNP*) derivative of GlcNAc, e.g., *pNP*-β-D-*N*-acetylglucosaminide, which is shown in Figure 6. As can be seen, the *pNP*-β-D-*N*-acetylglucosaminide yielded a retention factor k' = 1.94 on the WGA column even with the eluting mobile phase containing 0.2 M GlcNAc (the hapten sugar). This retention is attributed to hydrophobic interaction of the *para*-nitrophenyl moiety of the sugar with the acrylate backbone of the monolith.

To further understand the affinity of the WGA column toward glycoconjugates, the column was examined for its affinity to some specific standard glycoproteins such as

transferrin, α_1-acid glycoprotein and κ-casein. The structures of *N*-glycans that have affinity to WGA are given in Chapter IV. As shown in Figure 7, and similarly to WGA silica-based monolithic column (see Chapter IV), the WGA acrylate column retains the majority of α_1-acid glycoprotein, which is known to have sialylated bi-, tri- and tetraantennary *N*-glycans of the complex type. Despite the fact that transferrin also possesses sialylated *N*-glycans of the complex type, the WGA acrylate column retained only a part of transferrin, see Figure 8, which suggests that the glycosylation sites of transferrin are more populated with biantennary *N*-glycans than with tri- and

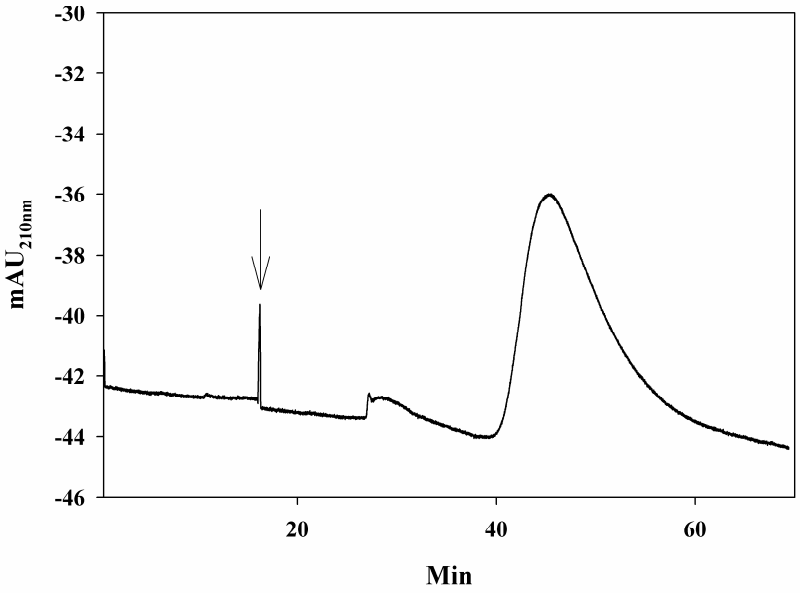

Figure 6. *Chromatogram of pNP-β-D-N-acetylglucosaminide on the WGA-immobilized acrylate-based (DIOL-EDMA) monolithic column. Conditions: column size, 25/33 cm × 100 μm ID; arrow indicates the change to the eluting mobile phase. Binding mobile phase: 20 mM BisTris, pH 6.0, containing 100 mM NaCl; eluting mobile phase: 0.2 M GlcNAc in the binding mobile phase; separation pressure, 10 bar; column temperature, 20 °C.*

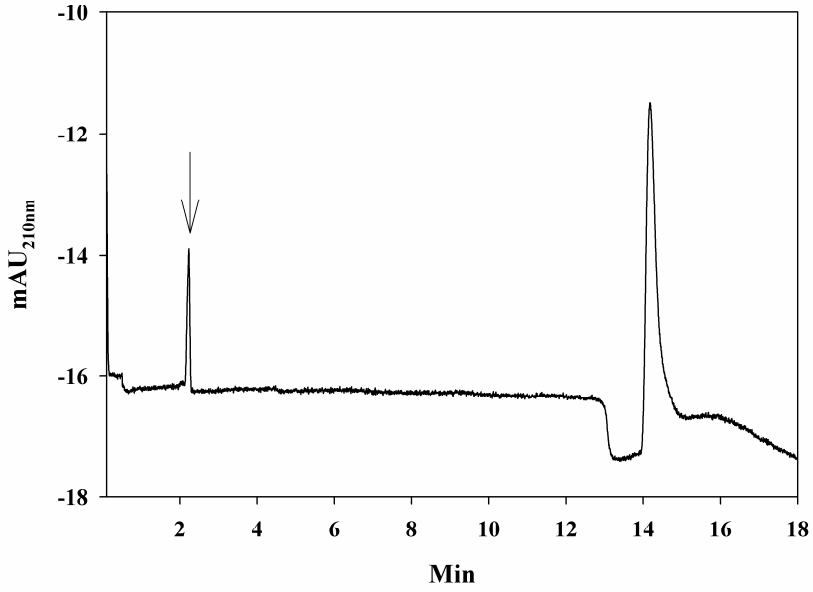

Figure 7. *Chromatogram of α_1-acid glycoprotein on the WGA-immobilized acrylate-based (DIOL-EDMA) monolithic column. Conditions are the same as in Figure 6.*

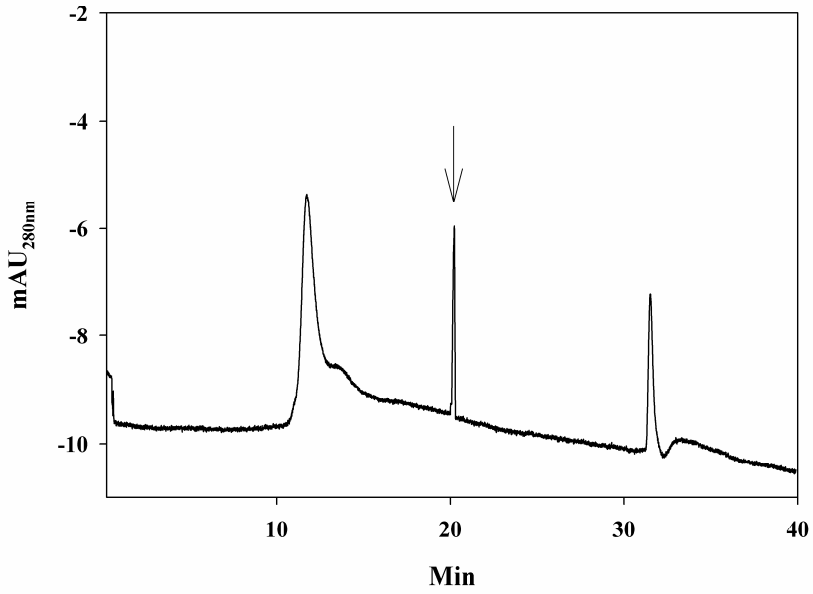

Figure 8. *Chromatogram of transferrin on the WGA-immobilized acrylate-based (DIOL-EDMA) monolithic column. Conditions are the same as in Figure 6.*

tetraantennary *N*-glycans. WGA which exhibits strong affinity to a cluster of sialic acids will certainly interact much stronger with multi-sialylated glycans such as tri- and tetraantennary *N*-glycans of the complex type.

The WGA acrylate column exhibited little or no nonspecific interactions with non glycosylated proteins. This is shown in Figure 9 where one can see that the WGA acrylate column exhibited affinity toward the specific glycoprotein (e.g., κ-casein) and no affinity toward non-glycosylated protein such myoglobin. Myoglobin is an oxygen-transport protein of the blood with a molecular weight of 17 kDa and has no carbohydrate moiety and thus no affinity to WGA. Myoglobin eluted in the column dead volume with the binding mobile phase while κ-casein had strong affinity with WGA and did not elute until the eluting mobile phase containing the hapten sugar GlcNAc was applied.

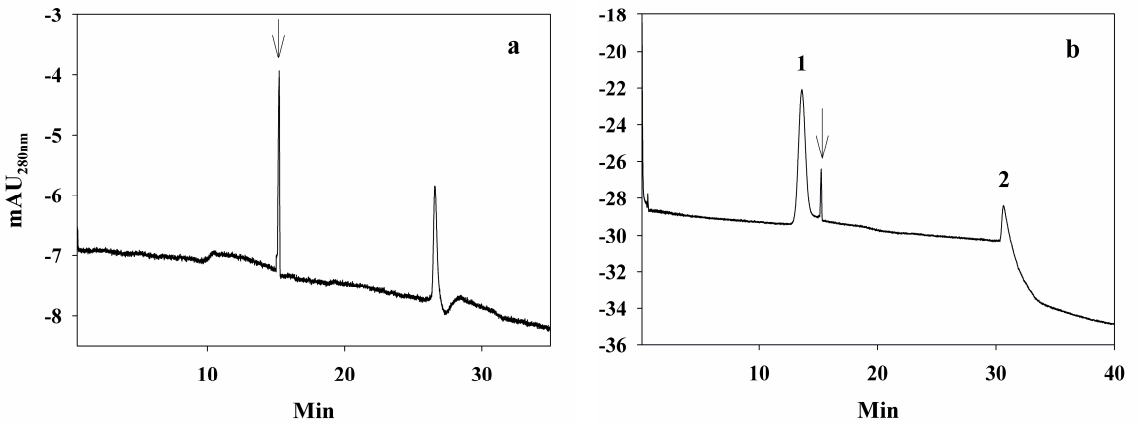

Figure 9. *Chromatograms of (a) κ-casein and (b) myoglobin and κ-casein on the WGA-immobilized acrylate-based (DIOL-EDMA) monolithic column. Conditions are the same as in Figure 6. Solutes: 1. myoglobin, 2. κ-casein.*

<u>*Ricinus communis* agglutinin-I (RCA-I) immobilized affinity monolith</u> RCA-I is a glycoprotein isolated from castor beans with a molecular weight of ~120 kDa. RCA-I

is a lectin that specifically interacts with the non-reducing terminal moieties of the outer chains of glycans. RCA-I recognizes the β-galactosyl residues of *N*-glycans and *O*-glycans [7]. While the Galβ1—›4GlcNAc group strongly binds to RCA-I and is eluted with 10 mM lactose, oligosaccharides with Galβ1—›3GlcNAcβ1—› or Galβ1—› 6 residues at the non reducing termini are only retarded with the binding mobile phase. The reactivity of RCA-I with specific oligosaccharides was confirmed by enzymatic digestion with exo- and endoglycosidases [7]. In fact, the digestion of oligosaccharide chains with diplococcal β-galactosidase which hydrolyzes the Galβ1—›4 linkage led to a loss of reactivity of the given oligosaccharides to RCA-I and consequently to the elution of these oligosaccharides from the RCA-I column in the column dead volume (i.e., pass through fraction) with the binding mobile phase. Also, glycoproteins with *O*-glycans having the Galβ1—›3GlcNAc group were reported to pass through an RCA-I column after endo-α-*N*-acetylgalactosaminidase digestion [7]. The specificity of the RCA toward the oligosaccharides is shown in Figure 10 [9, 10]. Since galactose (Gal) is a common part of the oligosaccharides for many glycoproteins, RCA-I can be used for the purification of glycoproteins containing either *O*-glycans or *N*-glycans or both types of glycans. As shown in Figure 10, RCA-I interacts strongly with bisected hybrid type *N*-glycans, bisected as well as non bisected complex type *N*-glycans of the biantennary, triantennary and tetraantennary types. The hapten monosaccharide for RCA is the β-D-galactose (Gal).

On the basis of the above considerations as far as the reactivity of RCA-I with glycoproteins is concerned, it is safe to say that RCA-I is a lectin with a much broader reactivity that the other lectins studied in this investigation. Consequently, the RCA-I

1. Structures exhibiting strong binding and requiring 0.1 M galactose for elution

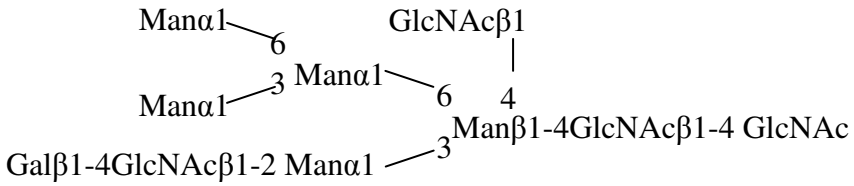

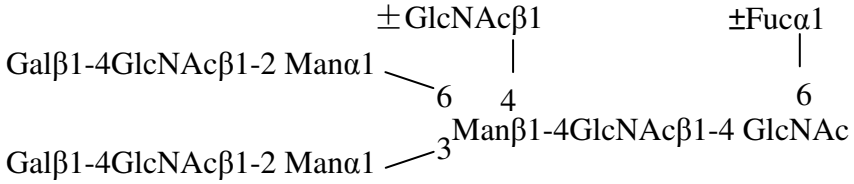

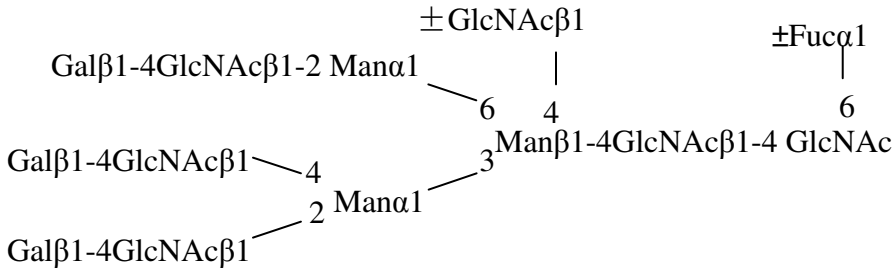

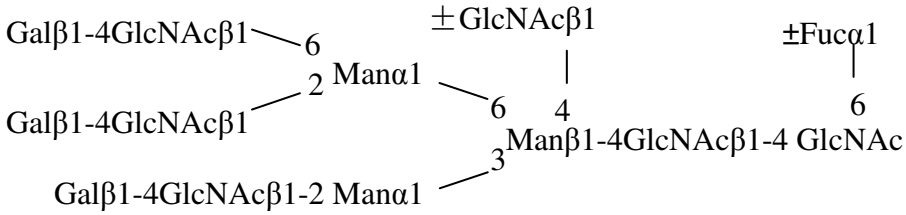

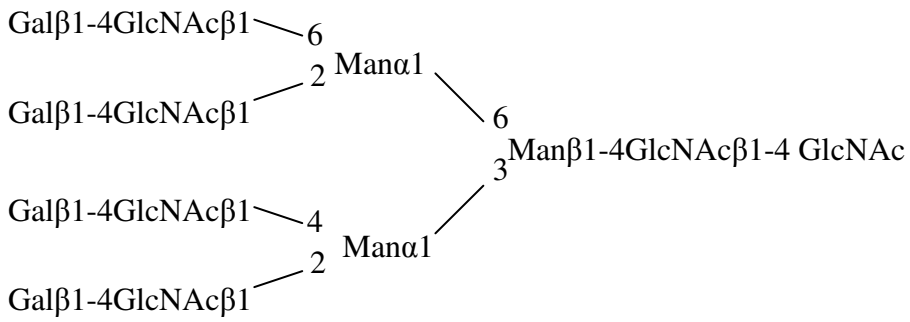

2. Structures exhibiting weak binding

Galβ1-6Galβ1-R

Galβ1-3GlcNAcβ1-R

Galβ1-3GalNAc

R: Manα1-6(Manα1-3)(±GlcNAcβ1-4)Manβ1-4GlcNAcβ1-4(±Fucα1-6)

Figure 10. *Specificity of RCA-I toward glycans* [9, 10].

monolithic column developed in this study was tested for its affinity interactions with a broad range of standard glycoproteins whose glycan structures are more or less well known, including those possessing *N*-glycans such as transferrin, α_1-acid glycoprotein, collagen, avidin and lipoxidase (see Figures 11-15), and those glycoproteins possessing *O*-glycans including κ-casein, mucin and fetuin (with fetuin containing both *N*- and *O*-glycans) (see Figures 16-18).

As shown in Figures 11 through 15, which display the chromatogams of transferrin, α_1-acid glycoprotein, avidin, lipoxidase and collagen, respectively, obtained on the RCA-I monolithic column, the different glycoproteins were, as expected, fully retained on the column simply because these glycoproteins have in common the

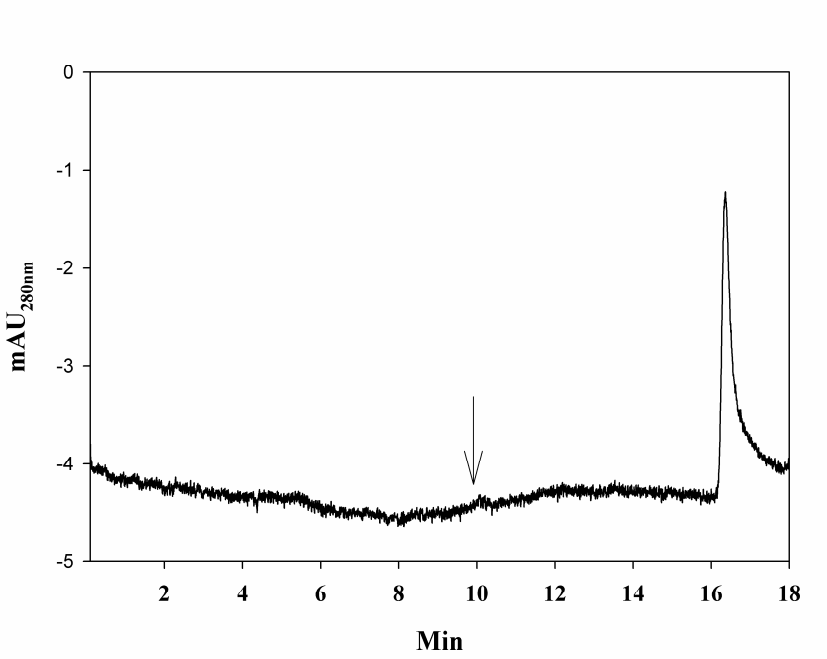

Figure 11. *Chromatogram of transferrin on the RCA-I-immobilized acrylate-based (DIOL-EDMA) monolithic column. Conditions: column size, 25/33 cm × 100 μm ID; arrow indicates the change to the eluting mobile phase. Binding mobile phase: 20 mM BisTris, pH 6.0, containing 100 mM NaCl,; eluting mobile phase: 0.2 M galactose in the binding mobile phase; separation pressure, 10 bar; column temperature, 20 °C.*

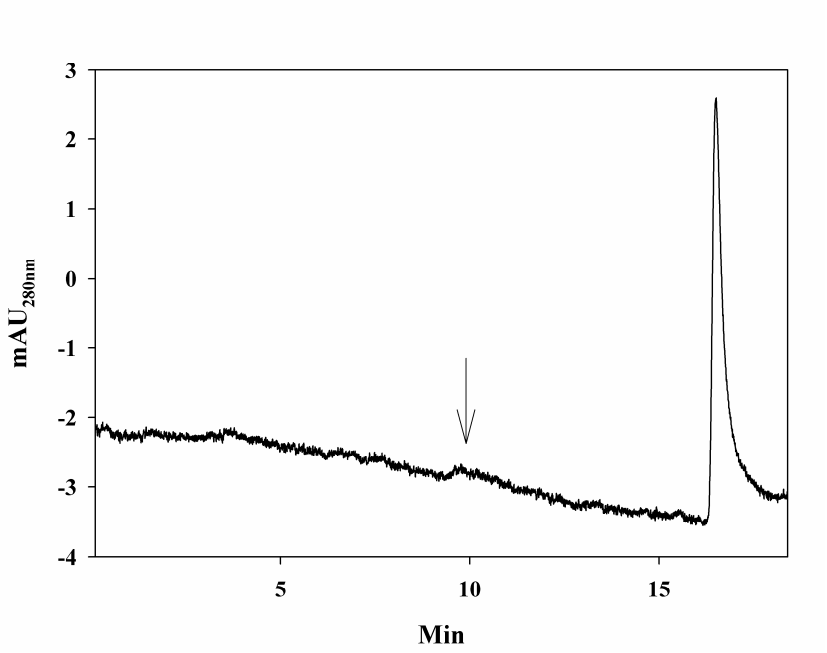

Figure 12. *Chromatogram of α_1-acid glycoprotein on the RCA-I-immobilized acrylate-based (DIOL-EDMA) monolithic column. Conditions are the same as in Figure 11.*

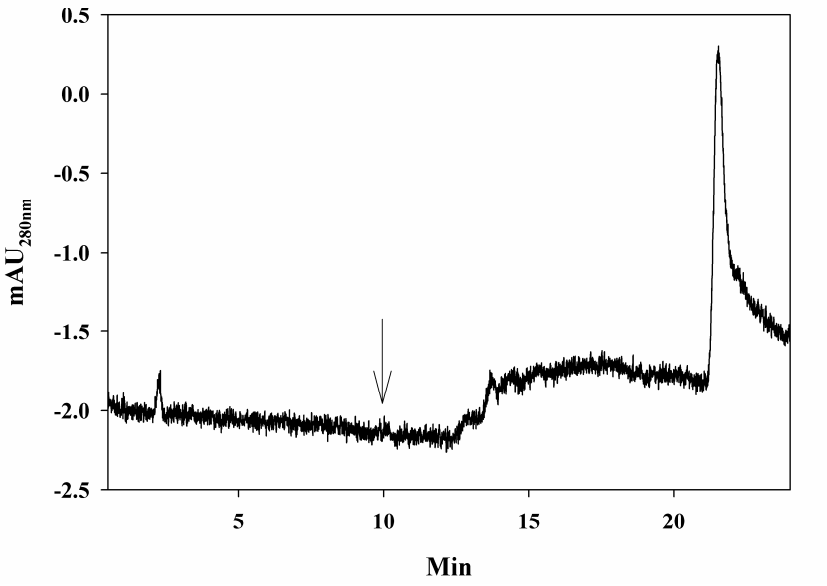

Figure 13. *Chromatogram of lipoxidase on the RCA-I-immobilized acrylate-based (DIOL-EDMA) monolithic column. Conditions are the same as in Figure 11.*

saccharide motifs that are reactive with RCA-I. For the glycan structures of these glycoproteins, see previous chapters and also below.

Lipoxidase, an oxidoreductase (also called lipoxygenase), is a glycoprotein of ~94 kDa isolated from the leaves of soybean (*Glycine max* [L.] Merr.) [11, 12]. It was reported that the monosaccharides glucosamine, galactose and to a lesser extent mannose were present on the oligosaccharide chains of this glycoprotein [13]. As indicated in Figure 13, most of the lipoxidase was retained by the RCA affinity column. The binding of lipoxidase to the immobilized RCA-I would suggest the presence of Gal and GlcNAc residues, which are required for the RCA-I recognition of glycans.

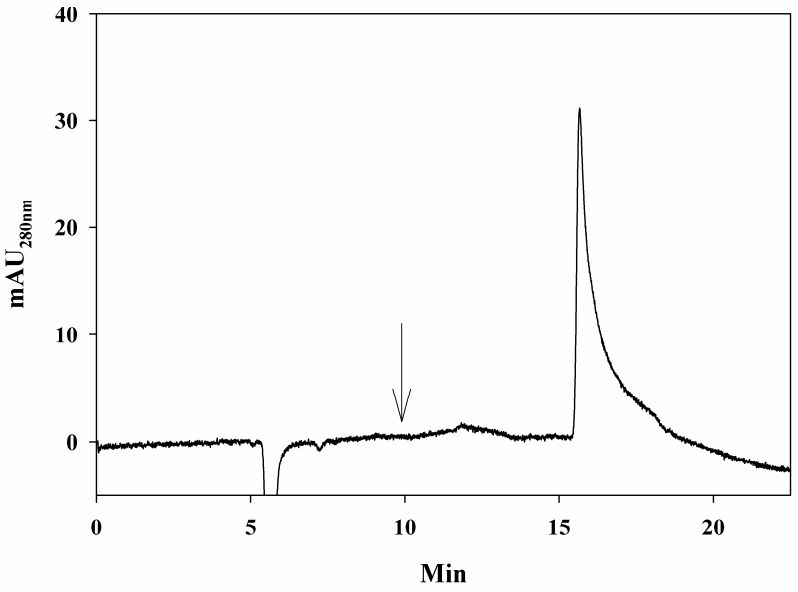

Figure 14. *Chromatogram of avidin on the RCA-I-immobilized acrylate-based (DIOL-EDMA) monolithic column. Conditions are the same as in Figure 11.*

Avidin is a tetrameric glycoprotein from the egg white of birds, reptiles and amphibians. It has a pI of ~10.5 and a molecular weight of 68 kDa [14]. Of the 10-

asparagine residues of each subunit, only Asn-17 is glycosylated. The carbohydrate moiety accounts for ~19% of the molecular weight of the protein and exhibits extensive microheterogeneity [15]. Avidin contains at least 3 distinct *N*-glycans composed of three to four *N*-acetylglucosamines and four to five mannoses [16, 17]. More information about avidin can be found in Chapter III, and the proposed structures of *N*-glycans attached to avidin are listed in Table 5 of Chapter III. Figure 14 shows that the majority of avidin had strong affinity with RCA-I.

Collagen type VI glycoprotein from human placenta is a heterotrimer with 19 potential sites for attachment of *N*-glycans. The oligosaccharide is a heterogeneous biantennary *N*-acetyllactosamine type. The heterogeneity reflects the presence or absence of five Gal residues at the non-reducing end and the presence of a fucose residue

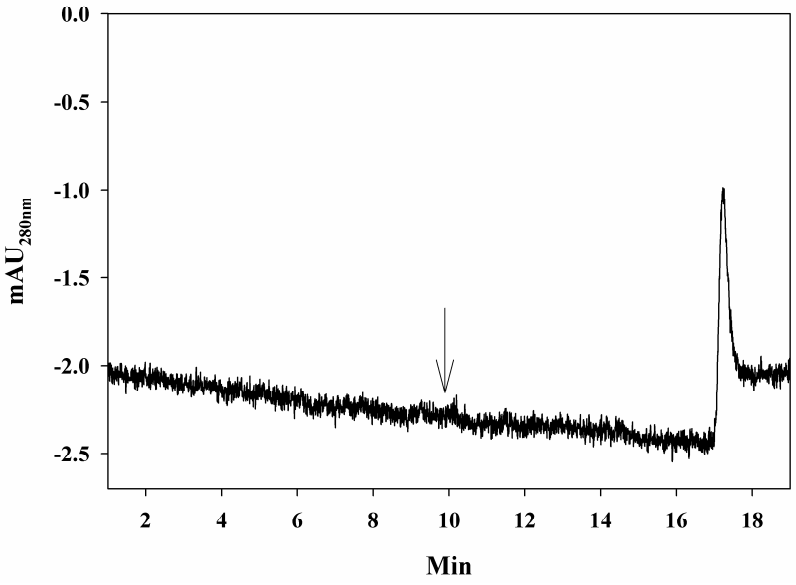

Figure 15. *Chromatogram of collagen on the RCA-I-immobilized acrylate-based (DIOL-EDMA) monolithic column. Conditions are the same as in Figure 11.*

at the reducing end [18]. The high degree of glycosylation of the type VI collagen and presence of Gal residues in its *N*-glycans may explain the affinity of this glycoprotein to RCA-I (Figure 15).

Glycoproteins with *O*-glycans or both *N*- and *O*-glycans were investigated for their affinity toward RCA-I. These were κ-casein, mucin and fetuin (with fetuin containing both *N*- and *O*-glycans). As shown in Figures 16 through 18, the RCA-I lectin retained all three glycoproteins under investigation. As described in Chapter IV, κ-casein has at least five *O*-glycans, which are populated by the saccharide motifs reactive with RCA-I, see Figure 16.

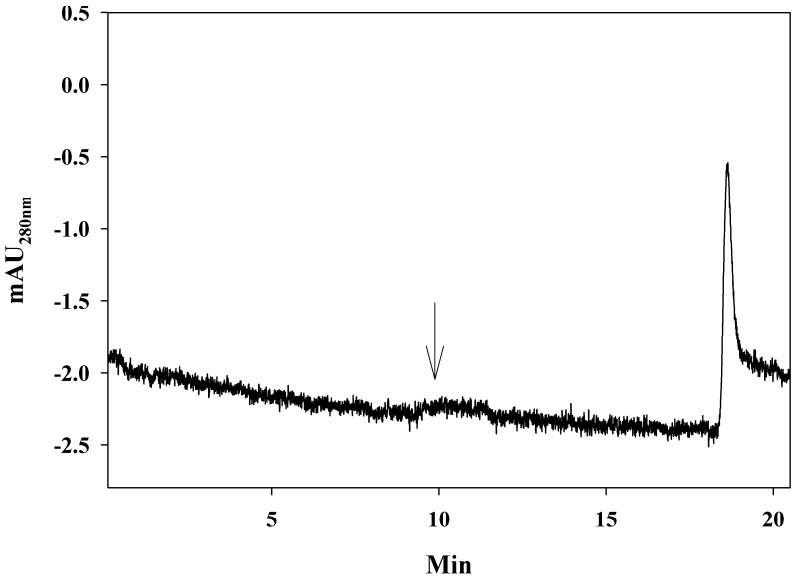

Figure 16. *Chromatogram of κ-casein on the RCA-I-immobilized acrylate-based (DIOL-EDMA) monolithic column. Conditions are the same as in Figure 11.*

TABLE 2.

PROPOSED *N*-GLYCANS DERIVED FROM FETUIN [19]

(1)

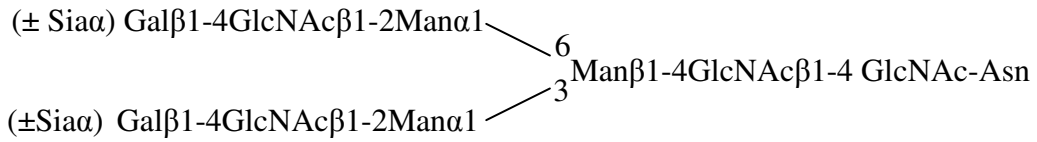

(2)

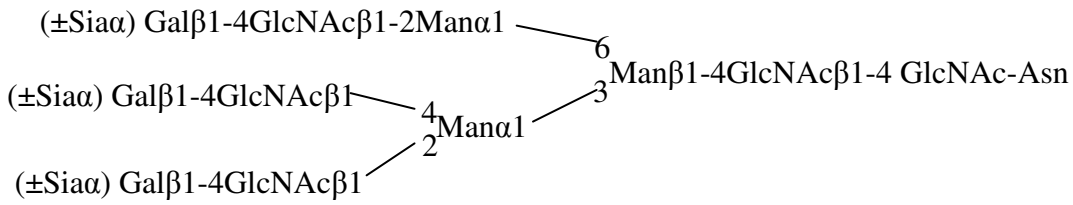

(3)

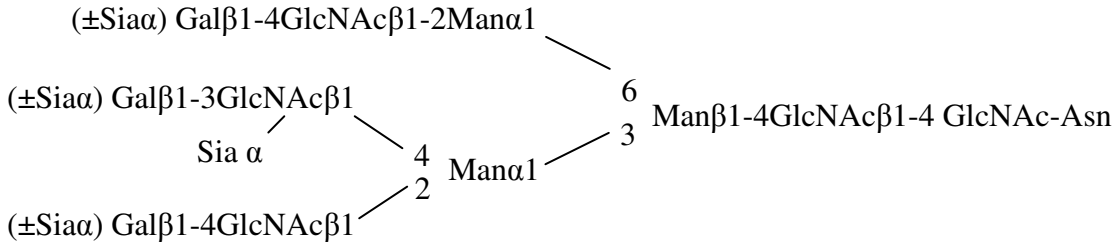

+: With the residue; -: without the residue

TABLE 3.

PROPOSED *O*-GLYCANS DERIVED FROM FETUIN [20, 21]

Siaα2-3Galβ1-6GalNAc-Ser/Thr

Siaα2-3Galβ1-3(Siaα2-6)GalNAc-Ser/Thr

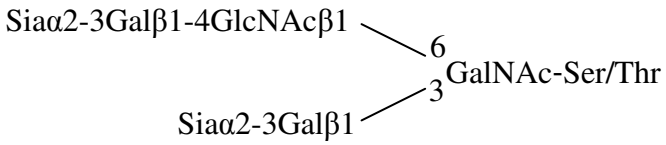

Fetuin (M. W. ~48 kDa) is the major protein in fetal calf serum, which is made in liver and secreted into blood stream. Fetuin has both *N*-glycans and *O*-glycans that account for 80% and 20% of the total fetuin-bound carbohydrates, respectively [19]. The majority of the *N*-glycans are tribranched glycans accounting for 83% and the dibranched *N*-glycans account for 17%. Both of these two kinds of glycans are sialylated to various degrees. Table 2 lists the proposed *N*-glycans released from the bovine fetuin [19]. Table 3 lists the structures of the *O*-glycans from fetuin in fetal calf serum. The number of the units of the tri-, tetra- and hexasaccharides were 2.13, 0.72 and 0.15, respectively [20, 21]. Since RCA-I binds to *N*-glycans of the complex type and *O*-glycans, the peak

eluted at ~22 min in Figure 17 by a step gradient with the eluting mobile phase is thought to include both kinds of the glycans of fetuin.

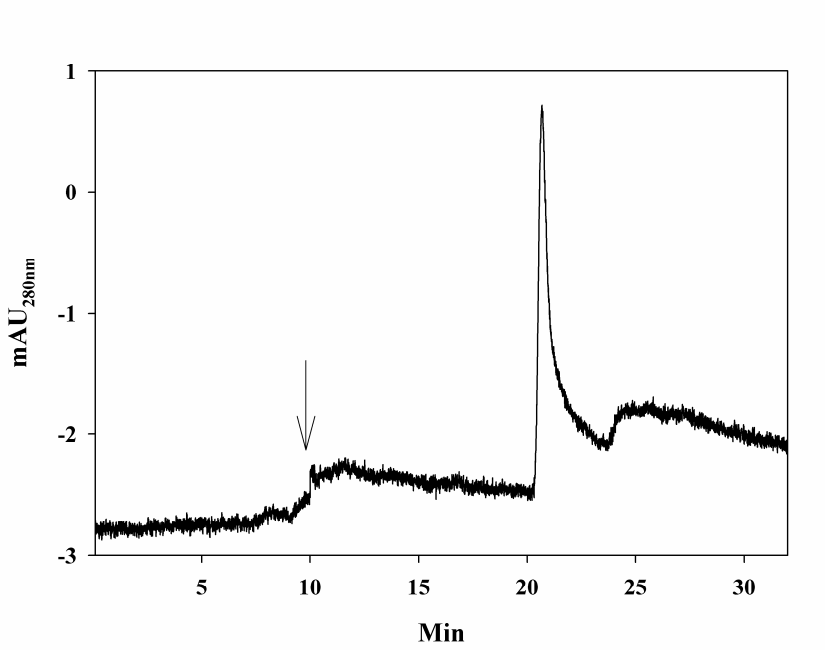

Figure 17. *Chromatogram of fetuin on the RCA-I-immobilized acrylate-based (DIOL-EDMA) monolithic column. Conditions are the same as in Figure 11.*

Mucin is a heavily glycosylated protein, which is usually found in various secretions and tissues of human and animals, e. g., saliva and the lining of the stomach, etc. About 26% of the proteins in the saliva are mucins. 40% - 80% of the mass of the mucin are *O*-glycans [22]. The structures of the oligosaccharides released from bovine submaxillary mucin are shown in Table 4 [23]. Figure 18 shows that mucin might have different forms (i.e., glycoforms) as indicated by the peaks after the arrow. The peak at the 22 min after the stepwise application of the eluting mobile phase is thought to consist of the glycoforms with strong affinity for RCA-I, that is, the molecules of mucin with the saccharide motifs that are reactive with RCA-I.

TABLE 4.

GLYCANS DERIVED FROM MUCIN [23]

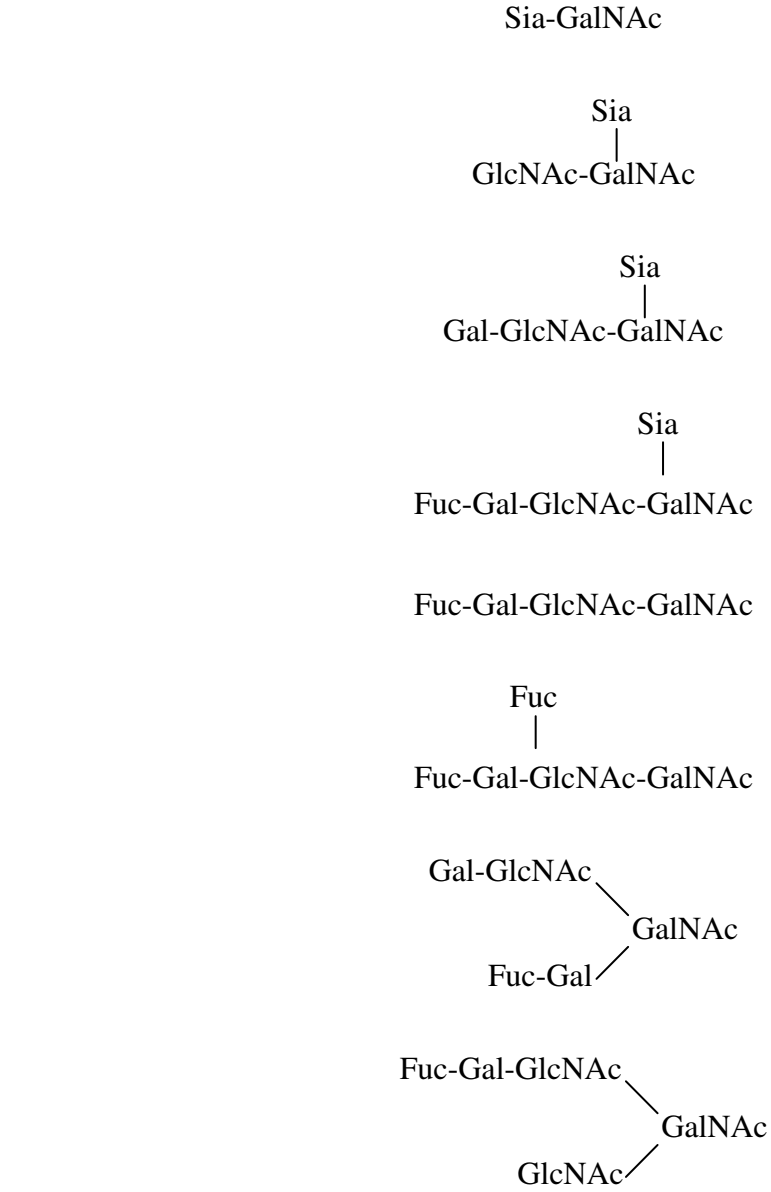

Note: adapted from reference [23].

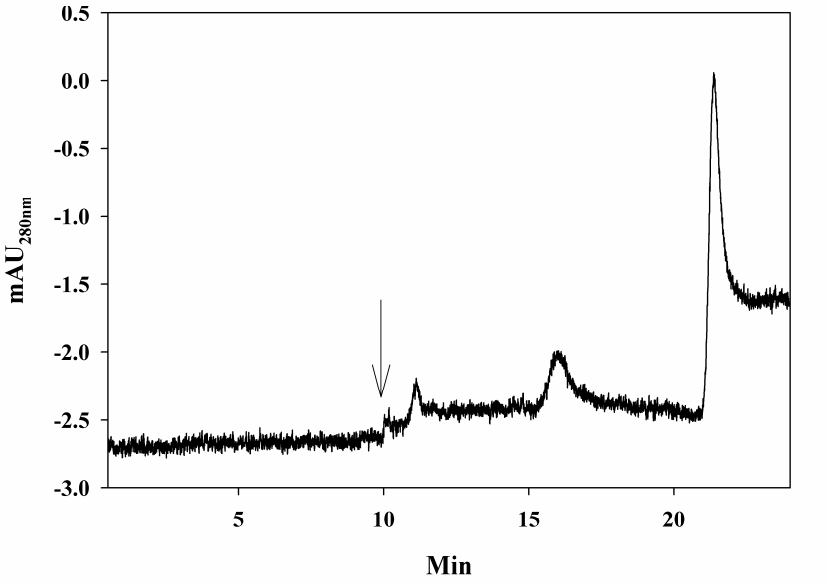

Figure 18. *Chromatogram of mucin on the RCA-I immobilized acrylate-based (DIOL-EDMA) monolithic column. Conditions are the same as in Figure 11.*

Jacalin immobilized affinity monolith Jacalin is a lectin with a molecular weight of ~66 kDa isolated from the Jack fruit (*Artocarpus integrifolia)* seeds. Jacalin binds only *O*-glycans, and preferentially those with the structure Galβ1→3GalNAc, which is known as the Thomsen-Friedenreich antigen, generally called T-antigen that is expressed in more than 85% of human carcinomas [24]. It also binds the disaccharide Galβ1→3GalNAc in its sialylated form. In fact, jacalin has been shown to bind *O*-glycosylated glycoproteins (i.e., glycoproteins with *O*-glycans) even without prior desialylation [9, 25]. In another study, it has been shown that the desialylated form of fetuin bound equally well to immobilized jacalin, showing that binding was not dependent on the presence of the sialic acid residues. Removal of galactose from the *N*-acetylgalactosamine residue of fetuin reduced but did not abolish the ability to bind to

jacalin, indicating the *N*-acetylgalactosamine is an important part of the carbohydrate structure required for binding [26]. Galactose is the hapten sugar for jacalin.

The affinity interaction between the immobilized jacalin monolithic column and fetuin is shown in Figure 19. It is believed that the peak before the arrow belonged to fetuin molecules (called glycoforms) rich in *N*-glycans (i.e., *N*-glycans that do not have the saccharide motifs reactive with jacalin, for *N*-glycan structures see Table 1), and those after the arrow are believed to be the fetuin molecules with the *O*-glycans.

Another important glycoprotein for testing the jacalin immobilized monolithic column was mucin. For structures of the *O*-glycans of this protein see Table 4. The

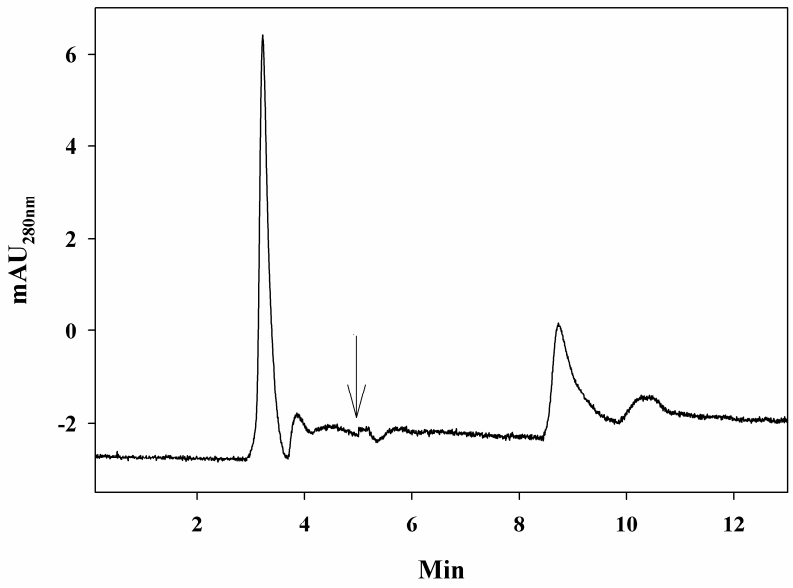

Figure 19. *Chromatogram of fetuin on the jacalin-immobilized acrylate-based (DIOL-EDMA) monolithic column. Conditions: column size, 25/33 cm × 100 μm ID; arrow indicates the change to the eluting mobile phase. Binding mobile phase: 20 mM BisTris, pH 6.0, containing 100 mM NaCl; eluting mobile phase: 0.2 M galactose in the binding mobile phase; separation pressure, 10 bar; column temperature, 20 °C.*

structure of the Gal-GalNAc with or without sialylation on the *O*-glycans of the mucin [22] contributed to most of the mucin retention by the immobilized jacalin (see Figure 20).

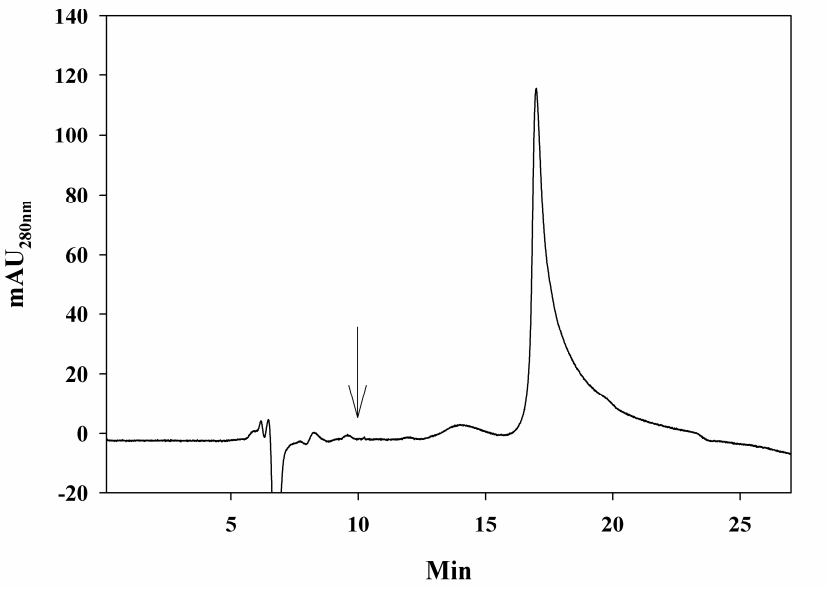

Figure 20. *Chromatogram of mucin on the jacalin-immobilized acrylate-based (GMA-EDMA) monolithic column. Conditions are the same as in Figure 19.*

SNA immobilized on the GMA-EDMA monolith SNA is a lectin isolated from *Sambucus nigra* (elderberry) bark. It has a molecular weight of ~150 kDa. SNA does not interact with sugar chains containing terminal β-Gal or β-*N*-GalNAc. However, SNA binds to oligosaccharides with sialic acid attached to terminal Gal in (α-2,6) linkage preferentially and in (α-2,3) linkage to a lesser degree. The lectin does not bind to sialylated *N*-acetylgalactosamine [27]. Therefore, immobilized SNA should be effective for separating and determining the structures of glycans with (α-2,6) linked sialic acid residues. The structures of *N*- and *O*-glycans that bind to SNA are given in Figure 21 [7].

Siaα2-6Galβ1-4GlcNAcβ1-R

Siaα2-6GalNAc-Ser/Thr

R: Manα1-6(Manα1-3)(±GlcNAcβ1-4)Manβ1-4GlcNAcβ1-4(±Fucα1-6)

Figure 21. *Specificity of SNA toward glycans (Structures exhibiting strong binding and requiring 0.2 M galactose for elution)* [7].

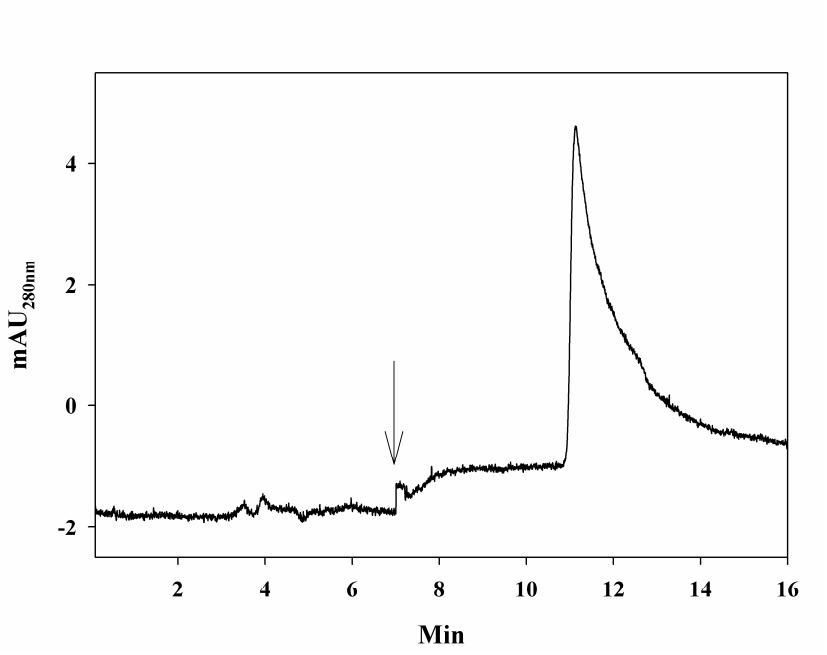

Figure 22. *Chromatogram of transferrin on the SNA-immobilized GMA-EDMA monolithic column. Conditions: column size, 25/33 cm × 100 μm ID; arrow indicates the change to the eluting mobile phase. Binding mobile phase: 20 mM BisTris, pH 6.0, containing 100 mM NaCl; eluting mobile phase: 0.2 M galactose in the binding mobile phase; separation pressure, 10 bar; column temperature, 20 °C.*

The affinity interactions between the SNA and the glycoproteins such as transferrin, glucose oxidase, collagen, fetuin and mucin were studied in this chapter (see Figures 22-25). Since all of the *N*-glycans of transferrin have at least one residue ending with (α-2,6) sialic acid, all of the transferrin was retained on the SNA affinity column (see Figure 22).

The fact that collagen type VI glycoprotein *N*-glycans of the biantennary *N*-acetyllactosamine type (i.e., Galβ1—›4GlcNAc) may explain the observed large fraction retained by the immobilized SNA (see Figure 23). Despite the fact that glucose oxidase contains carbohydrates that are constituted of mostly mannose (14% D-mannanose) and to lesser extent GlcNAc and Gal (2.3% D-glucosamine and 0.3% D-galactose) [28, 29], the SNA column exhibited a strong affinity toward glucose oxidase (see Figure 24). The sialic acid residues attached to the terminal galatose of the *O*-glycans on the mucin *via*

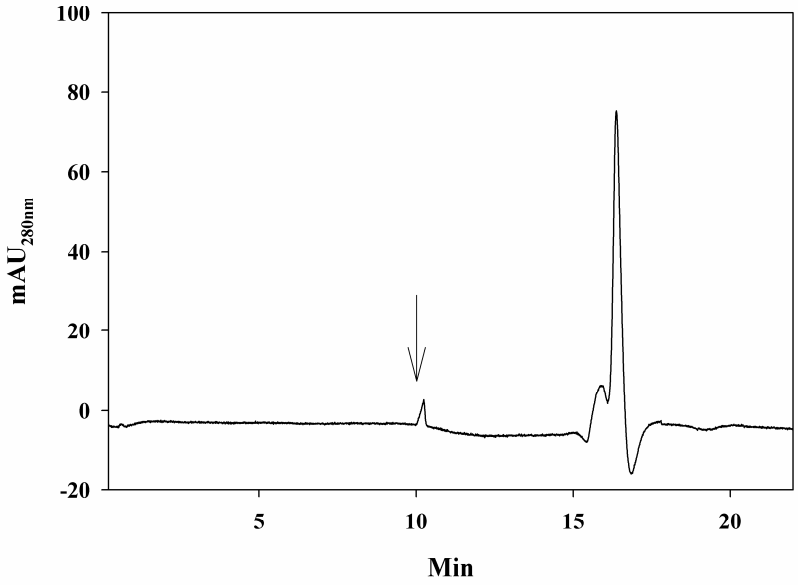

Figure 23. *Chromatogram of collagen VI on the SNA-immobilized GMA-EDMA monolithic column. Conditions are the same as in Figure 22.*

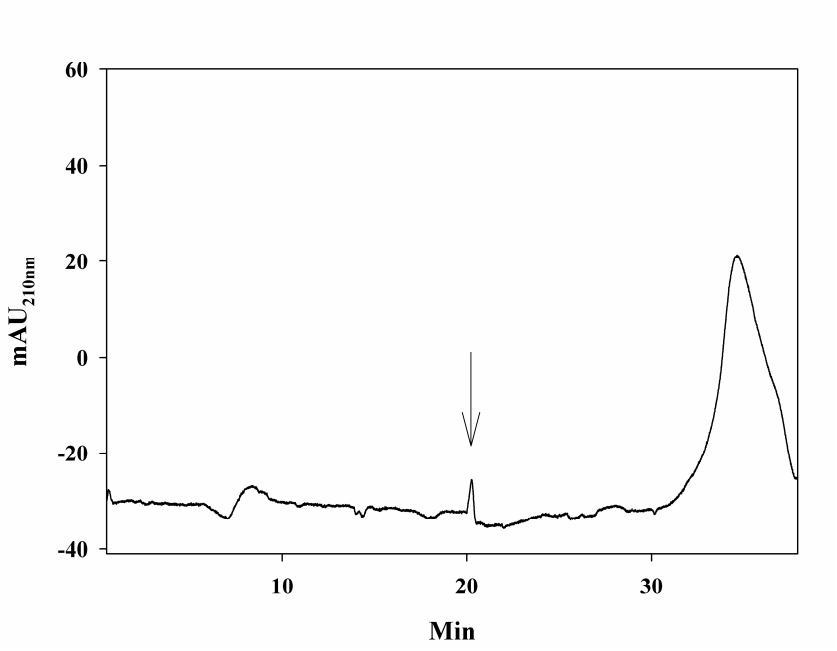

Figure 24. *Chromatogram of glucose oxidase on the SNA-immobilized GMA-EDMA monolithic column. Conditions are the same as in Figure 22.*

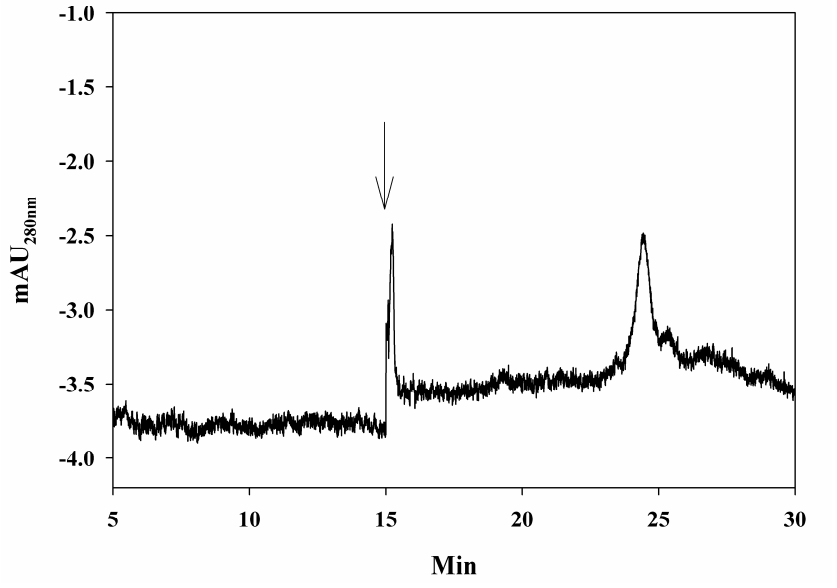

Figure 25. *Chromatogram of mucin on the SNA-immobilized GMA-EDMA monolithic column. Conditions are the same as in Figure 22.*

the linkage of (α-2,6) constituted the saccharide motifs that are responsible for the large retained fraction of mucin on the SNA column (see Figure 25). Since fetuin has *N*-glycans with residues of sialylated galactose and *O*-glycans with residues of sialylated galactose in the (α-2,3) linkage, most of the fetuin was retained by the SNA as shown in Figure 26.

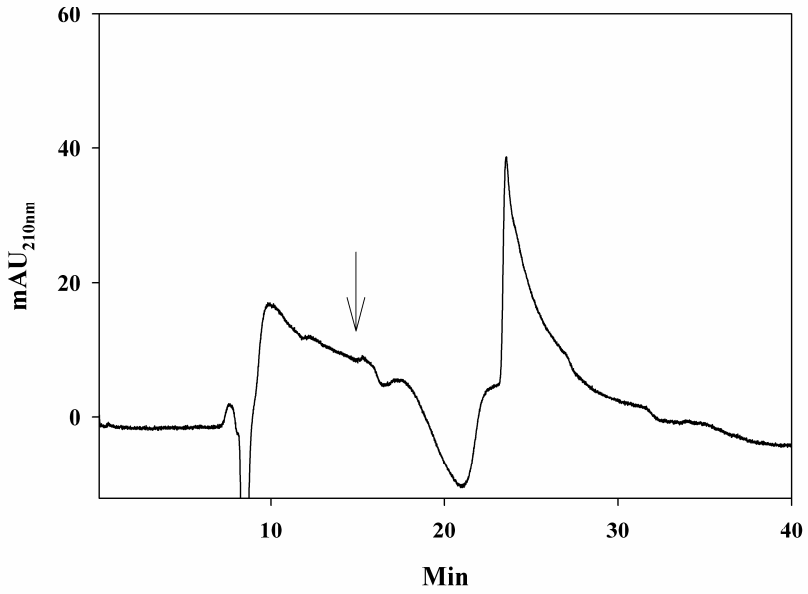

Figure 26. *Chromatogram of fetuin on the SNA-immobilized GMA-EDMA monolithic column. Conditions are the same as in Figure 22.*

Glycan Fractionations by Lectin Affinity Columns

The *N*-glycans derived from the glycoproteins such as transferrin, α_1-acid glycoprotein and ovalbumin were separated by the lectin affinity columns including Con A, WGA and RCA immobilized monolithic columns. The identification of the glycans was based on the specific UV spectra of the 2-AB derivatized glycans (see Chapter III).

The 2-AB derivatized glycans are labeled with an asterisk (*) on the chromatograms in the following sections. The brackets placed on sections of the chromatograms represent the different elution regions.

As shown in Figure 27, the 2-AB derivatized glycans derived from transferrin were detected at 37 min after the elution mobile phase was applied at 20 min. The peaks in the elution region (II) are thought to belong to the biantennary glycans of the complex type, which had affinity with the Con A lectin (see Table 4 in Chapter III). This is

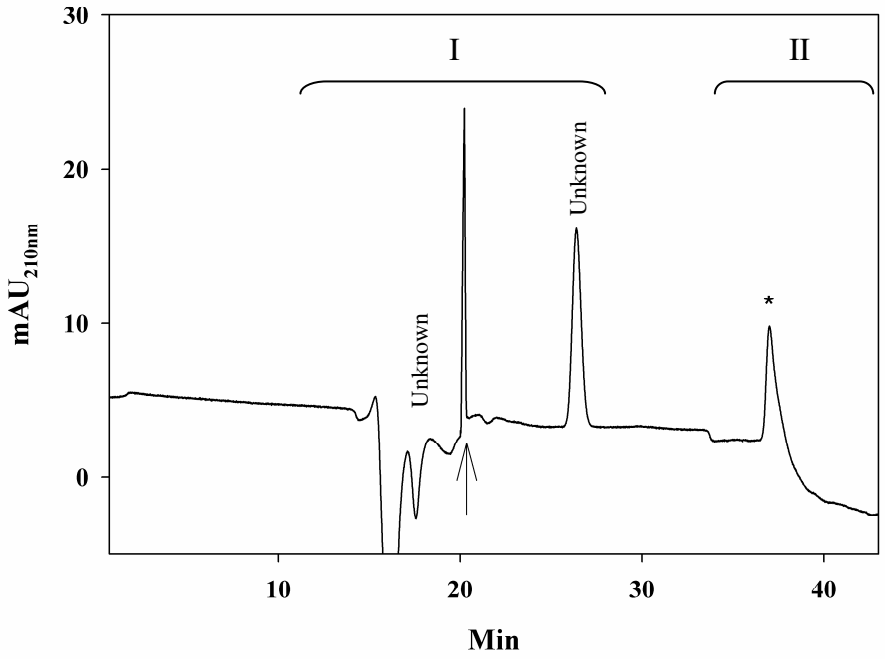

Figure 27. *Chromatogram of glycans derived from transferrin on the Con A-immobilized monolithic column. Conditions: column size, 25/33 cm × 100 μm ID; arrow indicates the change to the eluting mobile phase. Binding mobile phase: 20 mM BisTris, pH 6.0, containing 100 mM NaCl, 1 mM Ca^{2+}, 1 mM Mn^{2+} and 1 mM Mg^{2+}; eluting mobile phase: 0.2 M Me-α-D-Man in the binding mobile phase; separation pressure, 10 bar; column temperature, 20 °C.*

consistent with the affinity chromatogram of transferrin on the Con A immobilized column (see Figure 3). This result supports the assumption that the tri- and tetraantennary complex-type glycans attached to transferrin were in low content compared to that of the biantennary glycans. This also explains why a higher fraction of transferrin was retained by the Con A affinity column as indicated in Figure 3 in this chapter and Figure 9 in Chapter IV.

2-AB derivatized glycans derived from the α_1-acid glycoprotein were detected before and after the application of the eluting mobile phase to the Con A column (see Figure 28). The glycans in the elution region (II) are believed to belong to the biantennary complex type *N*-glycans. Those in the elution region (I) are thought to be the tri- and tetraantennary complex type *N*-glycans (see Table 3 in Chapter III). On the

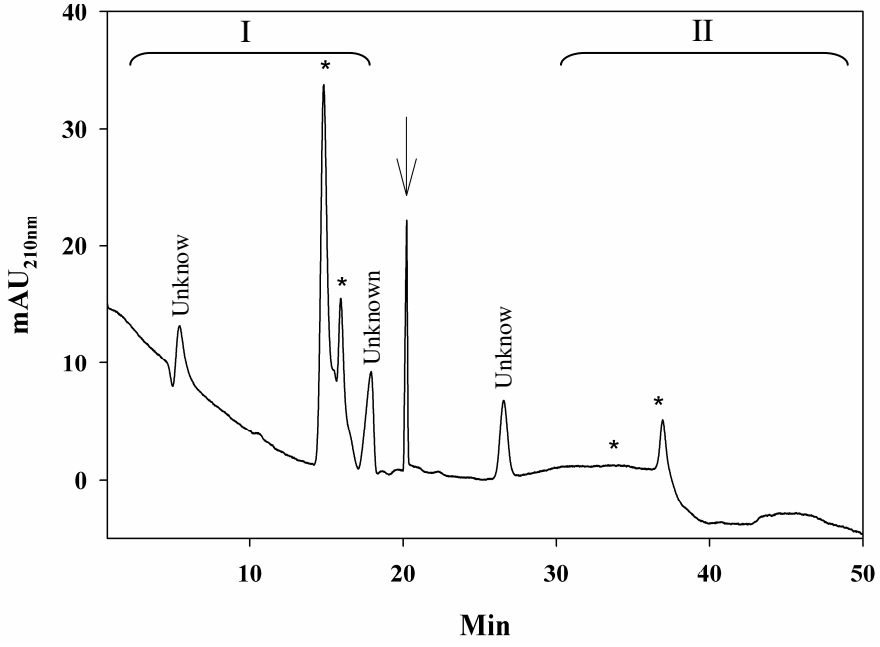

Figure 28. *Chromatogram of glycans derived from α_1-acid glycoprotein on the Con A-immobilized monolithic column. Conditions are the same as in Figure 27.*

basis of this assumption, the ratio of the peaks in Figure 28 shows that α_1-acid glycoprotein contained fewer biantennary glycans, and the majority of the glycans were of the tri- and tetraantennary oligosaccharides when compared to transferrin. This result is also consistent with the affinity chromatogram of α_1-acid glycoprotein on the Con A immobilized column (see Figure 5 in this chapter and Figure 11 in Chapter IV).

Ovalbumin contains high mannose type and hybrid type *N*-glycans (see Table 2 in Chapter III). Based on the affinity of ovalbumin to immoblized Con A, we can sort out the peaks of the *N*-glycans into two kinds. The *N*-glycans in the elution region (I) are believed to be those oligosaccharide chains with the structures of 6, 7 and 8 (i.e., hybrid type) in Table 2 in Chapter III, while those glycans in the elution region (II) belong to those oligosaccharides with the structures of 1-5 (i.e., high mannose type) in Table 2 of

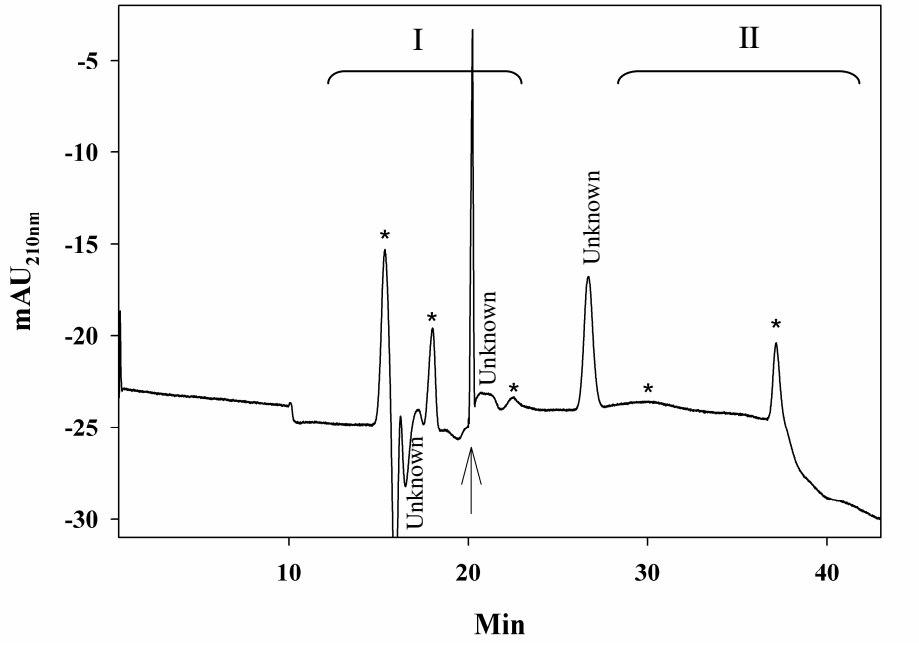

Figure 29. *Chromatogram of glycans derived from ovalbumin on a Con A-immobilized monolithic column. Conditions are the same as in Figure 27.*

Chapter III (see Figure 29).

Figure 30 shows the fractionation of the *N*-glycans derived from α_1-acid glycoprotein on the WGA immobilized column. WGA has strong affinity to clusters of sialic acid residues. The glycans in the elution region (II) are believed to be the highly sialylated complex type oligosaccharides (e.g., tri- and tetraantennary complex type) while the glycan peaks in the elution region (I) might imply that some of the sialic acids have dissociated from the oligosaccharides during the enzymatic cleavage of the glycans from the glycoprotein or that these glycans belong to the biantennary complex type.

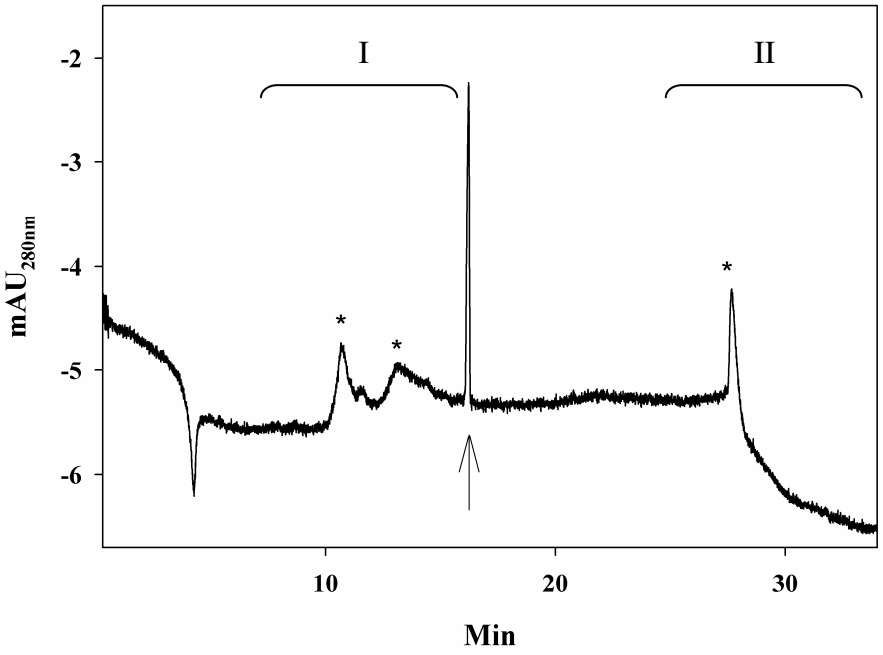

Figure 30. *Chromatogram of N-glycans derived from α_1-acid glycoprotein on the WGA-immobilized monolithic column. Conditions: column size, 25/33 cm × 100 μm ID; arrow indicates the change to the eluting mobile phase. Binding mobile phase: 20 mM BisTris, pH 6.0, containing 100 mM NaCl; eluting mobile phase: 0.2 M GlcNAc in the binding mobile phase; separation pressure, 10 bar; column temperature, 20 °C.*

As discussed in the previous section, the WGA retained the highly sialylated tri- and tetraantennary glycans, while the biantennary glycans were not retained and eluted with the binding mobile phase. As can be seen in Figure 31 that shows the *N*-glycans derived from transferrin, the first peak is believed to belong to the biantennary glycans. The second peak that eluted at ~ 28 min by the stepwise elution with the hapten sugar did not yield the UV spectrum typical of 2-AB derivatized glycans. One reason for this behavior is the relatively low concentration of the retained glycans. Another reason is that the 0.2 M GlcNAc used as the hapten sugar in the eluting mobile phase had high absorbance at the detection wavelength.

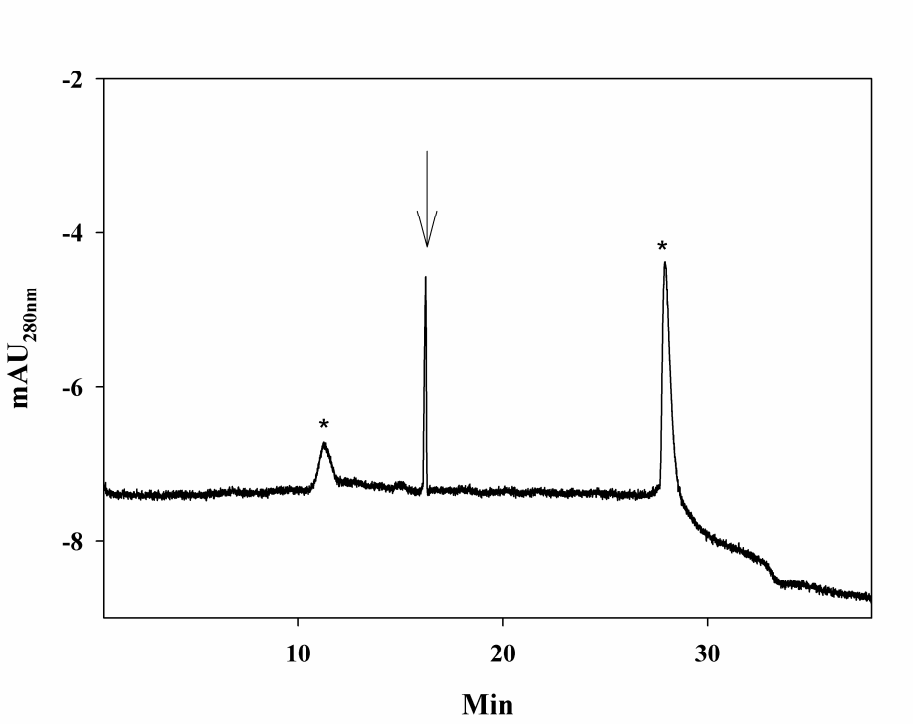

Figure 31. *Chromatogram of glycans derived from transferrin on the WGA-immobilized monolithic column. Conditions are the same as in Figure 30.*

RCA-I binds to any glycans that have the structure of Galβ1-4GlcNAc, which most of the glycoproteins possess. This is why the RCA-I column exhibited affinity for a wide range of glycoproteins and glycans. As an example, Figure 32 shows the fractionations of the *N*-glycans derived from α_1-acid glycoprotein on the RCA-immobilized monolithic column. Most of the glycans derived from the α_1-acid glycoprotein were retained on the RCA column which was indicated by the peak after the arrow. Only a small fraction of glycans which eluted with the binding mobile phase were detected.

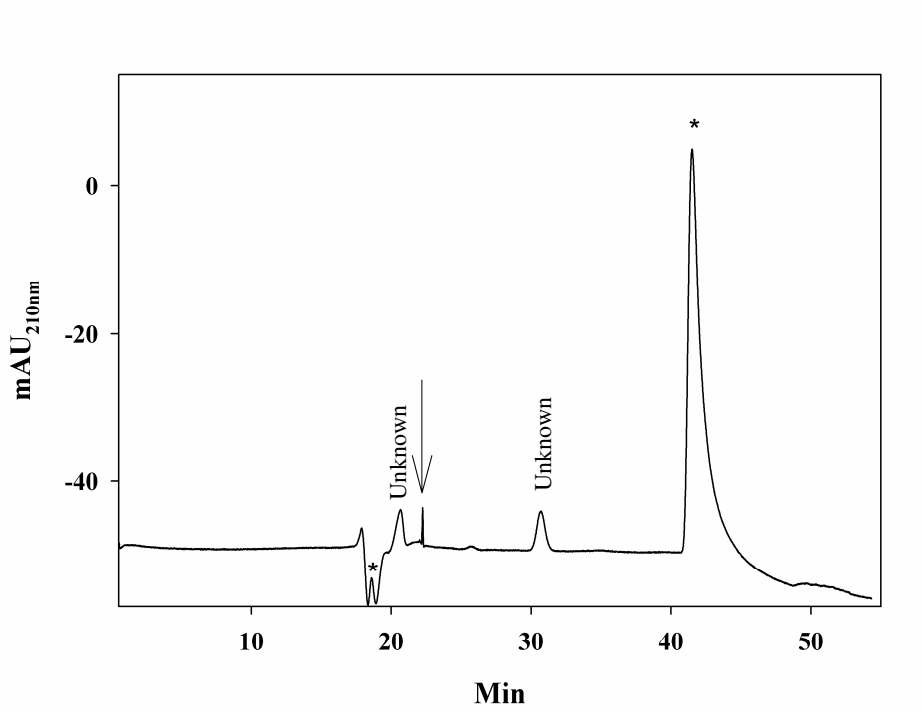

Figure 32. *Chromatogram of glycans derived from α_1-acid glycoprotein on the RCA-I-immobilized monolithic column. Conditions: column size, 25/33 cm × 100 µm ID; arrow indicates the change to the eluting mobile phase. Binding mobile phase: 20 mM BisTris, pH 6.0, containing 100 mM NaCl; eluting mobile phase: 0.2 M galactose in the binding mobile phase; separation pressure, 10 bar; column temperature, 20 °C.*

Conclusions

The acrylate-based monoliths, which were prepared *via* an *in situ* polymerization reaction employing glyceryl monomethacrylate or GMA as the functional monomer, and EDMA as the crosslinker were successfully immobilized with lectins of various specificities directed to various portions of glycans and type of glycans. The lectin affinity monoliths proved useful in nano-LAC, and exhibited affinity interactions at varying degrees with particular glycoproteins and glycans. While immobilized Con A and WGA, which belong to the category of lectins with specificities directed to the core portion of *N*-glycans, exhibited narrow selectivity toward defined glycoconjugates, RCA-I whose specificity is directed to the non-reducing terminal moieties of outer glycan chains offered a much broader affinity toward various glycoconjugates. Immobilized jacalin with specific affinity to *O*-glycans and immobilized SNA with specific affinity to some *N*-glycans and *O*-glycans complemented the other three lectins (i.e., Con A, WGA and RCA-I) in nano-LAC. The set of immobilized lectin affinity monoliths developed in this study are expected to find general use in the field of glycomics and glycoproteomics.

REFERENCES

[1] Hahn, R., Jungbauer, A., *Anal. Chem.* **2000**, *72*, 4853.

[2] Mallik, R., Hage, D. S., *J. Sep. Sci.* **2006**, *29*, 1686.

[3] Bedair, M., El Rassi, Z., *j. Chromatogr. A* **2005**, *1079*, 236.

[4] Pan, Z., Zou, H., Mo, W., Huang, X., Wu, R., *Anal. Chim. Acta* **2004**, *466*, 141.

[5] Okanda, F. M., El Rassi, Z., *Electrophoresis* **2006**, *27*, 1020.

[6] Hage, D. S., Bian, M., Burks, R., Karle, E., Ohnmacht, C., Wa, C., *Bioaffinity Chromatography*, in: Hage, D. S. (Ed.), *Handbook of Affinity Chromatography*
Taylor & Francis Group, Boca Raton **2006**, pp. 101.

[7] Kobata, A., Yamshita, K., *Fractionation of oligosaccharides by serial affinity chromatography with use of immobilized lectin columns*, in: Fukuda, M., Kobata, A. (Eds.), *Glycobiology A Practical Approach*, Oxford University Press, New York **1993**, pp. 103.

[8] Lee, B., Krishnanchettiar, S., Lateef, S. S., Lateef, N. S., Gupta, S., *Rapid Commun. Mass Spectrom.* **2005**, *19*, 2629.

[9] Fukuda, M., Kobata, A., *Glycobiology A Practical Approach*, Oxford University Press, New York **1993**.

[10] Yamamoto, K., Tsuji, T., Osawa, T., *Analysis of Asparagine-Linked Oligosaccharides by Sequential Lectin-Affinity Chromatography*, in: Hounsell, E. F. (Ed.), *Glycoanalysis Protocols*, Humana Press, Totowa, New Jersey **1998**.

[11] Tranbarger, T. J., Franceschi, V. R., Hildebrand, D. F., Grimes, H. D., *The Plant Cell* **1991**, *3*, 937.

[12] Wittenbach, V. A., *Plant Physiol.* **1983**, *73*, 125.

[13] Franceschi, V. R., Giaquinta, R. T., *Planta* **1983**, *157*, 422.

[14] Korpela, J., *Med. Bio.* **1984**, *62*, 5.

[15] Bruch, R. C., White, H. B., *Biochemistry* **1982**, *21*, 5334.

[16] Green, N., *Advances in Protein Chemistry* **1975**, *29*, 85.

[17] DeLange, R., Huang, T., *J. Biol. Chem.* **1971**, *246*, 698.

[18] Noelken, M. E., Hudson, B. G., in: Montreuil, J., Schachter, H., Vliegenthart, J. F. G. (Eds.), *Glycoproteins*, Elsevier Amsterdam **1995**, pp. 589.

[19] Green, E. D., Adelt, G., Baenziger, J. U., *J. Biol. Chem.* **1988**, *263*, 18253.

[20] Edge, A. S. B., Spiro, R. G., *J. Biol. Chem.* **1987**, *262*, 16135.

[21] Spiro, R. G., Bhoyroo, V. D., *J. Biol. Chem.* **1974**, *249*, 5704.

[22] Zalewska, A., Zwierz, K., Zolkowski, K., Gindzienski, A., *Acta Biochim. Polonica* **2000**, *47*, 1067.

[23] Davies, M. J., Smith, K. D., Carruthers, R. A., Chai, W., Lawson, A. M., *J. Chromatogr.* **1993**, *646*, 317.

[24] Jeyaprakash, A. A., Rani, P. G., Reddy, G. B., Banumathi, S., Betzel, C., Sekar, K., Surolia, A., Vijayan, M., *J. Molecul. Biol.* **2002**, *321*, 637.

[25] Sastry, M. V. K., Banarjee, P., Patanjali, S. R., Swamy, M. J., Swarnalatha, G. V., Surolia, A., *J. Biol. Chem.* **1986**, *261*, 11726.

[26] Vector Laboratories, *Specificity of Jacalin Binding*, *www.vectorlabs.com/data/descriptions/pdf/L1150.pdf* **2008**.

[27] *Vector Laboratories*, Vector Laboratories Inc., Burlingame **2003-2004**.

[28] Wilson, R., Turner, A. P. F., *Biosensors & Bioelectronics* **1992**, *7*, 165.

[29] Pazur, J. H., Keppe, K., Ball, E. M., *Arch. Biochem.* **1963**, *103*, 513.

VITA

Hengwen Zhong

Candidate for the Degree of

Doctor of Philosophy

Thesis: SILICA- AND ORGANIC POLYMER-BASED MONOLITHIC STATIONARY PHASES FOR MODERN LIQUID PHASE SEPARATIONS

Major Field: Chemistry

Biographical:

Personal Data: Born in Guangxi, P.R. China, the daughter of Youye Zhong and Songfang Huang.

Education: Received Bachelor of Science degree in July, 1990 from Peking University, China; received Master of Science degree in July, 2005 from Oklahoma State University; completed the requirements for the Doctor of Philosophy in Chemistry at Oklahoma State University, Stillwater, Oklahoma in December, 2008.

Experience: July 1990 to July 2002, employee of Guangxi Research Institute of Chemical Industry, China; April 1999 to March 2000, visiting scholar, Kumamoto University, Japan; August 2002 to present, graduate research and teaching assistant, Oklahoma State University.

Professional Memberships: American Chemical Society

Name: Hengwen Zhong Date of Degree: December, 2008

Institution: Oklahoma State University Location: Stillwater, Oklahoma

Title of Study: SILICA- AND ORGANIC POLYMER-BASED MONOLITHIC STATIONARY PHASES FOR MODERN LIQUID PHASE SEPARATIONS

Pages in Study: 178 Candidate for the Degree of Doctor of Philosophy

Major Field: Chemistry

Scope and Method of Study: Scope and Method of Study: The aim of this study was, firstly, to introduce novel polar silica-based and acrylate-based monolithic columns for liquid normal phase chromatography (NPC) and electrochromatography of biomolecules and secondly, to develop silica-based and acrylate-based lectin affinity monolithic columns for the fractionation of glycoproteins and their glycan fragments by lectin affinity chromatography. The monolithic phases were obtained by *in situ* polymerization *via* sol-gel process in the case of silica monoliths and by vinyl co-polymerization of an acrylate functional monomer (e.g., glyceryl monomethacrylate) and a crosslinker (e.g., ethylene dimethacrylate) in the case of acrylate-based monoliths in the presence of porogens and initiators with gentle heating overnight. The silica monoliths were first functionalized with an epoxy silane and then with 1*H*-imidazole-4,5-dicarbonitrile to yield the so called 2CN-OH polar phases or with immobilized lectins *via* epoxy ring opening reactions. The acrylate-based monoliths had the diol functionalities on their surface which readily yielded polar diol monoliths or were conveniently converted to aldehyde monoliths prior to lectin immobilization. The polar and lectin affinity monolithic stationary phases were exploited in nano liquid chromatography and capillary electrochromatography using fused silica capillary columns of 100 μm I.D.

Findings and Conclusions: The investigation has yielded a simplified and time efficient method to fabricate acrylate-based monolithic stationary phases which can be effectively further modified into affinity stationary phases, and can also be applied readily as a polar stationary phase for NPC. The new acrylate-based lectin affinity monoliths exhibited strong interactions with target glycoproteins and 2-aminobenzamide (2-AB) derivatized glycans. The 2CN-OH silica-based monolith exhibited relatively high retention and selectivity toward a wide range of polar species, and proved useful in the separation of 2-AB derivatized glycans. The lectin silica-based monoliths were effective in the fractionation of selected acidic glycoproteins and the separation of some nitrophenyl derivatized monosaccharides.

ADVISER'S APPROVAL: Ziad El Rassi